

1           **Transverse energy analysis of**  
2           **relativistic heavy ion collisions**  
3   **through the use of identified particles**  
4           **spectra**

5                   A Thesis Presented for the  
6                   Master of Science  
7                   Degree  
8           The University of Tennessee, Knoxville

9                   Biswas Sharma

10                  May 2018

11

© by Biswas Sharma, 2018

12

All Rights Reserved.

# 13 Table of Contents

14	<b>1 Introduction</b>	<b>1</b>
15	<b>2 Theoretical Background</b>	<b>3</b>
16	2.1 Quantum Chromodynamics . . . . .	3
17	2.2 Phase Transitions . . . . .	4
18	2.3 Quark-Gluon Plasma . . . . .	5
19	<b>3 Relativistic Heavy Ion Collisions</b>	<b>7</b>
20	3.1 RHIC and LHC . . . . .	7
21	3.2 Collision Energy and Geometry . . . . .	9
22	3.3 QGP Evolution . . . . .	10
23	3.4 Detection of Collision Products . . . . .	11
24	3.5 Detection of QGP Signatures . . . . .	12
25	3.5.1 Bjorken Energy Density . . . . .	12
26	3.5.2 Elliptic Flow . . . . .	14
27	3.5.3 Prompt and Thermal Photons . . . . .	14
28	3.5.4 Strangeness Enhancement . . . . .	16
29	3.5.5 Jet Quenching . . . . .	17
30	3.6 The Beam Energy Scan Program . . . . .	17
31	<b>4 Measurement of Transverse Energy</b>	<b>20</b>
32	4.1 Definition of Transverse Energy . . . . .	20
33	4.2 $E_T$ Measurement with Calorimeters . . . . .	21

34	4.2.1	Calorimeter . . . . .	21
35	4.2.2	$E_T$ from PHENIX Calorimetry . . . . .	22
36	4.3	$E_T$ Measurement with Tracking Detectors . . . . .	23
37	4.3.1	Tracking and Particle Identification . . . . .	23
38	4.3.2	Calculation of $\frac{dE_T}{d\eta}$ from $p_T$ spectra . . . . .	24
39	4.3.3	Tracking Detectors in STAR . . . . .	25
40	<b>5</b>	<b>Data Analysis</b>	<b>27</b>
41	5.0.1	STAR $p_T$ spectra . . . . .	27
42	5.1	Extrapolation of Spectra . . . . .	28
43	5.1.1	Boltzmann-Gibbs Blast Wave . . . . .	29
44	5.1.2	Fitting Spectra to BGBW . . . . .	29
45	5.2	Calculations from the Spectral Fits . . . . .	30
46	5.2.1	Calculation of $\frac{dE_T}{dy}$ , $\frac{dE_T}{d\eta}$ , $\frac{dN_{ch}}{dy}$ , and $\frac{dN_{ch}}{d\eta}$ . . . . .	30
47	5.2.2	Corrections for Unidentified Particles and Estimation of Total $E_T$ . .	30
48	5.2.3	Lambdas Centralitiy Adjustments and $E_T$ Interpolations . . . . .	31
49	5.3	Uncertainties . . . . .	31
50	<b>6</b>	<b>Results</b>	<b>32</b>
51	<b>7</b>	<b>Conclusion</b>	<b>38</b>
52	<b>8</b>	<b>Future Work</b>	<b>39</b>
53	8.1	Goodness of Fit . . . . .	39
54	8.2	Bjorken Energy Density Estimate . . . . .	39
55	8.3	Asymmetric beams . . . . .	40
56		<b>Bibliography</b>	<b>41</b>
57		<b>Appendices</b>	<b>75</b>
58	A	Kinematic Variables . . . . .	76

# 59 List of Tables

<small>60</small>	3.1 Colliding species and associated collision energies at RHIC [28]. . . . .	10
<small>61</small>	5.1 Isospin states of different identified particles. . . . .	30

# List of Figures

63	2.1	Schematic of the QCD phase diagram [9]. . . . .	6
64	3.1	Initial layout of the RHIC [30]. . . . .	8
65	3.2	An illustration of a mid-central collision of two nuclei traveling in the z	
66		direction. The X-axis is parallel to the line joining the centers of the two	
67		nuclei at the time of collision [15]. . . . .	11
68	3.3	An illustration of a collision consisting of participants (solid red) and	
69		spectators (open blue) within the colliding nuclei labeled A and B. $t_c$ denotes	
70		the time of maximum overlap of the two nuclei. The apparent narrowing of	
71		the volumes of the nuclei in the z-direction is due to Lorentz contraction [42].	12
72	3.4	Evolution of the QGP represented in a lightcone diagram. $\tau_0$ denotes the	
73		formation time of the QGP. $T_c$ is the critical temperature of the transition	
74		from the QGP to the hadron gas phase. $T_{ch}$ and $T_{fo}$ stand for the temperatures	
75		at, respectively, chemical freeze-out and thermal freeze-out [15]. . . . .	13
76	3.5	Minimum-bias Au+Au ( $\sqrt{s_{NN}} = 200\text{GeV}$ ) elliptic flow spectra for identified	
77		particles: (a) $v_2$ vs $p_T$ and (b) $v_2$ vs $KE_T$ [4]. . . . .	15
78	3.6	Minimum-bias Au+Au ( $\sqrt{s_{NN}} = 200\text{GeV}$ ) elliptic flow spectra for identified	
79		particles: (a) $\frac{v_2}{n_q}$ vs $\frac{p_T}{n_q}$ and (b) $\frac{v_2}{n_q}$ vs $\frac{KE_T}{n_q}$ [4]. . . . .	16
80	3.7	Feynman diagram representing the production of photons from quarks and	
81		gluons. (a) and (b) represent annihilation processes, whereas (c) and (d)	
82		represent Compton processes [44]. . . . .	17

83	3.8	Illustration of jet quenching. Two jets are produced from each of the hard	
84		scatterings occuring at the locations of the solid dots. Jets originating closer	
85		to the initial surface are more probable to propagate outside the medium, as	
86		shown. Jets opposite to them interact with the medium, losing their energy	
87		and resulting in bow front shock waves [41]. . . . .	18
88	4.1	Energy loss distribution in the STAR TPC for primary and secondary particles	
89		[8]. . . . .	26
90	5.1	Transverse momentum spectra for $\pi^+$ , $\pi^-$ , $K^+$ , $K^-$ , $p$ , and $\bar{p}$ at midrapidity	
91		( $ y  < 0.1$ ) from 39 GeV Au+Au collisions at RHIC. The fitting curves	
92		on the 0-5% central collision spectra for pions, kaons, and protons/anti-	
93		protons represent, respectively, the Bose-Einstein, $m_T$ -exponential, and	
94		double-exponential functions [2]. . . . .	28
95	5.2	Red curve shows the Boltzmann-Gibbs blast wave functional fit on the PRE-	
96		LIMINARY transverse momentum spectrum for lambda particles identified	
97		by the STAR detector for 19.6 GeV Au+Au collisions (10-15% central).	
98		Parameters extracted from the chi-square goodness-of-fit test, as well as other	
99		statistics, are shown in the box on the top right. . . . .	30
100	6.1	Parallel coordinates plot for 270 different spectra relating 6 different identified	
101		particles (color-coded) to their respective collision centrality classes, good-fit	
102		parameters, and the transverse energy calculated using said parameters. . . .	32
103	6.2	$(dE_T/d\eta)/0.5N_{part}$ at midrapidity as a function of $\sqrt{s_{NN}}$ for different central-	
104		ities. The dashed line represents a power-law fit to the 0-5% central data in	
105		the form $y = ax^{2b}$ , where $x$ and $y$ are the placeholders for the quantities in	
106		the plot axes. $\chi^2/n.d.f$ for the fit was 1.806, and the good-fit parameters were	
107		$a = 0.4838 \pm 0.0429$ and $b = 0.2005 \pm 0.01466$ . The shaded area represents	
108		the uncertainty bounds for the 0-5% central PHENIX data from [3]. . . . .	33
109	6.3	$(dE_T/d\eta)/(dN_{ch}/d\eta)$ at midrapidity as a function of $\sqrt{s_{NN}}$ for different	
110		centralities. . . . .	34

111	6.4	$(dE_T/d\eta)/0.5N_{part}$ at midrapidity as a function of $N_{part}$ for different collision	
112		energies. . . . .	34
113	6.5	$(dE_T/d\eta)/(dN_{ch}/d\eta)$ at midrapidity as a function of $N_{part}$ for different collision	
114		energies. . . . .	35
115	6.6	$(dE_T/dy)/0.5N_{part}$ at midrapidity as a function of $\sqrt{s_{NN}}$ for different centralities.	35
116	6.7	$(dE_T/dy)/(dN_{ch}/dy)$ at midrapidity as a function of $\sqrt{s_{NN}}$ for different	
117		centralities. . . . .	36
118	6.8	$(dE_T/dy)/0.5N_{part}$ at midrapidity as a function of $N_{part}$ for different collision	
119		energies. . . . .	36
120	6.9	$(dE_T/dy)/(dN_{ch}/dy)$ at midrapidity as a function of $N_{part}$ for different collision	
121		energies. . . . .	37
122	6.10	$\frac{dE_T}{d\eta}/0.5N_{part}$ for 0-5% central collisions at midrapidity as a function of $\sqrt{s_{NN}}$ .	
123		The PHENIX data are from [3]. The error bars represent the total statistical	
124		and systematic uncertainties. . . . .	37



# Chapter 1

## Introduction

The Big Bang model is based on observational evidence, such as the cosmic microwave background radiation and the cosmological expansion, and suggests that at the beginning the universe must have been at a state of really high density and temperature. As the universe expanded, it went through several stages of cooling characterized by the formation of matters with different compositions. The matter we mostly observe today exists at temperatures and densities much lower compared to those in the early universe.

The Large Hadron Collider (LHC) at CERN and the Relativistic Heavy Ion Collider (RHIC) at the Brookhaven National Laboratory have the ability to collide heavy nuclei, such as those of gold and uranium, at nearly the speed of light, reaching temperatures of trillions of degrees Celcius. These laboratories have provided evidence of the formation of an exotic state of matter, called the quark-gluon plasma (QGP). It only exists for a brief amount of time after such collisions and instantly freezes out into a plethora of new particles, which carry the signatures we can use to deduct QGP properties. Its properties suggest that it should be similar to the matter that existed within microseconds of the genesis of the universe.[? ].

One of the methods to probe the properties of this matter is by analyzing the conversion of the beam-direction energy at the time of collision into transverse energy after the collision. These measurements can be used to estimate the energy density of the QGP. This analysis is generally done by using data from the calorimeters placed around the collision site. In this

thesis, I use the data collected by tracking detectors, instead of the conventional calorimeters,  
to calculate the transverse energy.

This thesis is structured as follows. Chapter 2 touches on the theoretical background  
associated with the concept of the quark-gluon plasma. In chapter 3, I summarize the  
experimental concepts pertaining to relativistic heavy-ion collisions and the production and  
detection of QGP. Chapter 4 consists of the formalism of the measurement of transverse  
energy using calorimeters as well as tracking detectors. It also describes what has been done  
using calorimeters. Chapter 5 describes the data used to perform the analysis in this thesis  
and notes the relevant details of the analysis. In chapter 6, I present the results and compare  
them to the ones in literature obtained using a different method. Chapter 7 concludes the  
thesis and discusses its implications. Finally, in chapter 8, I present arguments on what can  
be done in the future using the results of and the software developed for this analysis.

# Chapter 2

## Theoretical Background

### 2.1 Quantum Chromodynamics

The strong force is one of the four fundamental interactions in physics. At large scales, it is also known as the residual strong force, and it is responsible for binding the nucleons together to give the nucleus its structure. At smaller scales, it is called the fundamental nuclear force, and it binds the fundamental units of subnuclear matter, the quarks, together to form the nucleons. The force carriers of the interaction are the mesons at the former scale and the gluons at the latter. The electrodynamic interaction between charged particles such as protons and electrons is described by quantum electrodynamics (QED) as mediated by photons; the strong interaction, albeit more complicated, is explained under the framework of quantum chromodynamics (QCD) [25, 37]. The quarks and gluons of QCD are collectively known as partons. Gluons are the gauge bosons of the Yang-Mills theory.

The Yang-Mills theory is a non-Abelian gauge theory. It has a Lagrangian with several degrees of freedom, some of which are redundant and need to be gauged. This is done by a mathematical treatment as prescribed under a gauge theory [7]. The gauge theory associated with the Yang-Mills theory is based on the  $SU(N)$  group. It is non-Abelian as represented by the non-commutative transformations. QCD is a gauge theory that describes the application of the  $SU(3)$  symmetry transformations on the triplet (what does the tripleness imply?????????) of color charges, namely red, blue, and green. The electroweak interaction,

178 on the other hand, can be formalized under the gauge group  $SU(2) \times U(1)$ . Together, they  
179 form the  $SU(3) \times SU(2) \times (U(1))$  gauge theory called the standard model.

180 One of the ways QCD is different from QED is the confinement of partons. In QED, the  
181 fundamental particles are bound together by the Coulomb potential, which diminishes with  
182 distance between the charge-carrying particles, as demonstrated by the relation 2.1:

$$V_C \propto \frac{1}{r} \tag{2.1}$$

183 where  $V_C$  is the Coulomb potential, and  $r$  is the spatial separation between the particles.  
184 This means that bound QED particles can be isolated by increasing their spatial separation.  
185 The QCD potential, on the other hand, has an extra linear term in it, which means that  
186 the potential increases linearly with distance at large distances, and so an infinite amount of  
187 energy is required to separate quarks [10]. Hence, we never observe isolated quarks and they  
188 are said to be confined, not just bound, to form composite structures called hadrons [34].  
189 A quark and an anti-quark forms a meson and three quarks forms a baryon. In addition to  
190 having a color charge, a quark also carries a flavor. There are six different quarks based on  
191 the flavors they carry: up, down, top, bottom, beauty, and strange.

## 192 2.2 Phase Transitions

193 In everyday life, we observe matter existing in four distinct phases: solid, liquid, gas, and  
194 plasma. Changes in physical conditions can lead to a transition from one of these phases  
195 to another, exemplified by the commonly observed conversion of ice to water. Distinctions  
196 among the various phases can be represented in a chart called the phase diagram.

197 The phase diagram consists of thermodynamic observables such as temperature and  
198 density on its axes. Curves in the phase diagram represent boundaries of physical conditions  
199 separating one phase from another: crossing a boundary represents an abrupt transition from  
200 one phase to another. This abruptness is mathematically characterized by the discontinuity  
201 in the change of the derivative of the free energy – a thermodynamic variable – with respect  
202 to the physical quantities in the axes. Such an abrupt transition is called a first-order phase

transition. Along the boundary represented by the curve, there can be a point beyond which the phase transition is continuous instead of being abrupt, and the distinction between two phases is not clear. This point is called a critical point, and the phase transition that takes place beyond this point is called a crossover.

One of the main focuses of current experimental and theoretical nuclear physics research is the study of the phase diagram of strongly interacting matter at a range of temperatures and baryon chemical potentials. In experiments involving the collisions of heavy ions at high and low energies, different regions of the phase diagram can be probed by varying the collision energy [3]. For instance, the high-baryon chemical potential regime corresponds to lower beam energies and higher temperatures correspond to higher beam energies. The results of these experiments and model calculations can be used to study the nature of transitions in the QCD phase diagram.

A schematic representing the QCD phase diagram as a function of the temperature ( $T$ ) and quark chemical potential ( $\mu$ ) is shown in Figure 2.1 [9]. A crossover is predicted at low baryon chemical potentials (close to baryon-antibaryon symmetry) and high temperatures reminiscent of the early universe. Methods to study this region of the phase space will be explored in this thesis. At low temperatures and high net baryon densities, loose predictions have been made regarding the existence of exotic phases of high density matter, and programs, such as the Compressed Baryonic Matter experiment at the Facility for Antiproton and Ion Research in Germany, are being designed to study this region of the phase diagram [21].

## 2.3 Quark-Gluon Plasma

The confinement of quarks into the hadronic phase of QCD matter, as described in section 2.1, has its limitations. At very high densities, when the wave function of a single hadron overlaps with the spatial regions covered by multiple such hadrons, it is impossible to classify which pair or triplet of quarks belongs to which meson or baryon. As long as a particular quark is close enough to the other quarks in the volume, it is deconfined in such a way that it can freely move anywhere in the volume [34]. QCD predicts such phase transition, at energy

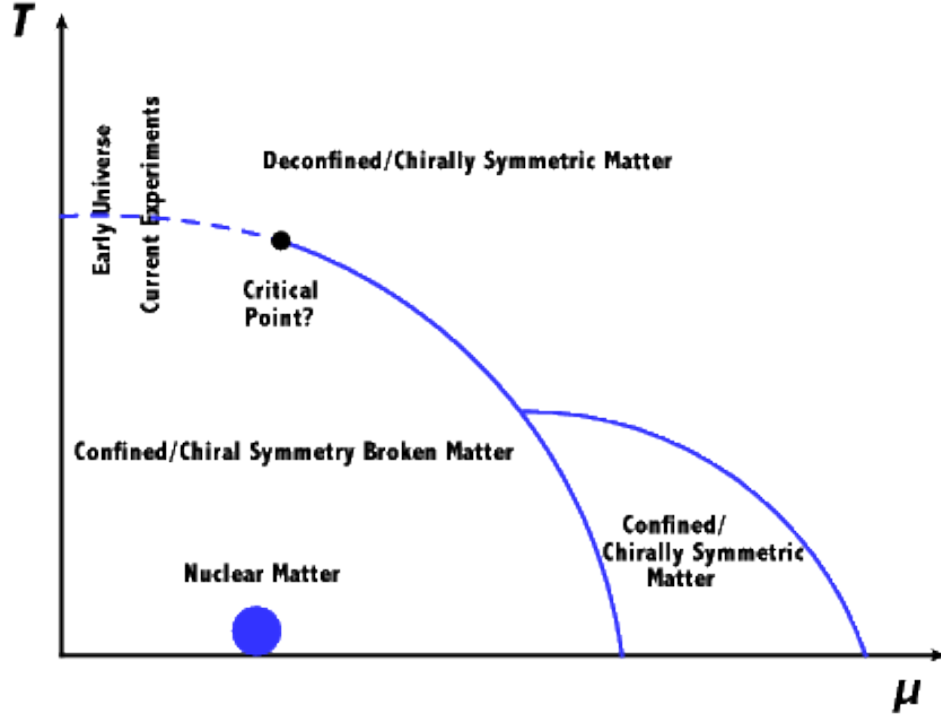


**Figure 2.1:** Schematic of the QCD phase diagram [9].

231 densities above  $0.2\text{--}1\text{ GeV/fm}^3$  [1] and around a critical temperature of about 160 MeV [18],  
 232 of strongly interacting matter to a phase with quarks and gluons in thermal and chemical  
 233 equilibrium representing the relevant degrees of freedom and behaving like an almost perfect  
 234 fluid [13]. This deconfined state of quarks and gluons is termed the quark-gluon plasma  
 235 (QGP) in analogy to the quantum electrodynamical plasma phase of matter.

## Chapter 3

# Relativistic Heavy Ion Collisions

The experimental evidence for the QGP come from the collisions of heavy nuclei. The signatures of such evidence are described in section 3.5. Physicists proposed the existence of such matter since as far back as 1984, when nuclei were accelerated and collided with stationary targets [20]. They were able to agree on a conclusive discovery of this matter during the 2000s, after colliding accelerated nuclei with other such nuclei or smaller species (protons, deuterons) at unprecedented energies and with improved detection schemes [39]. With further increases in collision energies and enhancements in detector technology, modern accelerator facilities provided additional evidence and estimates of some of the properties as well as the dynamics of the evolution of the QGP. The following sections describe two such facilities, the physics of the collisions and what happens after the collisions.

### 3.1 RHIC and LHC

The Relativistic Heavy Ion Collider (RHIC) is located in Upton, New York in the premises of the Brookhaven National Laboratory (BNL). Its construction started in 1991 and was completed in 1999. Figure 3.1 shows the layout, at the time of construction, of the collider along with the Alternating Gradient Synchrotron (AGS) complex and the locations of the original four detectors: Solenoidal Tracker At RHIC (STAR), Pioneering High Energy Nuclear Interaction eXperiment (PHENIX), Phobos and BRAHMS (Broad RAnge Hadron Magnetic Spectrometers). Phobos, BRAHMS, and PHENIX were decommissioned after the

completion of their science objectives, but STAR is still functional. The AGS was part of BNL before the construction of the RHIC, and its capabilities were augmented with the construction of the AGS Booster in 1991.

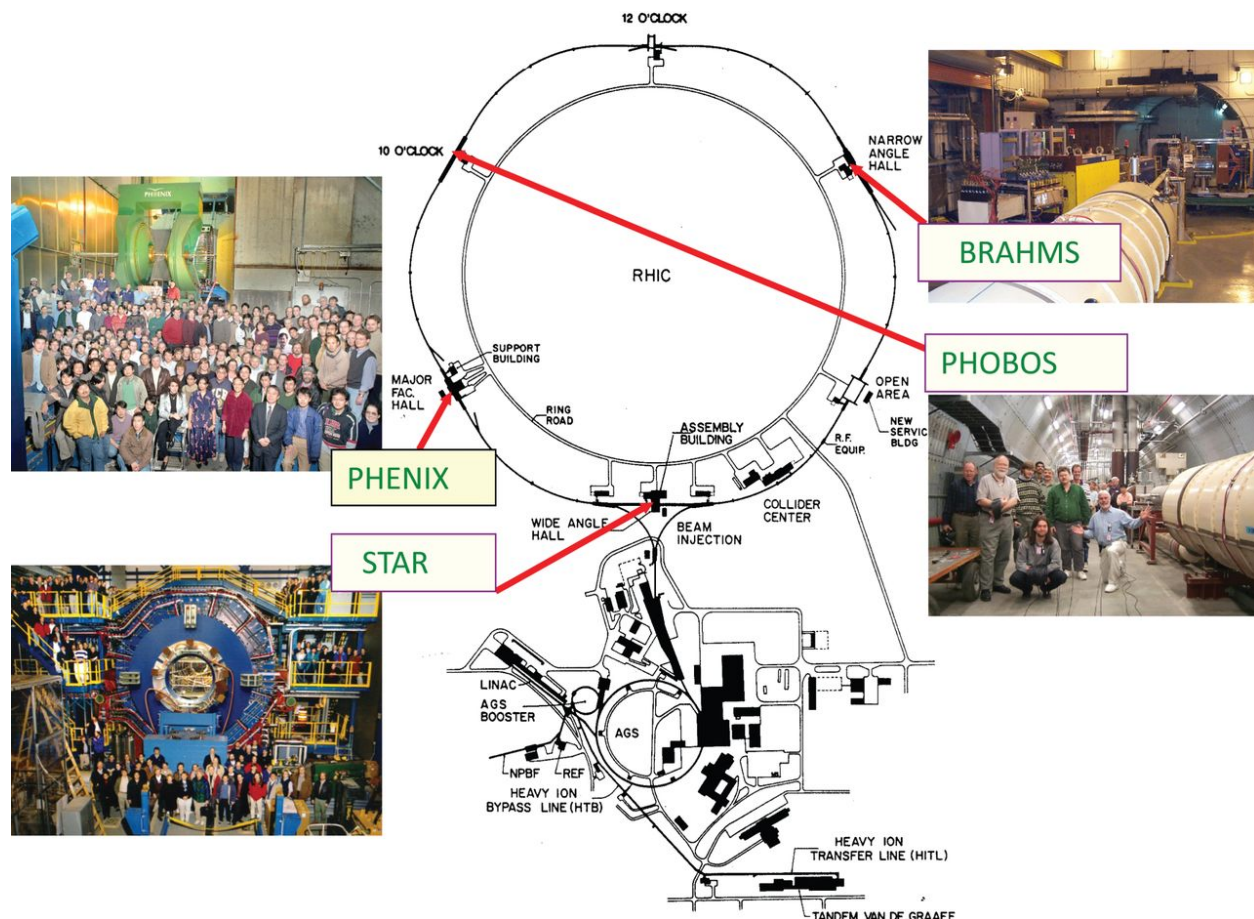


Figure 3.1: Initial layout of the RHIC [30].

Heavy ion beams in RHIC are created in a series of steps before collision. In case of gold ions, a pulsed sputter source produces negatively charged ions, which are stripped of some of their electrons with a foil on the positive end of the high-voltage Tandem Van de Graaff. The ions are now positively charged and are accelerated to 1MeV/u toward the negative terminal of the Tandem. Upon exiting it, some more stripping takes place. The bending magnets then selectively deliver +32 charge states of the ions to the Booster Synchrotron, which accelerates them to 95MeV/u and strips them to a +77 charge state before injecting them to the AGS. The AGS accelerates them to 10.8 GeV/u and strips them of the remaining two electrons at the exit. The gold ions are then injected through the AGS-to-RHIC Beam Transfer Line to



the two RHIC rings. These rings carry beams moving in opposite directions and intersect at six symmetric locations in the 3.8 km circumference. The original four detectors are located in four of these six locations where the beams undergo head-on collisions.

The Large Hadron Collider (LHC) is located underground (between 45m and 170m) beneath the France-Switzerland border near the city of Geneva. The two rings of the collider were constructed between 1998 and 2008 by the European Organization for Nuclear Research (CERN) in the 26.7 km circular tunnel originally housing CERN's Large Electron-Positron collider. Analogous to the RHIC, the LHC gets its beams prepared by a series of machines in the CERN accelerator complex. The collisions occur at the locations of the four big LHC experiments: Compact Muon Solenoid (CMS), A Toroidal LHC ApparatuS (ATLAS), Large Hadron Collider beauty (LHCb) experiment, and A Large Ion Collider Experiment (ALICE). ALICE is dedicated to the study of heavy-ion collisions [17].

## 3.2 Collision Energy and Geometry

What happens in the aftermath of a collision depends on how much energy is available at the time of the collision as well as the geometry of the collision. The collision energy is determined by the collider configuration. The geometry of the collision is deduced from the constraints imposed by the static (eg. rest mass) and dynamic (eg. trajectory) properties of the detected products.

In collision experiments, it is convenient to use a reference frame in which the net momentum of the pair of colliding species is zero. This frame is called the center-of-mass frame. In this frame, the total energy of the species in the two beams is a function of the number of nucleons and the center-of-mass energy per nucleon. The collision energy is reported as the center-of-mass energy per nucleon pair,  $\sqrt{s_{NN}}$ .

RHIC has the unique capability of colliding species at a range of energies spanning almost two orders of magnitude. Table 3.1 lists the collision energies produced so far at RHIC for various collision systems. The LHC boasts the highest amount of collision energy for any collider on earth. It collided species (p+p, p+A, Pb+Pb) at a center of mass energy upto

295 2.76 TeV per nucleon pair at the end of 2010. At the end of 2015, 5.02 TeV Pb+Pb (13 TeV  
 296 p+p) collisions were successfully completed [19].

Collision system	$\sqrt{s_{NN}}(GeV)$
p+p	200, 500
d+Au	200
Cu+Cu	62, 200
Au+Au	9, 20, 62, 130, 200

**Table 3.1:** Colliding species and associated collision energies at RHIC [28].

297 In general, any collision between two nuclei is not perfectly head-on. Some collisions are  
 298 close to being head-on and are called central collisions. Some are glancing and are called  
 299 peripheral collisions. By convention, 0% is the centrality of a perfectly head-on collision  
 300 and 100% is that of the least head-on, i.e., the most peripheral collision. In practice, each  
 301 collision event is deducted to belong to a specific centrality bin. For instance, 0-5% would  
 302 be the centrality for an identified  $N_{ch}$  value which would be the minimum charged particle  
 303 multiplicity produced by at most 5% of the total number of collisions. This identification of  
 304 the  $N_{ch}$  value is often achieved by using the a Glauber model [15, 27]. Figure 3.2 illustrates  
 305 the aftermath of a mid-central collision, i.e, a collision in which about half of the volume of  
 306 each of the nuclei intersects the other.

307 The collision of two nuclei can be modeled as collisions of the constituents that make  
 308 up the nuclei. The nucleons that take part in the collisions and are called participants.  
 309 The rest of the nucleons are known as spectators. Figure 3.3 illustrates the distribution of  
 310 participants and spectators in two colliding nuclei.

### 311 3.3 QGP Evolution

312 The evolution of the QGP is shown in a lightcone diagram in figure 3.4 [15]. The initial state  
 313 of the colliding nuclei is not well known and is the topic of research for upcoming experiments.  
 314 During the collision, the participants scatter off of each other while the spectators keep  
 315 traveling almost unperturbed in their original direction. The immediate aftermath of a  
 316 central collision of heavy ions at RHIC and LHC energies is the formation of a hot fireball.

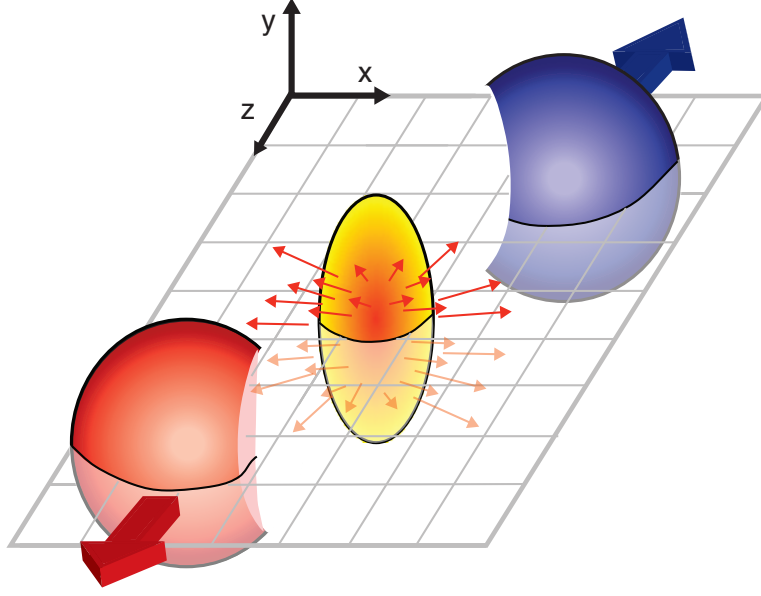


**Figure 3.2:** An illustration of a mid-central collision of two nuclei traveling in the  $z$  direction. The  $X$ -axis is parallel to the line joining the centers of the two nuclei at the time of collision [15].

317 This fireball evolves in time to form a liquid-like medium of quarks and gluons. This medium  
 318 attains a local equilibrium and remains in such a state, depending on the collision energy,  
 319 for about 1-10 fm/c. This equilibrium is broken as the liquid QGP evolves by expanding and  
 320 cooling to attain a density and temperature at which the deconfinement of quarks and gluons  
 321 is lost and they undergo a chemical freeze-out to form a hadron gas. Collisions between the  
 322 constituents of this gas become scant as it evolves with further expansion and cooling, and  
 323 the hadrons undergo a thermal freeze-out to attain their final energies and momenta [15].

### 324 3.4 Detection of Collision Products

325 Detectors are placed around the collision site to perform measurements on the final state  
 326 particles emitting from the thermal freeze-out of the medium. These measurements typically  
 327 include the reconstruction of the particle tracks, estimation of the the types of particles, and  
 328 the momenta and energies they carry.

329 Generally, a tracking detector surrounds the collision site, and there are particle identifiers  
 330 followed by calorimeters around it. A magnetic field is applied parallel to the beam direction

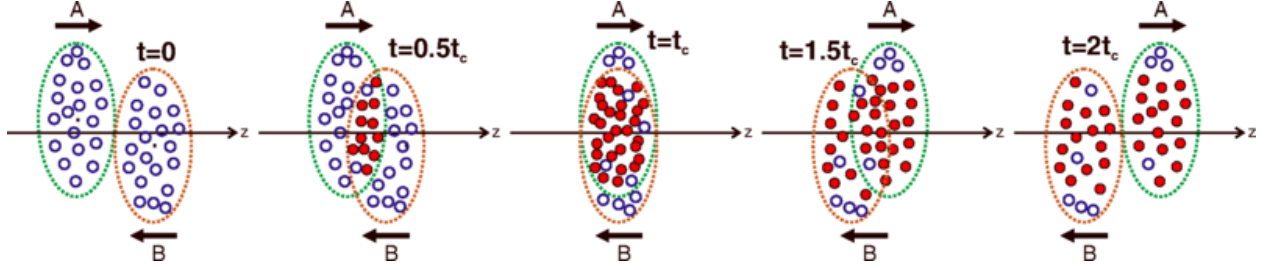


**Figure 3.3:** An illustration of a collision consisting of participants (solid red) and spectators (open blue) within the colliding nuclei labeled A and B.  $t_c$  denotes the time of maximum overlap of the two nuclei. The apparent narrowing of the volumes of the nuclei in the z-direction is due to Lorentz contraction [42].

around the collision site. Due to this orientation of the magnetic field, the spectators traveling parallel to it move undeflected and the final state charged particles with components of velocity transverse to the beam axis get deflected around the beam axis with radius given by

$$r = \frac{p_T}{qB}, \quad (3.1)$$

where  $p_T$  is the transverse momentum of the particle,  $q$  is its electric charge, and  $B$  is the applied magnetic field. Two kinds of detectors most relevant to this thesis, tracking detectors and calorimeters, are described in chapter 4.

## 3.5 Detection of QGP Signatures

The existence and properties of the QGP in the aftermath of high-energy heavy-ion collisions can be probed using different techniques relevant to several theoretical characteristics of the medium. No signature can alone be used to claim the production of the QGP, and some of the probes, which should be interpreted together, are described below.

### 3.5.1 Bjorken Energy Density

In 1983, J.D. Bjorken[12] prescribed a formula to use the final state particles to estimate the initial energy density,  $\epsilon_0$ , in a nucleus-nucleus collision. With slight changes in the original

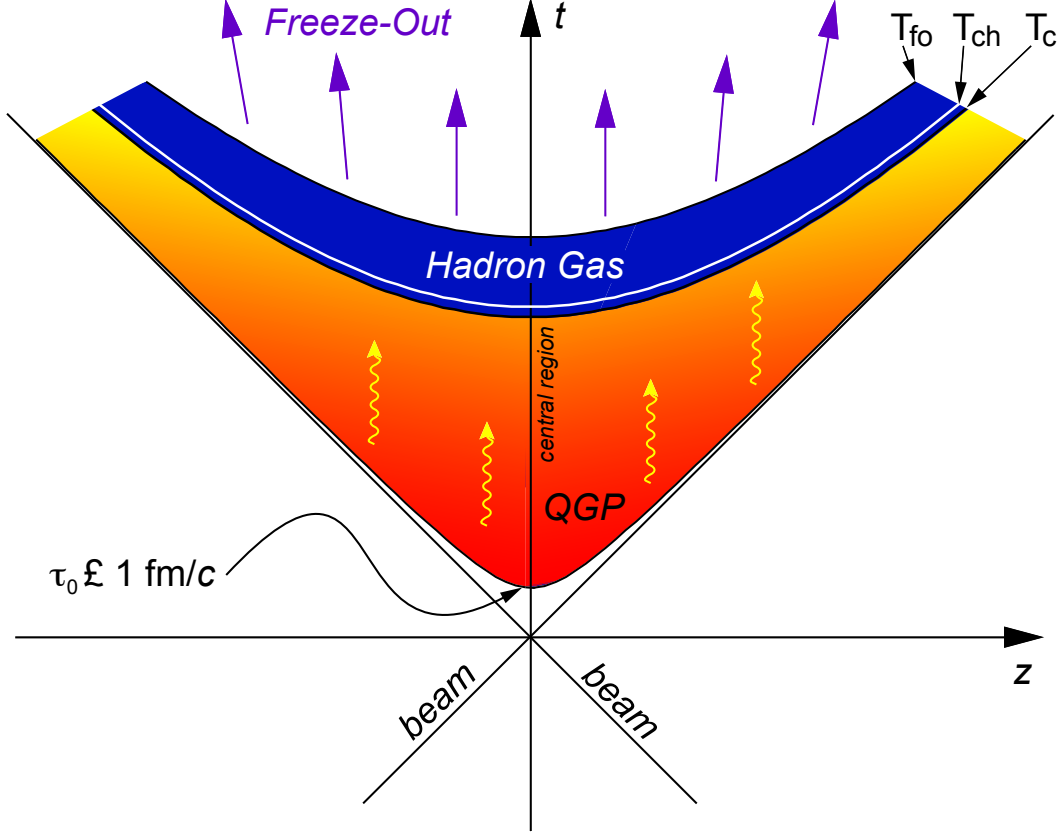


**Figure 3.4:** Evolution of the QGP represented in a lightcone diagram.  $\tau_0$  denotes the formation time of the QGP.  $T_c$  is the critical temperature of the transition from the QGP to the hadron gas phase.  $T_{ch}$  and  $T_{fo}$  stand for the temperatures at, respectively, chemical freeze-out and thermal freeze-out [15].

formula, the energy density is given by:

$$\epsilon_0 = \frac{1}{\tau_0 A_T} \left\langle \frac{dE_T}{dy} \right\rangle, \quad (3.2)$$

where  $\tau_0$  is the formation time of QGP equilibration,  $A_T$  is the transverse area of the intersection of the two nuclei, and  $\langle \frac{dE_T}{dy} \rangle$  is the mean transverse energy per unit rapidity.  $\tau_0$  is model-dependent and is normally estimated to be  $1 fm/c$ .  $A_T$  depends on the centrality of the collision and can be estimated using the Glauber models discussed earlier.  $\langle \frac{dE_T}{dy} \rangle$  is found from the measurement of the transverse energy carried by the final state particles from the collision and is the central theme of this thesis. Details about it are in the following chapters. The estimate of the initial energy density from Bjorken formula can be compared with the

QCD prediction of the critical energy density[1] to check if the results from a collision imply the achievement of the critical physical condition required for the phase transition [24].

### 3.5.2 Elliptic Flow

The evolution of the medium produced after relativistic heavy ion collisions can be well described under the framework of relativistic hydrodynamics [35, 40]. This description indicates the presence of a collective flow, and hence a liquid-like (awkward?????) and thermalized nature, of the constituents that make up the system. The momentum distribution of the final state particles emitted out of the collectively flowing system can be decomposed into its azimuthal Fourier components. The second harmonic coefficient,  $\nu_2(y, p_T)$ , of this decomposition characterizes what is known as the elliptic flow [23]. The magnitude of the elliptic flow from a non-central collision represents the anisotropy in azimuthal momentum space of the thermalized post-collision system [38]. The elliptic flow of the medium, as a function of the momentum or the kinetic energy in the transverse direction, points towards quarks, rather than hadrons, being the relevant degrees of freedom in the QGP. Figure 3.5 shows  $\nu_2$  as a function of the transverse momentum and the transverse kinetic energy for identified particles. The spectra scale consistently at lower values of both  $p_T$  and  $KE_T$ . However, they branch out at higher values:  $p_T \gtrsim 2\text{GeV}/c$  and  $KE_T \gtrsim 1\text{GeV}$ . Figure 3.6, on the other hand, is similar to figure 3.5, with the exception that both the axes have quantities that are normalized by the number of quarks,  $n_q$ . In this case, the  $KE_T$  spectra strongly exhibits a scaling which is more comprehensively consistent with the number of quarks than in case of figure 3.5. This universal quark-number scaling can be interpreted as the degrees of freedom of the system being quark-like [4].

### 3.5.3 Prompt and Thermal Photons

Most of the photons observed after relativistic heavy ion collisions are the results of the decay of the neutral pion into two gammas. When these photons are subtracted from the observations, the remaining photons are called direct photons [31]. These direct photons are produced within the fireball via different mechanisms as discussed below.

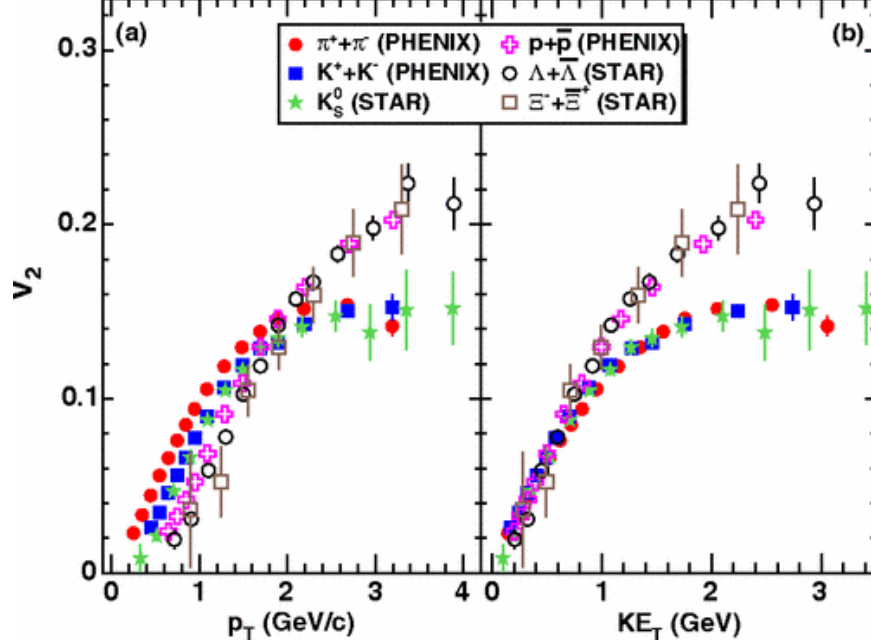


**Figure 3.5:** Minimum-bias Au+Au ( $\sqrt{s_{NN}} = 200 \text{ GeV}$ ) elliptic flow spectra for identified particles: (a)  $v_2$  vs  $p_T$  and (b)  $v_2$  vs  $KE_T$  [4].

381 In the QGP, a quark and an antiquark can annihilate to produce a photon and a gluon.  
 382 It is also possible for the pair to annihilate and produce two photons, but the probability  
 383 of this process is smaller than the former by about two orders of magnitude. Furthermore,  
 384 a quark (or an antiquark) can interact with a gluon to produce an antiquark (or a quark)  
 385 and a photon, a process analogous to Compton scattering in QED. The photons produced  
 386 from the hard scattering processes between the partons are called direct photons, and their  
 387 multiplicity scales with the number of binary collisions. Photons can also be produced  
 388 due to scatterings of partons within the thermalized medium, and these photons are called  
 389 thermal photons. The nature of the  $p_T$  distribution is different in this case as the emission  
 390 process mimics blackbody radiation. This difference helps distinguish these photons from  
 391 the direct photons produced by partonic interactions. Just like the leptons described in  
 392 the previous section, the photons produced in the QGP can only interact with the medium  
 393 electromagnetically. Therefore, they undergo minimal scattering before being detected, and  
 394 hence can be used to probe the thermodynamical state of the medium at the time of their  
 395 creation [44, 31, 43].

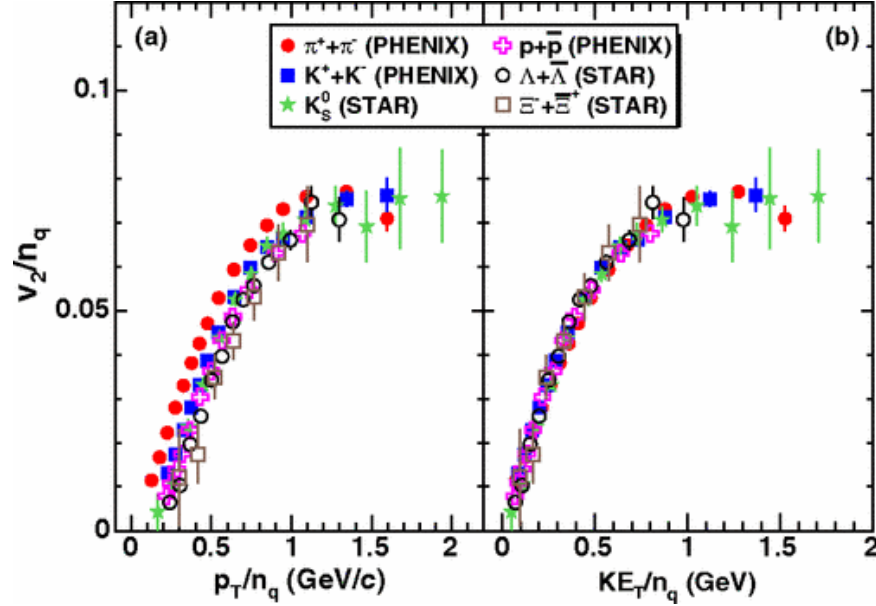


**Figure 3.6:** Minimum-bias Au+Au ( $\sqrt{s_{NN}} = 200\text{GeV}$ ) elliptic flow spectra for identified particles: (a)  $\frac{v_2}{n_q}$  vs  $\frac{p_T}{n_q}$  and (b)  $\frac{v_2}{n_q}$  vs  $\frac{KE_T}{n_q}$  [4].

### 3.5.4 Strangeness Enhancement

One of the implications of the formation of QGP is chiral symmetry restoration. At the energy scale of this phenomenon, strange quarks lose their masses, and hence it is feasible to produce a lot of them. The interacting nuclei carry no net strangeness before colliding, and so an observation of strange and multi-strange particles after the collision can be used to probe the properties of the post-collision medium [16]. Strangeness can also be produced in hadron-hadron collisions. However, it is enhanced in nucleus-nucleus collisions in which a large number of hadrons are produced and are in chemical equilibrium at very high temperatures. The enhancement is exemplified by the ratio of the production of the strange kaons to that of the non-strange pions, which are the most abundant hadrons produced from nucleus-nucleus collisions. Kaon yield increases more rapidly than does pion yield as the temperature increases. This can be shown mathematically by treating the system as a hadron gas in thermal and chemical equilibrium that follows the Bose-Einstein distribution, but it is beyond the scope of this thesis [44]. ..... connect to big picture... why is strangeness enhancement interesting? .... phase space suppression? ..... chiral symmetry restoration.....?



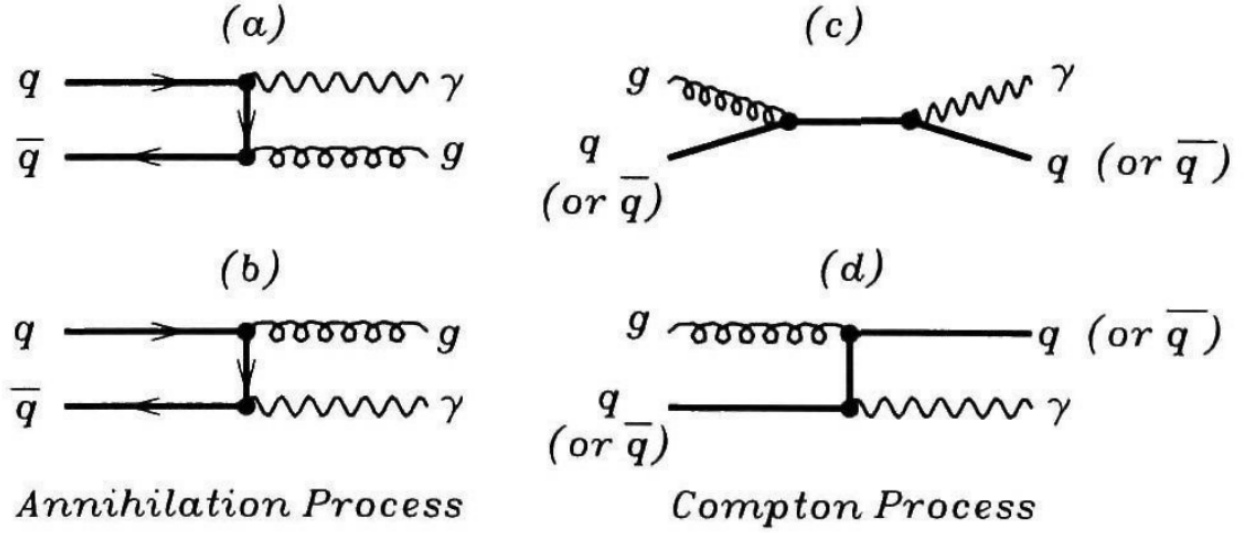


**Figure 3.7:** Feynman diagram representing the production of photons from quarks and gluons. (a) and (b) represent annihilation processes, whereas (c) and (d) represent Compton processes [44].

### 3.5.5 Jet Quenching

A scattering event in which the participants transfer a large amount of their original momenta is called hard scattering. The products of the scattering are called jets. Ultimately, jets are what are recognized by a jet finder algorithm as jets. In heavy-ion collisions, most hard scatterings are the results of two partons from the opposite nuclei scattering off of each other. These partons can lose their momenta by strongly interacting with a medium made of deconfined quarks and gluons. Therefore, the properties of the jets, as carried by the final state hadrons, should be different for collisions that produce the QGP as compared to those that do not, and hence they can be used as signatures and probes of QGP. Figure 3.8 illustrates the quenching of jets that have to travel long distances in the medium. Formalisms developed to study jet quenching due to radiative and collisional energy losses are detailed in [33].

## 3.6 The Beam Energy Scan Program

The RHIC, in 2010, started a multi-phase Beam Energy Scan (BES) program to study the QCD phase diagram. Between 2010 and 2011, during the exploratory phase I of the BES

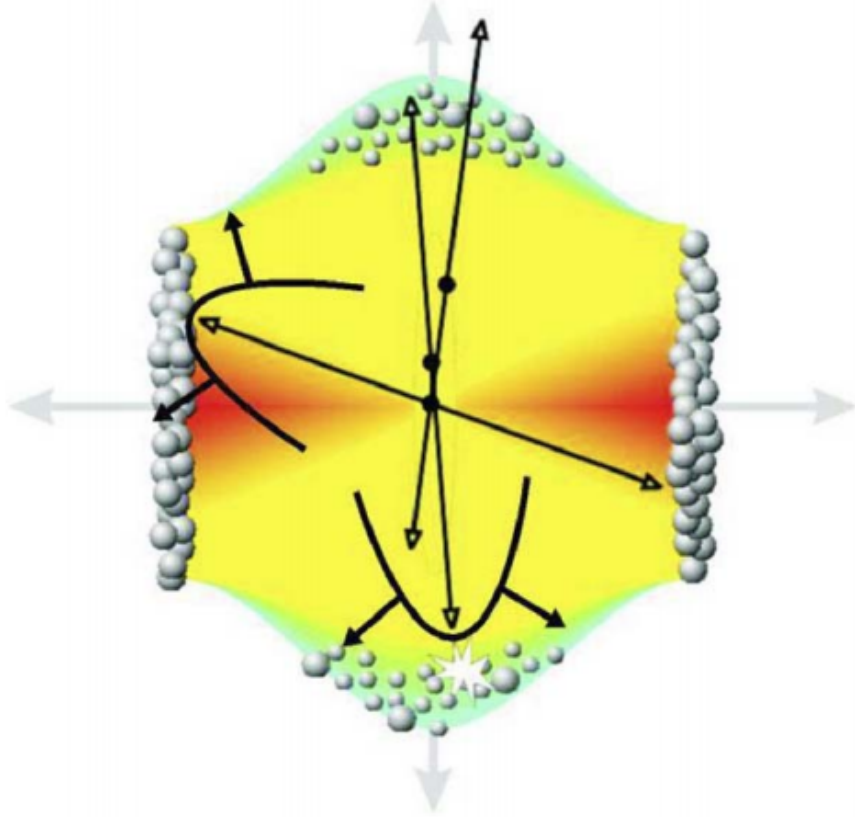


**Figure 3.8:** Illustration of jet quenching. Two jets are produced from each of the hard scatterings occurring at the locations of the solid dots. Jets originating closer to the initial surface are more probable to propagate outside the medium, as shown. Jets opposite to them interact with the medium, losing their energy and resulting in bow front shock waves [41].

426 program, the collider provided Au+Au collisions at 7.7, 11.5 (not completed in PHENIX),  
 427 19.6, 27, and 39 GeV. Together with the data formerly collected by the RHIC at higher  
 428 collision energies, BES phase I data can scan the interval from 450 MeV to 20 MeV in  $\mu_B$   
 429 space [29, 26]. One of the things that can be studied with the data associated with this region  
 430 of the phase space is the possibility of a “turn-off of new phenomena already established  
 431 at higher RHIC energies”[29]. Results corresponding to the high- $\mu_B$  region might provide  
 432 evidence of a first order phase transition, and possibly the critical point [26].

433 The manifestation of such phenomena would be in terms of the fluctuations or other  
 434 properties of the post-collision system. One can, for instance, study the scaling of the  
 435 transverse energy after the collision with the longitudinal energy at the time of the collision,  
 436  $\sqrt{s_{NN}}$ . This can be done in multiple ways using a detector like STAR or PHENIX that is

437 made up of sub-systems such as the Time Of Flight (TOF) detectors, Time Projection  
438 Chambers (TPCs)/Time Expansion Chambers, as well as calorimeters. The next chapter  
439 describes the measurement of transverse energy using BES data from PHENIX calorimeters.  
440 Also, the next chapter and the ones after it contain the procedures and the results of the  
441 analysis of the BES data from STAR using the identified particles spectra.

## Chapter 4

# Measurement of Transverse Energy

This chapter introduces the definitions of transverse energy, ways to measure it using different detectors, and particular examples for the detectors at the RHIC.

### 4.1 Definition of Transverse Energy

The transverse energy,  $E_T$ , from a collision can be defined as the sum of the transverse masses,  $m_T$ , of all the particles produced in the collision, i.e.,

$$E_T \equiv \sum_i m_{T,i} \quad (4.1)$$

with

$$m_T \equiv \sqrt{p_T^2 + m^2} \quad (4.2)$$

where  $m$  is the rest mass of the particle and  $p_T$  is its transverse momentum. Using this definition to calculate the  $E_T$  requires perfect identification of all the particles. It has not been possible to do so in experiments, and so a more feasible, operational definition of  $E_T$  is used. A commonly accepted definition in case of the feasibility of calorimetric measurements is [5, 13]:

$$E_T = \sum_i E_i \sin \theta_i, \quad (4.3)$$

455

$$\frac{dE_T}{d\eta} = \sin\theta \frac{dE}{d\eta}, \quad (4.4)$$

456 where the index  $i$  runs over all the particles going into a fixed solid angle for each event,  
 457  $\theta$  is the polar angle, i.e, the angle with respect to the beam axis,  $\eta$  is the pseudorapidity  
 458 defined as

$$\eta \equiv -\ln \tan \frac{\theta}{2}, \quad (4.5)$$

459 and  $E_i$  is the energy deposited in the calorimeter by the  $i^{th}$  particle.  $E_i$  is considered to be,  
 460 by convention [6], the following

$$E_i = \begin{cases} E_i^{tot} - m_0 & \text{for baryons} \\ E_i^{tot} + m_0 & \text{for anti-baryons} \\ E_i^{tot} & \text{otherwise} \end{cases} \quad (4.6)$$

461 where  $E_i^{tot}$  is the total energy of the  $i^{th}$  particle defined canonically as

$$E^{tot} \equiv \sqrt{p^2 + m_0^2} \quad (4.7)$$

462 and  $m_0$  is the particle's rest mass.

463  $E_i$  given by equation 4.6 is what would be observed by a calorimeter. In order to  
 464 account for the portion of the emitted transverse energy not detected or overestimated by  
 465 the calorimeters, corrections are made based on simulations.

## 466 **4.2 $E_T$ Measurement with Calorimeters**

### 467 **4.2.1 Calorimeter**

468 A calorimeter in a particle or nuclear physics experiment is a device used to measure the  
 469 energy carried by a particle by analyzing the signal generated by the shower of particles  
 470 produced by the interaction of the incoming particle with the material of the device [? ,  
 471 (<http://pdg.lbl.gov/2016/download/rpp-2016-booklet.pdf>)] In theory, a single calorimeter

can be made to measure the energy deposited by different kinds of particles. However, it makes more sense to have two different kinds of calorimeters: one optimized to measure the energy deposited by particles like electrons (or positrons) and photons, called an electromagnetic calorimeter (EMCal), and the other optimized to measure the energy deposited by hadronic particles, called a hadronic calorimeter (HCal). This is because of the difference in the particle showers that these two categories of particles generate. Electrons and photons mostly lose their energies in the calorimeter material via bremsstrahlung, Compton scattering and pair production. They generate particle showers made of electrons and photons which cannot travel much farther into the medium before losing all their energies in a series of interactions producing an avalanche of sequential showers. However, hadrons can interact inelastically with the nucleus generating a shower of hadrons. These secondary hadrons have much larger masses than the secondary electrons in the shower generated by the electrons and photons. This means they are not deflected nearly as much by the electric forces in the material and travel much farther into the calorimeter. For this reason, EMCals are comparably smaller in depth and are placed before the HCals in a detector assembly.

## 4.2.2 $E_T$ from PHENIX Calorimetry

Adare et al. [3] use electromagnetic calorimetry in PHENIX to analyze the transverse energy corresponding to several different pairs of species colliding at a range of energies. They use the raw transverse energy measured by the EMCal,  $E_{TEMC}$ , to obtain the total  $E_T$  by making corrections in three different steps.

They first scale the data by a constant factor, 4.188, calculated to account for the fiducial acceptance in azimuth and pseudorapidity. The second factor is calculated to adjust for the effects of the calorimeter towers that are disabled. The third factor,  $k$ , is the ratio of  $E_T$  and  $E_{TEMC}$  and is computed as follows:

$$k = k_{response} \times k_{inflow} \times k_{losses} \quad (4.8)$$

where  $k_{response}$  corresponds to hadronic particles only depositing a fraction of their total energy while passing through the EMCal,  $k_{inflow}$  is attributable to the energy deposited

by particles coming from outside the EMCal's fiducial aperture, and  $k_{losses}$  accounts for the energy not registered in the EMCal due to energy thresholds, edge effects, and more importantly due to the particles that make it into the fiducial aperture but decay into products outside the aperture.

$k_{response}$  is estimated using simulations of event generation and particle detection. With 3/4 of the incident energy measured by the EMCal in the simulation,  $k_{response} = 1/(3/4) = 1.33$ . 24% of the energy measured by the EMCal is found to be associated with the 'inflow' particles, and so  $k_{inflow} = 1-0.24 = 0.76$ . 22% of the energy is lost due to aforementioned reasons (10% + 6% + 6%), and so  $k_{losses} = 1/(1-0.22) = 1.282$ . From equation 4.8, then,  $k = 1.30$ , and this factor was found to vary for all the data sets by less than 1%.

The systematic uncertainties due to several contributions (listed in Table II in [3]) are added in quadrature to obtain the total systematic uncertainties in  $dE_T/d\eta$ . The uncertainty is low for the correction related to the acceptance (2%) as compared to that for the  $k$  factor: 3% for losses and inflow and 4.5%-4.7% for the energy response.

## 4.3 $E_T$ Measurement with Tracking Detectors

Transverse energy analysis can be done using tracking detectors as well if they are able to produce measurements of other physical quantities that implicitly contain information about the transverse energy. Specifically, the charged particle multiplicity distributions with respect to the transverse momenta can be used, with assumptions involving particle ratios (section 5.2.2) and mean  $p_T$ , to calculate the particle's transverse energy. Since the corrections related to the tracking detectors are very different from those related to the calorimeters, results from the two different methods can be used to test the assumptions involved in each.

### 4.3.1 Tracking and Particle Identification

The tracking detectors in experiments such as the STAR (Solenoidal Tracker At RHIC) experiment and ALICE (A Large Ion Collider Experiment) at CERN include Time Projection Chambers (TPCs) and Time-of-Flight (TOF) detectors that can be used to measure the  $p_T$  spectra, yields and particle ratios of the identified charged hadrons [32, 2]. The TPCs provide

525 measurements of particle trajectories that can be used to determine the momenta for low-  
526 momentum particles. They also provide measurements of their specific energy loss,  $\frac{dE}{dx}$ , which  
527 can be used in combination with the momenta to identify particles using the Bethe-Bloch  
528 formula [11]. The particle identification (PID) capabilities of STAR are discussed in section  
529 4.3.3. TOF detectors cover the high-momentum part of the measurements. In ALICE, the  
530 combination of the measurements of the TPC with those of the Inner Tracking System (ITS)  
531 effectively adds the tracking length, thereby improving the resolution of the measured  $p_T$   
532 spectrum. Details about the PID and momentum determination capabilities of the detectors  
533 in ALICE can be found in [14].

534 The  $p_T$  spectra, reported as  $\frac{d^2N}{dydp_T}$  as a function of  $p_T$ , can be used to calculate  $\frac{dE_T}{d\eta}$  as  
535 formulated in the following section.

### 536 4.3.2 Calculation of $\frac{dE_T}{d\eta}$ from $p_T$ spectra

537 In relativistic heavy ion collisions, rapidity ( $y$ ) is defined as follows:

$$y \equiv \frac{1}{2} \ln \frac{E + p_z}{E - p_z}, \quad (4.9)$$

538 where  $E$  is given by equation 4.7 and  $p_z$  is the component of the momentum parallel to the  
539 beam axis. Pseudorapidity,  $\eta$ , is just  $y$  with  $m_0 = 0$ , which leads to equation 4.5. Taking  
540 the exponential of both sides of the equation 4.5 and using Euler's formula, we get:

$$\sin \theta = \frac{1}{\cosh \eta}. \quad (4.10)$$

Hence,

$$\begin{aligned} p &= \frac{p_T}{\sin \theta} \\ &= p_T \cosh \eta, \end{aligned}$$

541 and so we have

$$E_T = E \sin \theta = \frac{\sqrt{p_T^2 \cosh^2 \eta + m_0^2}}{\cosh \eta} \quad (4.11)$$



The Jacobian for the transformation from  $y$ -space to  $\eta$ -space is derived to be:

$$\frac{\partial y}{\partial \eta} = \frac{p_T \cosh \eta}{\sqrt{m_0^2 + p_T^2 \cosh^2 \eta}} \quad (4.12)$$

From equations 4.11 and 4.12, we can see that the product of  $E_T$  with the Jacobian is equal to  $p_T$ . That leads to a formulation of  $\frac{dE_T}{d\eta}$  as a function of only  $\eta$  and  $p_T$ :

$$\frac{dE_T}{d\eta} = \frac{1}{2a} \int_0^{10 \text{ GeV}/c} \int_{-a}^a p_T \frac{d^2 N}{dy dp_T} d\eta dp_T \quad (4.13)$$

where  $a$  and  $-a$  are the bounds for  $\eta$ . The estimate for the upper limit of  $p_T$  makes sense in accordance with the mean  $p_T$  of the spectra being comfortably an order of magnitude less than 10 GeV/c as discussed in chapter 5. More details on the kinematic variables  $y$  and  $\eta$  are in appendix ??.

### 4.3.3 Tracking Detectors in STAR

In the STAR experiment, the TPC is the primary tracking detector. It is 4.2 m long and it cylindrically encloses the accelerator beam pipe from its outside, with an inner diameter of 1 m and an outer diameter of 4 m [28]. It covers a pseudorapidity range of  $|y| < 1.8$  in all of azimuth for charged particles. It can identify particles with momenta over 100 MeV/c up to about 1 GeV/c as well as measure their momenta from 100 MeV/c to 30 GeV/c [8]. Figure 4.1 shows the PID capability of the STAR TPC for very high-multiplicity events [22]. Separation of pions from protons is demonstrated up to a little more than 1 GeV/c. At higher momenta, separating particles is more difficult because their energy loss has lower dependence on the rest mass [8]. The TOF system in STAR, with a time resolution of  $\lesssim 100$  ps, aids PID at higher momenta. However, at intermediate  $p_T$ , between  $\approx 2.0$  and 4.0 GeV/c, the TPC by itself cannot distinguish between pions and protons and the TOF by itself cannot separate pions from kaons. This problem is resolved by utilizing the fact that the dependence of the particle velocity on  $p_T$  – in case of the TPC – is different from that of the energy loss on  $p_T$  in case of the TPC; combining the results from the two, hence, makes PID feasible in this  $p_T$  range [36].

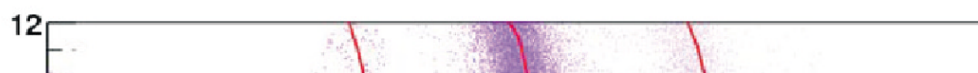


**Figure 4.1:** Energy loss distribution in the STAR TPC for primary and secondary particles [8].

## Chapter 5

# Data Analysis

The available spectra were extrapolated to calculate the transverse energies and charged particle multiplicities. Details follow.

### 5.0.1 STAR $p_T$ spectra

This thesis details the method of transverse energy analysis through the use of  $p_T$  spectra from the STAR BES data. As described in section 4.3.3, the TPCs and TOF detectors in STAR can identify particles as well as their trajectories and ultimately measure their multiplicity distributions with respect to the momenta. [1] reports the results for the  $p_T$  spectra for six different identified hadrons,  $\pi^+$ ,  $\pi^-$ ,  $K^+$ ,  $K^-$ ,  $p$ , and  $\bar{p}$ , from the STAR experiment. The spectra come from  $\sqrt{s_{NN}} = 7.7, 11.5$ , and 39 GeV Au+Au collisions data taken in the year 2010 and from  $\sqrt{s_{NN}} = 19.6$  and 27 GeV Au+Au collisions data taken in 2011 as part of the BES Program. Figure 5.1 [2] shows the spectra corresponding to 39 GeV collisions categorized into seven different collision centrality classes. Additionally, preliminary spectra were available from the STAR experiment for identified lambdas and anti-lambdas. These spectra were used to calculate an estimate of the total transverse energy per event per particle species. This result was then used to estimate the total transverse energy due to all the collision products.

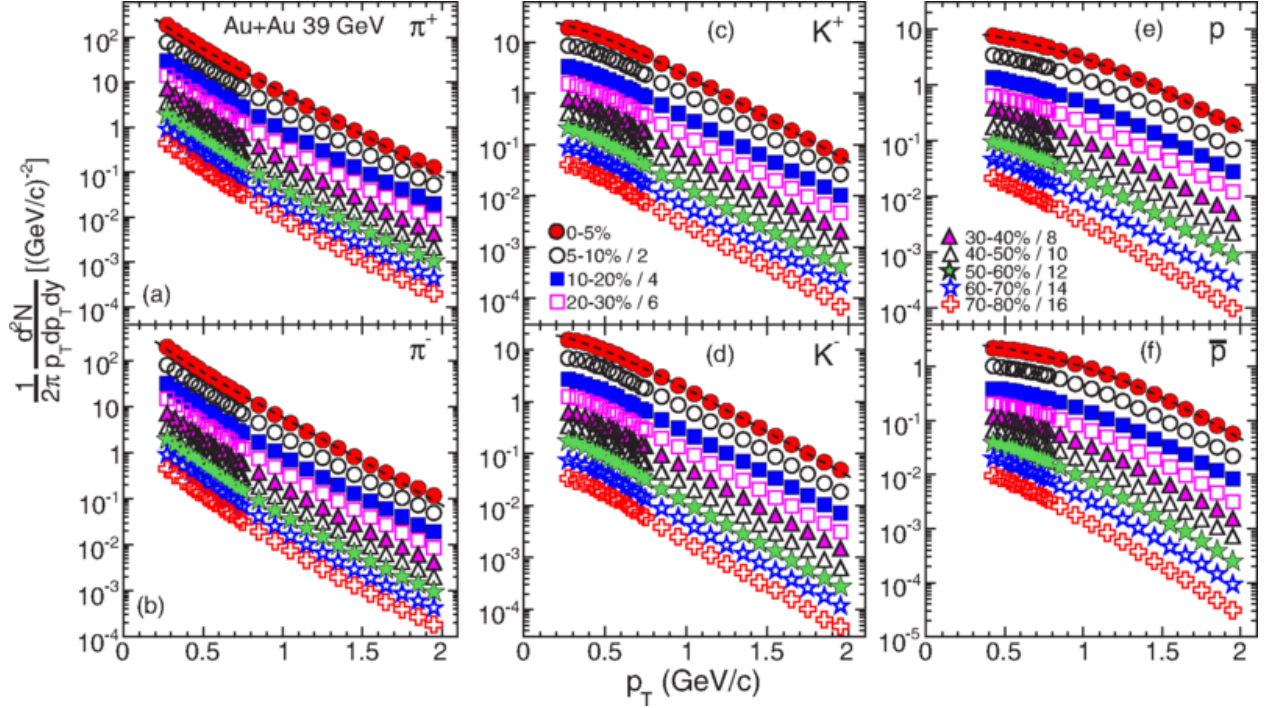


**Figure 5.1:** Transverse momentum spectra for  $\pi^+$ ,  $\pi^-$ ,  $K^+$ ,  $K^-$ ,  $p$ , and  $\bar{p}$  at midrapidity ( $|y| < 0.1$ ) from 39 GeV Au+Au collisions at RHIC. The fitting curves on the 0-5% central collision spectra for pions, kaons, and protons/anti-protons represent, respectively, the Bose-Einstein,  $m_T$ -exponential, and double-exponential functions [2].

The corrections applied by Adamczyk et al. [2] to the raw data to obtain the spectra and the reported systematic uncertainties in their results are discussed below (under construction)

.....

## 5.1 Extrapolation of Spectra

The available spectra were limited to a range of transverse momenta from around 0.25 GeV/c to around 2 GeV/c (for pions). To account for the transverse energy corresponding to the momenta for which there was no available data, an extrapolation had to be used. The model used for the extrapolation and the associated statistics are discussed below.

### 5.1.1 Boltzmann-Gibbs Blast Wave

The blast wave is a common model used in the analysis of the particle spectra.[????] The specific model used in this thesis is the Boltzmann-Gibbs blast wave (BGBW) as represented in equation ?? . It has the parameters mass, temperature, beta, v, and n. I assume that any anomalies in the magnitude of the normalization parameter do not affect the results significantly insomuch as they don't lead to:

- (a) unreasonable relative errors in the extrapolated values of the transverse energy,
- (b) any of the spectral fits having the extrapolated transverse energy more than that calculated from just the available spectra, and
- (c) for the 200 GeV collision samples, at least, the extrapolation at higher  $p_T$  being more than that at lower  $p_T$ .

$$BGBW \tag{5.1}$$

### 5.1.2 Fitting Spectra to BGBW

Figure 5.2 presents an example of a Boltzmann-Gibbs Blast Wave (BGBW) fit on one of the individual particle spectra with  $\chi^2/\text{n.d.f}$  as well as other statistics and the associated errors. A parallel-coordinates plot is presented in the next chapter in fig. 6.1, which shows the measured centralities, two of the good-fit parameters, and the calculated transverse energies for 270 different particles (lambdas not included).

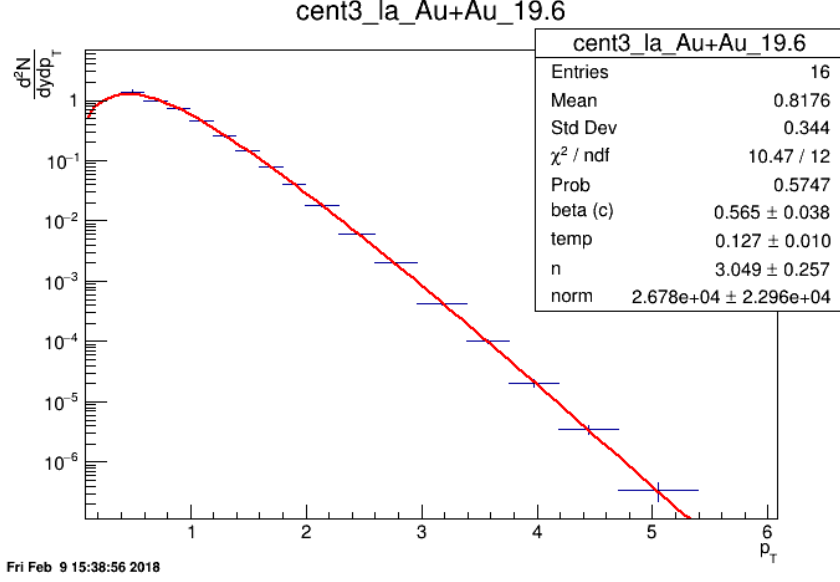


**Figure 5.2:** Red curve shows the Boltzmann-Gibbs blast wave functional fit on the PRELIMINARY transverse momentum spectrum for lambda particles identified by the STAR detector for 19.6 GeV Au+Au collisions (10-15% central). Parameters extracted from the chi-square goodness-of-fit test, as well as other statistics, are shown in the box on the top right.

## 5.2 Calculations from the Spectral Fits

### 5.2.1 Calculation of $\frac{dE_T}{dy}$ , $\frac{dE_T}{d\eta}$ , $\frac{dN_{ch}}{dy}$ , and $\frac{dN_{ch}}{d\eta}$

### 5.2.2 Corrections for Unidentified Particles and Estimation of Total $E_T$

It is reasonable to assume that, at high energies, there should be roughly the same multiplicity of all the isospin states of a final state particle. Table 5.1 lists the isospin states associated with the pion, the kaon, the proton, and the lambda particles.

Particle	Isospin multiplets
pion	$\pi^+, \pi^0, \pi^-$
kaon	$K^+, K^0, K^-, \bar{K}^0$
proton	$p, n, \bar{p}, \bar{n}$
lambda	$\Lambda, \bar{\Lambda}$

**Table 5.1:** Isospin states of different identified particles.

615 .....text content.....

$$E_T = 3E_T^\pi + 4E_T^K + 4E_T^p + 2E_T^\Lambda \quad (5.2)$$

616 .....text content.....

### 617 **5.2.3 Lambdas Centralitiy Adjustments and $E_T$ Interpolations**

618 The centrality bins corresponding to the lambdas spectra were slightly different from those  
619 corresponding to the rest of the particles.....

## 620 **5.3 Uncertainties**

621 ..... 100% correlated point-to-point and uncorrelated between particles..... ?

## Chapter 6

## Results

Present results and comparisons to Adare et al....

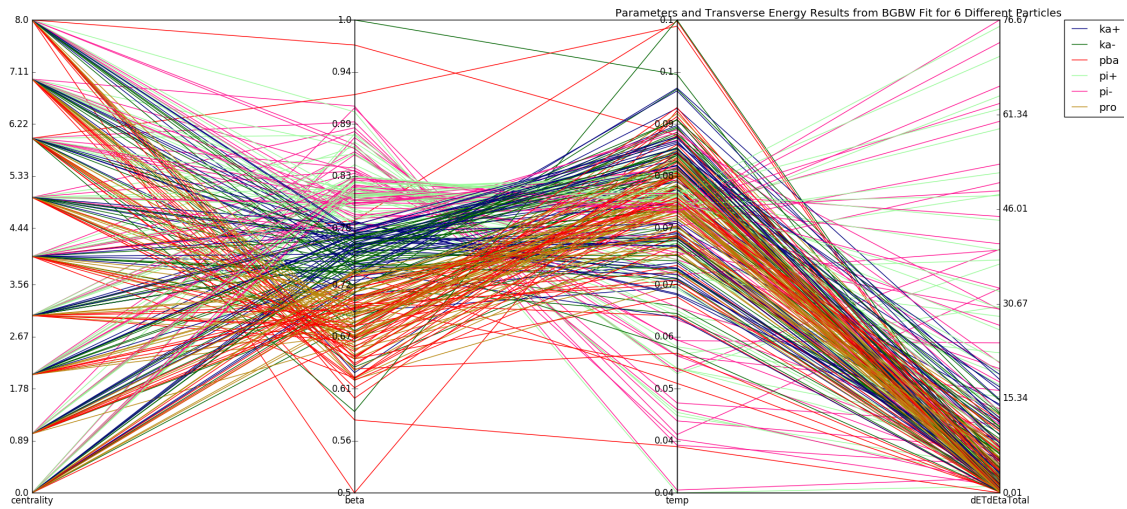


**Figure 6.1:** Parallel coordinates plot for 270 different spectra relating 6 different identified particles (color-coded) to their respective collision centrality classes, good-fit parameters, and the transverse energy calculated using said parameters.



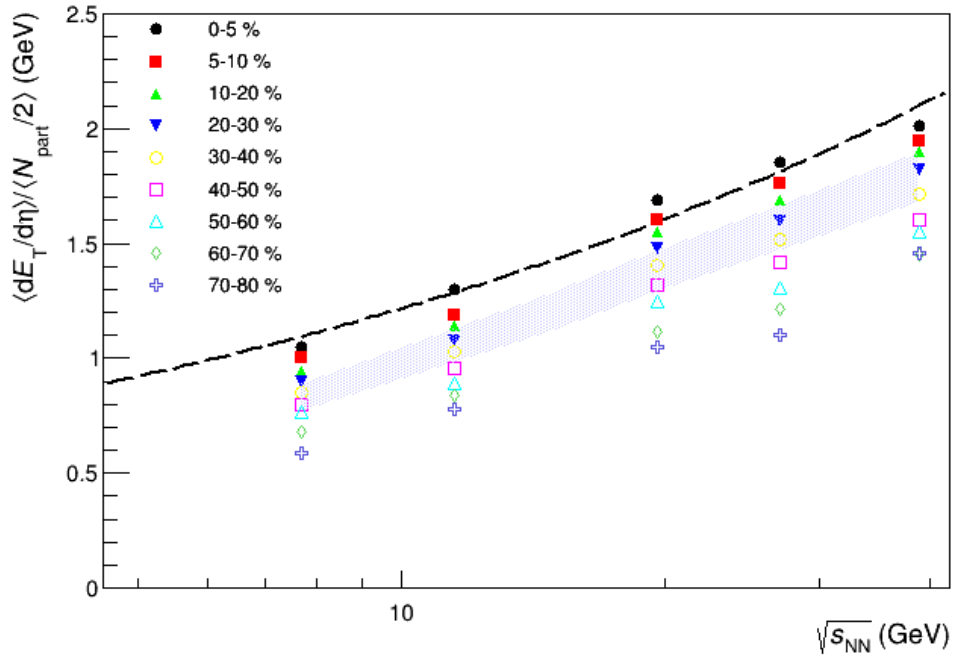


**Figure 6.2:**  $(dE_T/d\eta)/0.5N_{part}$  at midrapidity as a function of  $\sqrt{s_{NN}}$  for different centralities. The dashed line represents a power-law fit to the 0-5% central data in the form  $y = ax^{2b}$ , where  $x$  and  $y$  are the placeholders for the quantities in the plot axes.  $\chi^2/n.d.f$  for the fit was 1.806, and the good-fit parameters were  $a = 0.4838 \pm 0.0429$  and  $b = 0.2005 \pm 0.01466$ . The shaded area represents the uncertainty bounds for the 0-5% central PHENIX data from [3].

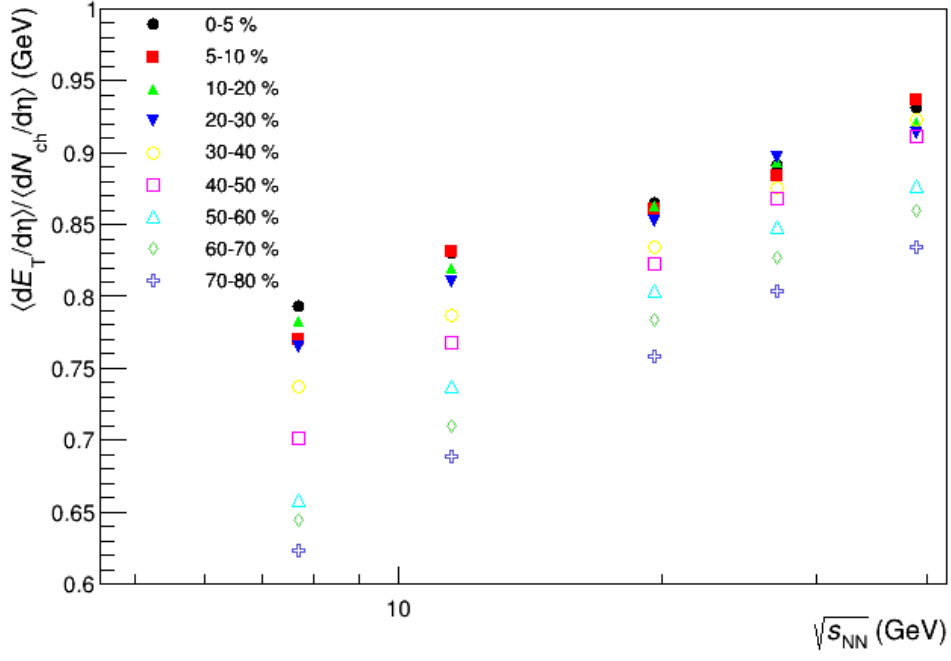


**Figure 6.3:**  $\langle dE_T/d\eta \rangle / \langle dN_{ch}/d\eta \rangle$  at midrapidity as a function of  $\sqrt{s_{NN}}$  for different centralities.

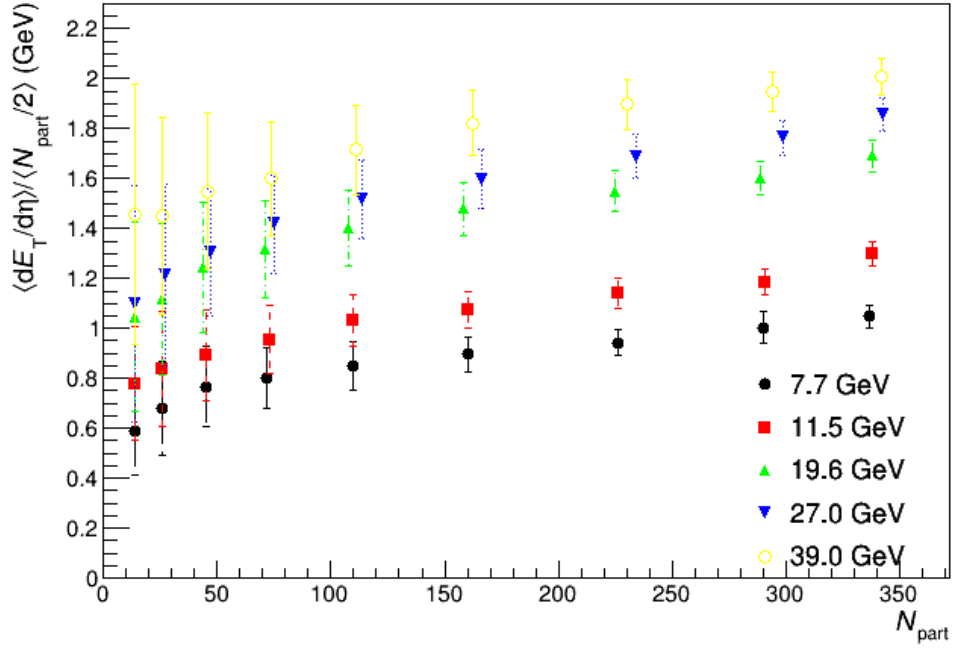


**Figure 6.4:**  $\langle dE_T/d\eta \rangle / 0.5N_{part}$  at midrapidity as a function of  $N_{part}$  for different collision energies.

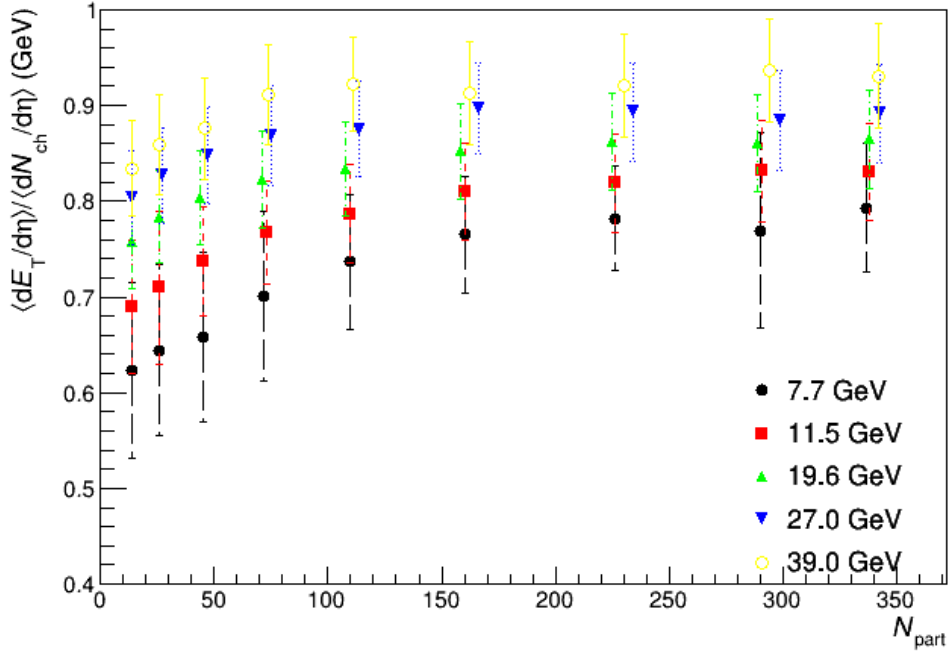


**Figure 6.5:**  $\langle dE_T/d\eta \rangle / \langle dN_{ch}/d\eta \rangle$  at midrapidity as a function of  $N_{part}$  for different collision energies.

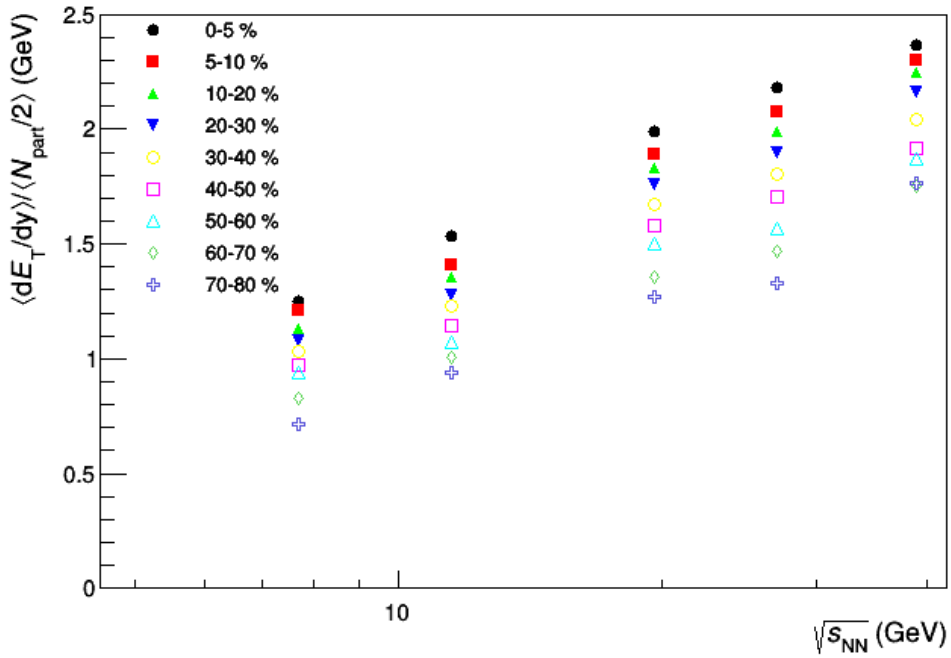


**Figure 6.6:**  $\langle dE_T/dy \rangle / 0.5N_{part}$  at midrapidity as a function of  $\sqrt{s_{NN}}$  for different centralities.

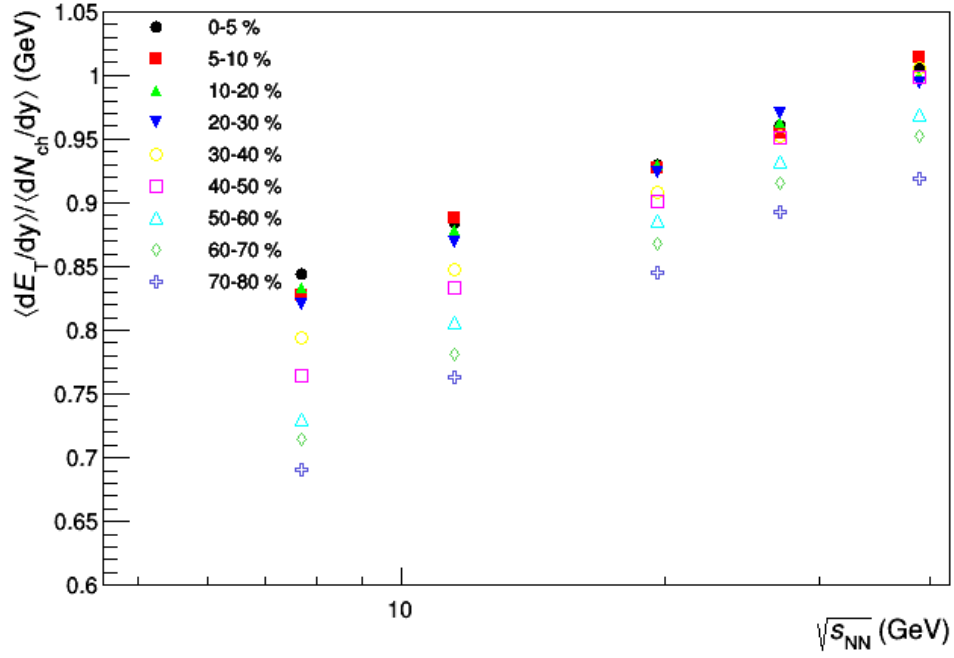


**Figure 6.7:**  $\langle dE_T/dy \rangle / \langle dN_{ch}/dy \rangle$  at midrapidity as a function of  $\sqrt{s_{NN}}$  for different centralities.

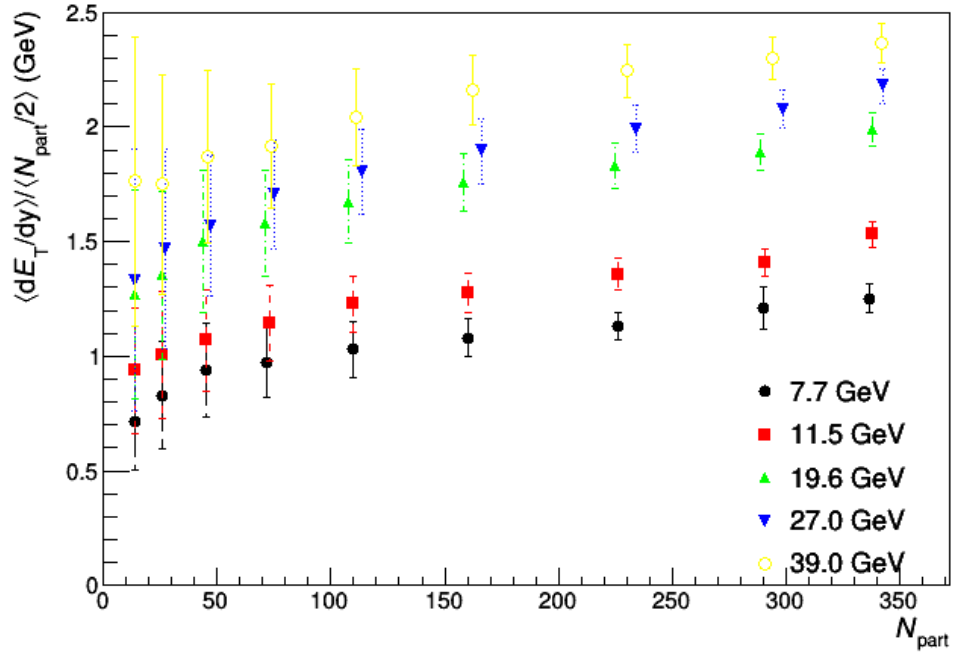


**Figure 6.8:**  $\langle dE_T/dy \rangle / 0.5N_{part}$  at midrapidity as a function of  $N_{part}$  for different collision energies.

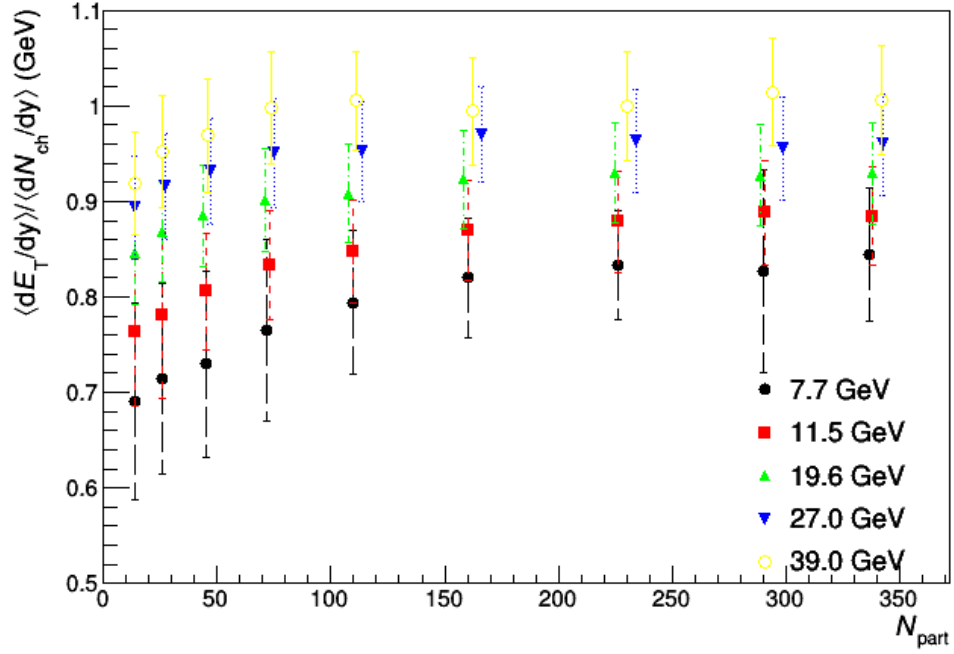


**Figure 6.9:**  $\langle dE_T/dy \rangle / \langle dN_{ch}/dy \rangle$  at midrapidity as a function of  $N_{part}$  for different collision energies.

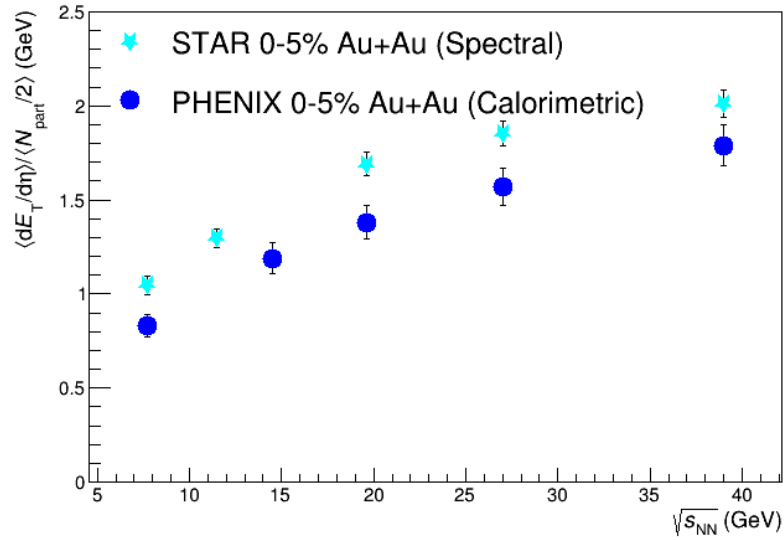


**Figure 6.10:**  $\frac{dE_T}{d\eta} / 0.5N_{part}$  for 0-5% central collisions at midrapidity as a function of  $\sqrt{s_{NN}}$ . The PHENIX data are from [3]. The error bars represent the total statistical and systematic uncertainties.

## 625 **Chapter 7**

## 626 **Conclusion**

627 Summary and implications

## Chapter 8

## Future Work

### 8.1 Goodness of Fit

A maximum likelihood? fit method can be adopted to compare the results with those using the chi-squared fits.

### 8.2 Bjorken Energy Density Estimate

Apart from the transverse energy, the calculation of the initial energy density,  $\epsilon$ , as given by the Bjorken formula in eq. 3.2, requires the estimate of other physical quantities. Adare et al.[3] use the Glauber model to determine  $A_T$ , the area of the intersection of the two nuclei in the transverse plane. Since the results in this thesis are cross-checked with those in [3], it would be reasonable to use the same model in the future work pertaining to this thesis.  $\tau_0$ , the proper time at the moment of QGP equilibration, also depends on the model of the collision. However, the product of  $\epsilon$  and  $\tau_0$  is often used instead of just  $\epsilon$  to study how the energy density scales with the collision energy and the number of participants.

## 642 **8.3 Asymmetric beams**

643 The codes in the repository can be used to analyze more data. In fact, since there is more  
644 data available on collisions of asymmetric systems such as d+Au?, we can expect it to be a  
645 test to tell if the assumptions? used in this analysis scale to such domains?



# Bibliography

647 [1] Adam, J., Adamova, D., Aggarwal, M. M., Aglieri Rinella, G., Agnello, M., Agrawal,  
 648 N., Ahammed, Z., Ahmad, S., Ahn, S. U., Aiola, S., Akindinov, A., Alam, S. N., Silva  
 649 De Albuquerque, D., Aleksandrov, D., Alessandro, B., Alexandre, D., Alfaro Molina,  
 650 J. R., Alici, A., Alkin, A., Millan Almaraz, J. R., Alme, J., Alt, T., Altinpinar, S.,  
 651 Altsybeev, I., Alves Garcia Prado, C., Andrei, C., Andronic, A., Anguelov, V., Anticic,  
 652 T., Antinori, F., Antonioli, P., Aphecetche, L. B., Appelshaeuser, H., Arcelli, S., Arnaldi,  
 653 R., Arnold, O. W., Arsene, I. C., Arslanok, M., Audurier, B., Augustinus, A., Averbek,  
 654 R. P., Azmi, M. D., Badala, A., Baek, Y. W., Bagnasco, S., Bailhache, R. M., Bala,  
 655 R., Balasubramanian, S., Baldisseri, A., Baral, R. C., Barbano, A. M., Barbera, R.,  
 656 Barile, F., Barnafoldi, G. G., Barnby, L. S., Ramillien Barret, V., Bartalini, P., Barth,  
 657 K., Bartke, J. G., Bartsch, E., Basile, M., Bastid, N., Basu, S., Bathen, B., Batigne,  
 658 G., Batista Camejo, A., Batyunya, B., Batzing, P. C., Bearden, I. G., Beck, H., Bedda,  
 659 C., Behera, N. K., Belikov, I., Bellini, F., Bello Martinez, H., Bellwied, R., Belmont Iii,  
 660 R. J., Belmont Moreno, E., Belyaev, V., Bencedi, G., Beole, S., Berceanu, I., Bercuci, A.,  
 661 Berdnikov, Y., Berenyi, D., Bertens, R. A., Berzano, D., Betev, L., Bhasin, A., Bhat, I. R.,  
 662 Bhati, A. K., Bhattacharjee, B., Bhom, J., Bianchi, L., Bianchi, N., Bianchin, C., Bielcik,  
 663 J., Bielcikova, J., Bilandzic, A., Biro, G., Biswas, R., Biswas, S., Bjelogrljic, S., Blair, J. T.,  
 664 Blau, D., Blume, C., Bock, F., Bogdanov, A., Boggild, H., Boldizar, L., Bombara, M.,  
 665 Book, J. H., Borel, H., Borissov, A., Borri, M., Bossu, F., Botta, E., Bourjau, C., Braun-  
 666 Munzinger, P., Bregant, M., Breitner, T. G., Broker, T. A., Browning, T. A., Broz, M.,  
 667 Brucken, E. J., Bruna, E., Bruno, G. E., Budnikov, D., Buesching, H., Bufalino, S., Buncic,  
 668 P., Busch, O., Buthelezi, E. Z., Bashir Butt, J., Buxton, J. T., Cabala, J., Caffarri, D.,  
 669 Cai, X., Caines, H. L., Calero Diaz, L., Caliva, A., Calvo Villar, E., Camerini, P., Carena,  
 670 F., Carena, W., Carnesecchi, F., Castillo Castellanos, J. E., Castro, A. J., Casula, E.  
 671 A. R., Ceballos Sanchez, C., Cepila, J., Cerello, P., Cerkala, J., Chang, B., Chapeland,  
 672 S., Chartier, M., Charvet, J.-L. F., Chattopadhyay, S., Chattopadhyay, S., Chauvin, A.,  
 673 Chelnokov, V., Cherney, M. G., Cheshkov, C. V., Cheynis, B., Chibante Barroso, V. M.,  
 674 Dobrigkeit Chinellato, D., Cho, S., Chochula, P., Choi, K., Chojnacki, M., Choudhury, S.,  
 675 Christakoglou, P., Christensen, C. H., Christiansen, P., Chujo, T., Chung, S.-U., Cicalo,  
 676 C., Cifarelli, L., Cindolo, F., Cleymans, J. W. A., Colamaria, F. F., Colella, D., Collu, A.,

677 Colocci, M., Conesa Balbastre, G., Conesa Del Valle, Z., Connors, M. E., Contreras Nuno,  
 678 J. G., Cormier, T. M., Corrales Morales, Y., Cortes Maldonado, I., Cortese, P., Cosentino,  
 679 M. R., Costa, F., Crochet, P., Cruz Albino, R., Cuautle Flores, E., Cunqueiro Mendez,  
 680 L., Dahms, T., Dainese, A., Danisch, M. C., Danu, A., Das, D., Das, I., Das, S., Dash,  
 681 A. K., Dash, S., De, S., De Caro, A., De Cataldo, G., De Conti, C., De Cuveland, J.,  
 682 De Falco, A., De Gruttola, D., De Marco, N., De Pasquale, S., Deisting, A., Deloff,  
 683 A., Denes, E. S., Deplano, C., Dhankher, P., Di Bari, D., Di Mauro, A., Di Nezza,  
 684 P., Diaz Corchero, M. A., Dietel, T., Dillenseger, P., Divia, R., Djuvsland, O., Dobrin,  
 685 A. F., Domenicis Gimenez, D., Donigus, B., Dordic, O., Drozhzhova, T., Dubey, A. K.,  
 686 Dubla, A., Ducroux, L., Dupieux, P., Ehlers Iii, R. J., Elia, D., Endress, E., Engel, H.,  
 687 Epple, E., Erasmus, B. E., Erdemir, I., Erhardt, F., Espagnon, B., Estienne, M. D.,  
 688 Esumi, S., Eum, J., Evans, D., Evdokimov, S., Eyyubova, G., Fabbietti, L., Fabris, D.,  
 689 Faivre, J., Fantoni, A., Fasel, M., Feldkamp, L., Feliciello, A., Feofilov, G., Ferencei, J.,  
 690 Fernandez Tellez, A., Gonzalez Ferreiro, E., Ferretti, A., Festanti, A., Feuillard, V. J. G.,  
 691 Figiel, J., Araujo Silva Figueredo, M., Filchagin, S., Finogeev, D., Fionda, F., Fiore, E. M.,  
 692 Fleck, M. G., Floris, M., Foertsch, S. V., Foka, P., Fokin, S., Fragiacomio, E., Francescon,  
 693 A., Frankenfeld, U. M., Fronze, G. G., Fuchs, U., Furget, C., Furs, A., Fusco Girard, M.,  
 694 Gaardhoeje, J. J., Gagliardi, M., Gago Medina, A. M., Gallio, M., Gangadharan, D. R.,  
 695 Ganoti, P., Gao, C., Garabatos Cuadrado, J., Garcia-Solis, E. J., Gargiulo, C., Gasik, P. J.,  
 696 Gauger, E. F., Germain, M., Gheata, M., Ghosh, P., Ghosh, S. K., Gianotti, P., Giubellino,  
 697 P., Giubilato, P., Gladysz-Dziadus, E., Glassel, P., Gomez Coral, D. M., Gomez Ramirez,  
 698 A., Sanchez Gonzalez, A., Gonzalez, V., Gonzalez Zamora, P., Gorbunov, S., Gorlich,  
 699 L. M., Gotovac, S., Grabski, V., Grachov, O. A., Graczykowski, L. K., Graham, K. L.,  
 700 Grelli, A., Grigoras, A. G., Grigoras, C., Grigoryev, V., Grigoryan, A., Grigoryan, S.,  
 701 Grynyov, B., Grion, N., Gronefeld, J. M., Grosse-Oetringhaus, J. F., Grosso, R., Guber,  
 702 F., Guernane, R., Guerzoni, B., Gulbrandsen, K. H., Gunji, T., Gupta, A., Gupta, R.,  
 703 Haake, R., Haaland, O. S., Hadjidakis, C. M., Haiduc, M., Hamagaki, H., Hamar, G.,  
 704 Hamon, J. C., Harris, J. W., Harton, A. V., Hatzifotiadou, D., Hayashi, S., Heckel, S. T.,  
 705 Hellbar, E., Helstrup, H., Herghelegiu, A. I., Herrera Corral, G. A., Hess, B. A., Hetland,  
 706 K. F., Hillemanns, H., Hippolyte, B., Horak, D., Hosokawa, R., Hristov, P. Z., Humanic,

707 T., Hussain, N., Hussain, T., Hutter, D., Hwang, D. S., Ilkaev, R., Inaba, M., Incani,  
 708 E., Ippolitov, M., Irfan, M., Ivanov, M., Ivanov, V., Izucheev, V., Jacazio, N., Jacobs,  
 709 P. M., Jadhav, M. B., Jadlovská, S., Jadlovsky, J., Jahnke, C., Jakubowska, M. J., Jang,  
 710 H. J., Janik, M. A., Pahula Hewage, S., Jena, C., Jena, S., Jimenez Bustamante, R. T.,  
 711 Jones, P. G., Jusko, A., Kalinak, P., Kalweit, A. P., Kamin, J. A., Kang, J. H., Kaplin,  
 712 V., Kar, S., Karasu Uysal, A., Karavichev, O., Karavicheva, T., Karayan, L., Karpechev,  
 713 E., Kebschull, U. W., Keidel, R., Keijndener, D. L., Keil, M., Khan, M. M., Khan, P.,  
 714 Khan, S. A., Khanzadeev, A., Kharlov, Y., Kileng, B., Kim, D. W., Kim, D. J., Kim,  
 715 D., Kim, H., Kim, J., Kim, M., Kim, S. Y., Kim, T., Kirsch, S., Kisel, I., Kiselev,  
 716 S., Kisiel, A. R., Kiss, G., Klay, J. L., Klein, C., Klein, J., Klein-Boesing, C., Klewin,  
 717 S., Kluge, A., Knichel, M. L., Knospe, A. G., Kobdaj, C., Kofarago, M., Kollegger, T.,  
 718 Kolozhvari, A., Kondratev, V., Kondratyeva, N., Kondratyuk, E., Konevskikh, A., Kopcik,  
 719 M., Kostarakis, P., Kour, M., Kouzinopoulos, C., Kovalenko, O., Kovalenko, V., Kowalski,  
 720 M., Koyithatta Meethalevedu, G., Kralik, I., Kravcakova, A., Krivda, M., Krizek, F.,  
 721 Kryshen, E., Krzewicki, M., Kubera, A. M., Kucera, V., Kuhn, C. C., Kuijer, P. G.,  
 722 Kumar, A., Kumar, J., Kumar, L., Kumar, S., Kurashvili, P., Kurepin, A., Kurepin, A.,  
 723 Kuryakin, A., Kweon, M. J., Kwon, Y., La Pointe, S. L., La Rocca, P., Ladron De Guevara,  
 724 P., Lagana Fernandes, C., Lakomov, I., Langoy, R., Lapidus, K., Lara Martinez, C. E.,  
 725 Lardeux, A. X., Lattuca, A., Laudi, E., Lea, R., Leardini, L., Lee, G. R., Lee, S., Lehas, F.,  
 726 Lemmon, R. C., Lenti, V., Leogrande, E., Leon Monzon, I., Leon Vargas, H., Leoncino, M.,  
 727 Levai, P., Li, S., Li, X., Lien, J. A., Lietava, R., Lindal, S., Lindenstruth, V., Lippmann,  
 728 C., Lisa, M. A., Ljunggren, H. M., Lodato, D. F., Lonne, P.-I., Loginov, V., Loizides, C.,  
 729 Lopez, X. B., Lopez Torres, E., Lowe, A. J., Luettig, P. J., Lunardon, M., Luparello,  
 730 G., Lutz, T. H., Maevskaya, A., Mager, M., Mahajan, S., Mahmood, S. M., Maire,  
 731 A., Majka, R. D., Malaev, M., Maldonado Cervantes, I. A., Malinina, L., Mal'Kevich,  
 732 D., Malzacher, P., Mamonov, A., Manko, V., Manso, F., Manzari, V., Marchisone, M.,  
 733 Mares, J., Margagliotti, G. V., Margotti, A., Margutti, J., Marin, A. M., Markert, C.,  
 734 Marquard, M., Martin, N. A., Martin Blanco, J., Martinengo, P., Martinez Hernandez,  
 735 M. I., Martinez-Garcia, G., Martinez Pedreira, M., Mas, A. J.-M., Masciocchi, S., Masera,  
 736 M., Masoni, A., Mastroserio, A., Matyja, A. T., Mayer, C., Mazer, J. A., Mazzoni,

737 A. M., Mcdonald, D., Meddi, F., Melikyan, Y., Menchaca-Rocha, A. A., Meninno, E.,  
 738 Mercado-Perez, J., Meres, M., Miake, Y., Mieskolainen, M. M., Mikhaylov, K., Milano,  
 739 L., Milosevic, J., Mischke, A., Mishra, A. N., Miskowiec, D. C., Mitra, J., Mitu, C. M.,  
 740 Mohammadi, N., Mohanty, B., Molnar, L., Montano Zetina, L. M., Montes Prado, E.,  
 741 Moreira De Godoy, D. A., Perez Moreno, L. A., Moretto, S., Morreale, A., Morsch, A.,  
 742 Muccifora, V., Mudnic, E., Muhlheim, D. M., Muhuri, S., Mukherjee, M., Mulligan, J. D.,  
 743 Gameiro Munhoz, M., Munzer, R. H., Murakami, H., Murray, S., Musa, L., Musinsky,  
 744 J., Naik, B., Nair, R., Nandi, B. K., Nania, R., Nappi, E., Naru, M. U., Ferreira Natal  
 745 Da Luz, P. H., Nattrass, C., Rosado Navarro, S., Nayak, K., Nayak, R., Nayak, T. K.,  
 746 Nazarenko, S., Nedosekin, A., Nellen, L., Ng, F., Nicassio, M., Niculescu, M., Niedziela,  
 747 J., Nielsen, B. S., Nikolaev, S., Nikulin, S., Nikulin, V., Noferini, F., Nomokonov, P.,  
 748 Nooren, G., Cabanillas Noris, J. C., Norman, J., Nyanin, A., Nystrand, J. I., Oeschler,  
 749 H. O., Oh, S., Oh, S. K., Ohlson, A. E., Okatan, A., Okubo, T., Olah, L., Oleniacz,  
 750 J., Oliveira Da Silva, A. C., Oliver, M. H., Onderwaater, J., Oppedisano, C., Orava, R.,  
 751 Oravec, M., Ortiz Velasquez, A., Oskarsson, A. N. E., Otwinowski, J. T., Oyama, K.,  
 752 Ozdemir, M., Pachmayer, Y. C., Pagano, D., Pagano, P., Paic, G., Pal, S. K., Pan, J.,  
 753 Pandey, A. K., Papikyan, V., Pappalardo, G., Pareek, P., Park, W., Parmar, S., Passfeld,  
 754 A., Paticchio, V., Patra, R. N., Paul, B., Pei, H., Peitzmann, T., Pereira Da Costa, H.  
 755 D. A., Peresunko, D. Y., Perez Lara, C. E., Perez Lezama, E., Peskov, V., Pestov, Y.,  
 756 Petracek, V., Petrov, V., Petrovici, M., Petta, C., Piano, S., Pikna, M., Pillot, P., Ozelin  
 757 De Lima Pimentel, L., Pinazza, O., Pinsky, L., Piyaathana, D., Ploskon, M. A., Planinic,  
 758 M., Pluta, J. M., Pochybova, S., Podesta Lerma, P. L. M., Poghosyan, M., Polishchuk,  
 759 B., Poljak, N., Poonsawat, W., Pop, A., Porteboeuf, S. J., Porter, R. J., Pospisil, J.,  
 760 Prasad, S. K., Preghenella, R., Prino, F., Pruneau, C. A., Pshenichnov, I., Puccio, M.,  
 761 Puddu, G., Pujahari, P. R., Punin, V., Putschke, J. H., Qvigstad, H., Rachevski, A., Raha,  
 762 S., Rajput, S., Rak, J., Rakotozafindrabe, A. M., Ramello, L., Rami, F., Raniwala, R.,  
 763 Raniwala, S., Rasanen, S. S., Rascanu, B. T., Rathee, D., Read, K. F., Redlich, K., Reed,  
 764 R. J., Rehman, A. U., Reichelt, P. S., Reidt, F., Ren, X., Renfordt, R. A. E., Reolon, A. R.,  
 765 Reshetin, A., Reygers, K. J., Riabov, V., Ricci, R. A., Richert, T. O. H., Richter, M. R.,  
 766 Riedler, P., Riegler, W., Riggi, F., Ristea, C.-L., Rocco, E., Rodriguez Cahuantzi, M.,

767 Rodriguez Manso, A., Roeed, K., Rogochaya, E., Rohr, D. M., Roehrich, D., Ronchetti,  
 768 F., Ronflette, L., Rosnet, P., Rossi, A., Roukoutakis, F., Roy, A., Roy, C. S., Roy, P. K.,  
 769 Rubio Montero, A. J., Rui, R., Russo, R., Di Ruzza, B., Ryabinkin, E., Ryabov, Y.,  
 770 Rybicki, A., Saarinen, S., Sadhu, S., Sadovskiy, S., Safarik, K., Sahlmuller, B., Sahoo, P.,  
 771 Sahoo, R., Sahoo, S., Sahu, P. K., Saini, J., Sakai, S., Saleh, M. A., Salzwedel, J. S. N.,  
 772 Sambyal, S. S., Samsonov, V., Sandor, L., Sandoval, A., Sano, M., Sarkar, D., Sarkar, N.,  
 773 Sarma, P., Scapparone, E., Scarlassara, F., Schiaua, C. C., Schicker, R. M., Schmidt, C. J.,  
 774 Schmidt, H. R., Schuchmann, S., Schukraft, J., Schulc, M., Schutz, Y. R., Schwarz, K. E.,  
 775 Schweda, K. O., Scioli, G., Scomparin, E., Scott, R. M., Sefcik, M., Seger, J. E., Sekiguchi,  
 776 Y., Sekihata, D., Selyuzhenkov, I., Senosi, K., Senyukov, S., Serradilla Rodriguez, E.,  
 777 Sevcenco, A., Shabanov, A., Shabetai, A., Shadura, O., Shahoyan, R., Shahzad, M. I.,  
 778 Shangaraev, A., Sharma, A., Sharma, M., Sharma, M., Sharma, N., Sheikh, A. I., Shigaki,  
 779 K., Shou, Q., Shtejer Diaz, K., Sibiryak, Y., Siddhanta, S., Sielewicz, K. M., Siemiarczuk,  
 780 T., Silvermyr, D. O. R., Silvestre, C. M., Simatovic, G., Simonetti, G., Singaraju, R. N.,  
 781 Singh, R., Singha, S., Singhal, V., Sinha, B., Sarkar Sinha, T., Sitar, B., Sitta, M., Skaali,  
 782 B., Slupecki, M., Smirnov, N., Snellings, R., Snellman, T. W., Song, J., Song, M., Song,  
 783 Z., Soramel, F., Sorensen, S. P., Derradi De Souza, R., Sozzi, F., Spacek, M., Spiriti, E.,  
 784 Sputowska, I. A., Spyropoulou-Stassinaki, M., Stachel, J., Stan, I., Stankus, P., Stenlund,  
 785 E. A., Steyn, G. F., Stiller, J. H., Stocco, D., Strmen, P., Alarcon Do Passo Suaide, A.,  
 786 Sugitate, T., Suire, C. P., Suleymanov, M. K. O., Suljic, M., Sultanov, R., Sumbera,  
 787 M., Sumowidagdo, S., Szabo, A., Szanto De Toledo, A., Szarka, I., Szczepankiewicz, A.,  
 788 Szymanski, M. P., Tabassam, U., Takahashi, J., Tambave, G. J., Tanaka, N., Tarhini,  
 789 M., Tariq, M., Tarzila, M.-G., Tauro, A., Tejeda Munoz, G., Telesca, A., Terasaki, K.,  
 790 Terrevoli, C., Teyssier, B., Thaeder, J. M., Thakur, D., Thomas, D., Tieulent, R. N.,  
 791 Tikhonov, A., Timmins, A. R., Toia, A., Trogolo, S., Trombetta, G., Trubnikov, V.,  
 792 Trzaska, W. H., Tsuji, T., Tumkin, A., Turrisi, R., Tveter, T. S., Ullaland, K., Uras, A.,  
 793 Usai, G., Utrobicic, A., Vala, M., Valencia Palomo, L., Vallero, S., Van Der Maarel, J.,  
 794 Van Hoorne, J. W., Van Leeuwen, M., Vanat, T., Vande Vyvre, P., Varga, D., Diozcora  
 795 Vargas Trevino, A., Vargyas, M., Varma, R., Vasileiou, M., Vasiliev, A., Vauthier, A.,  
 796 Vazquez Doce, O., Vechernin, V., Veen, A. M., Veldhoen, M., Velure, A., Vercellin, E.,

Vergara Limon, S., Vernet, R., Verweij, M., Vickovic, L., Viinikainen, J. S., Vilakazi, Z., Villalobos Baillie, O., Villatoro Tello, A., Vinogradov, A., Vinogradov, L., Vinogradov, Y., Virgili, T., Vislavicius, V., Viyogi, Y., Vodopyanov, A., Volkl, M. A., Voloshin, K., Voloshin, S., Volpe, G., Von Haller, B., Vorobyev, I., Vranic, D., Vrlakova, J., Vulpescu, B., Wagner, B., Wagner, J., Wang, H., Wang, M., Watanabe, D., Watanabe, Y., Weber, M., Weber, S. G., Weiser, D. F., Wessels, J. P., Westerhoff, U., Whitehead, A. M., Wiechula, J., Wikne, J., Wilk, G. A., Wilkinson, J. J., Williams, C., Windelband, B. S., Winn, M. A., Yang, P., Yano, S., Yasin, Z., Yin, Z., Yokoyama, H., Yoo, I.-K., Yoon, J. H., Yurchenko, V., Yushmanov, I., Zaborowska, A., Zaccolo, V., Zaman, A., Zampolli, C., Correia Zanolini, H. J., Zaporozhets, S., Zardoshti, N., Zarochentsev, A., Zavada, P., Zavyalov, N., Zbroszczyk, H. P., Zgura, S. I., Zhalov, M., Zhang, H., Zhang, X., Zhang, Y., Chunchui, Z., Zhang, Z., Zhao, C., Zhigareva, N., Zhou, D., Zhou, Y., Zhou, Z., Zhu, H., Zhu, J., Zichichi, A., Zimmermann, A., Zimmermann, M. B., Zinovjev, G., and Zyzak, M. (2016). Measurement of transverse energy at midrapidity in Pb-Pb collisions at  $\sqrt{s_{NN}} = 2.76$  TeV. *Phys. Rev. C*, 94(CERN-EP-2016-071. CERN-EP-2016-071):034903. 30 p. 30 pages, 14 captioned figures, 2 tables, authors from page 25, published version, figures at <http://aliceinfo.cern.ch/ArtSubmission/node/2400>. 6, 14

[2] Adamczyk, L., Adkins, J. K., Agakishiev, G., Aggarwal, M. M., Ahammed, Z., Ajitanand, N. N., Alekseev, I., Anderson, D. M., Aoyama, R., Aparin, A., Arkhipkin, D., Aschenauer, E. C., Ashraf, M. U., Attri, A., Averichev, G. S., Bai, X., Bairathi, V., Behera, A., Bellwied, R., Bhasin, A., Bhati, A. K., Bhattarai, P., Bielcik, J., Bielcikova, J., Bland, L. C., Bordyuzhin, I. G., Bouchet, J., Brandenburg, J. D., Brandin, A. V., Brown, D., Bunzarov, I., Butterworth, J., Caines, H., Calderón de la Barca Sánchez, M., Campbell, J. M., Cebra, D., Chakaberia, I., Chaloupka, P., Chang, Z., Chankova-Bunzarova, N., Chatterjee, A., Chattopadhyay, S., Chen, X., Chen, J. H., Chen, X., Cheng, J., Cherney, M., Christie, W., Contin, G., Crawford, H. J., Das, S., De Silva, L. C., Debbe, R. R., Dedovich, T. G., Deng, J., Derevschikov, A. A., Didenko, L., Dilks, C., Dong, X., Drachenberg, J. L., Draper, J. E., Dunkelberger, L. E., Dunlop, J. C., Efimov, L. G., Elsey, N., Engelage, J., Eppley, G., Esha, R., Esumi, S., Evdokimov, O., Ewigleben,

826 J., Eyser, O., Fatemi, R., Fazio, S., Federic, P., Federicova, P., Fedorisin, J., Feng, Z.,  
 827 Filip, P., Finch, E., Fisyak, Y., Flores, C. E., Fulek, L., Gagliardi, C. A., Garand, D.,  
 828 Geurts, F., Gibson, A., Girard, M., Grosnick, D., Gunarathne, D. S., Guo, Y., Gupta, A.,  
 829 Gupta, S., Guryn, W., Hamad, A. I., Hamed, A., Harlenderova, A., Harris, J. W., He, L.,  
 830 Heppelmann, S., Heppelmann, S., Hirsch, A., Hoffmann, G. W., Horvat, S., Huang, T.,  
 831 Huang, B., Huang, X., Huang, H. Z., Humanic, T. J., Huo, P., Igo, G., Jacobs, W. W.,  
 832 Jentsch, A., Jia, J., Jiang, K., Jowzaee, S., Judd, E. G., Kabana, S., Kalinkin, D., Kang,  
 833 K., Kauder, K., Ke, H. W., Keane, D., Kechechyan, A., Khan, Z., Kikoła, D. P., Kisel,  
 834 I., Kisiel, A., Kochenda, L., Kocmanek, M., Kollegger, T., Kosarzewski, L. K., Kraishan,  
 835 A. F., Kravtsov, P., Krueger, K., Kulathunga, N., Kumar, L., Kvapil, J., Kwasizur, J. H.,  
 836 Lacey, R., Landgraf, J. M., Landry, K. D., Lauret, J., Lebedev, A., Lednický, R., Lee,  
 837 J. H., Li, X., Li, C., Li, W., Li, Y., Lidrych, J., Lin, T., Lisa, M. A., Liu, H., Liu,  
 838 P., Liu, Y., Liu, F., Ljubicic, T., Llope, W. J., Lomnitz, M., Longacre, R. S., Luo, S.,  
 839 Luo, X., Ma, G. L., Ma, L., Ma, Y. G., Ma, R., Magdy, N., Majka, R., Mallick, D.,  
 840 Margetis, S., Markert, C., Matis, H. S., Meehan, K., Mei, J. C., Miller, Z. W., Minaev,  
 841 N. G., Mioduszewski, S., Mishra, D., Mizuno, S., Mohanty, B., Mondal, M. M., Morozov,  
 842 D. A., Mustafa, M. K., Nasim, M., Nayak, T. K., Nelson, J. M., Nie, M., Nigmatkulov,  
 843 G., Niida, T., Nogach, L. V., Nonaka, T., Nurushev, S. B., Odyniec, G., Ogawa, A.,  
 844 Oh, K., Okorokov, V. A., Olvitt, D., Page, B. S., Pak, R., Pandit, Y., Panebratsev, Y.,  
 845 Pawlik, B., Pei, H., Perkins, C., Pile, P., Pluta, J., Poniatowska, K., Porter, J., Posik,  
 846 M., Poskanzer, A. M., Pruthi, N. K., Przybycien, M., Putschke, J., Qiu, H., Quintero, A.,  
 847 Ramachandran, S., Ray, R. L., Reed, R., Rehbein, M. J., Ritter, H. G., Roberts, J. B.,  
 848 Rogachevskiy, O. V., Romero, J. L., Roth, J. D., Ruan, L., Rusnak, J., Rusnakova, O.,  
 849 Sahoo, N. R., Sahu, P. K., Salur, S., Sandweiss, J., Saur, M., Schambach, J., Schmäh,  
 850 A. M., Schmidke, W. B., Schmitz, N., Schweid, B. R., Seger, J., Sergeeva, M., Seyboth, P.,  
 851 Shah, N., Shahaliev, E., Shanmuganathan, P. V., Shao, M., Sharma, A., Sharma, M. K.,  
 852 Shen, W. Q., Shi, Z., Shi, S. S., Shou, Q. Y., Sichtermann, E. P., Sikora, R., Simko,  
 853 M., Singha, S., Skoby, M. J., Smirnov, N., Smirnov, D., Solyst, W., Song, L., Sorensen,  
 854 P., Spinka, H. M., Srivastava, B., Stanislaus, T. D. S., Strikhanov, M., Stringfellow, B.,  
 855 Sugiura, T., Sumbera, M., Summa, B., Sun, Y., Sun, X. M., Sun, X., Surrow, B., Svirida,



D. N., Tang, A. H., Tang, Z., Taranenko, A., Tarnowsky, T., Tawfik, A., Thäder, J., Thomas, J. H., Timmins, A. R., Tlusty, D., Todoroki, T., Tokarev, M., Trentalange, S., Tribble, R. E., Tribedy, P., Tripathy, S. K., Trzeciak, B. A., Tsai, O. D., Ullrich, T., Underwood, D. G., Upsal, I., Van Buren, G., van Nieuwenhuizen, G., Vasiliev, A. N., Videbæk, F., Vokal, S., Voloshin, S. A., Vossen, A., Wang, G., Wang, Y., Wang, F., Wang, Y., Webb, J. C., Webb, G., Wen, L., Westfall, G. D., Wieman, H., Wissink, S. W., Witt, R., Wu, Y., Xiao, Z. G., Xie, W., Xie, G., Xu, J., Xu, N., Xu, Q. H., Xu, Y. F., Xu, Z., Yang, Y., Yang, Q., Yang, C., Yang, S., Ye, Z., Ye, Z., Yi, L., Yip, K., Yoo, I.-K., Yu, N., Zbroszczyk, H., Zha, W., Zhang, Z., Zhang, X. P., Zhang, J. B., Zhang, S., Zhang, J., Zhang, Y., Zhang, J., Zhang, S., Zhao, J., Zhong, C., Zhou, L., Zhou, C., Zhu, X., Zhu, Z., and Zyzak, M. (2017). Bulk properties of the medium produced in relativistic heavy-ion collisions from the beam energy scan program. *Phys. Rev. C*, 96:044904. vii, 23, 27, 28

[3] Adare, A., Afanasiev, S., Aidala, C., Ajitanand, N. N., Akiba, Y., Akimoto, R., Al-Bataineh, H., Alexander, J., Alfred, M., Al-Jamel, A., Al-Ta'ani, H., Angerami, A., Aoki, K., Apadula, N., Aphecetche, L., Aramaki, Y., Armendariz, R., Aronson, S. H., Asai, J., Asano, H., Aschenauer, E. C., Atomssa, E. T., Auerbeck, R., Awes, T. C., Azmoun, B., Babintsev, V., Bai, M., Bai, X., Baksay, G., Baksay, L., Baldisseri, A., Bandara, N. S., Bannier, B., Barish, K. N., Barnes, P. D., Bassalleck, B., Basye, A. T., Bathe, S., Batsouli, S., Baublis, V., Bauer, F., Baumann, C., Baumgart, S., Bazilevsky, A., Beaumier, M., Beckman, S., Belikov, S., Belmont, R., Bennett, R., Berdnikov, A., Berdnikov, Y., Bhom, J. H., Bickley, A. A., Bjorndal, M. T., Black, D., Blau, D. S., Boissevain, J. G., Bok, J. S., Borel, H., Boyle, K., Brooks, M. L., Brown, D. S., Bryslawskyj, J., Bucher, D., Buesching, H., Bumazhnov, V., Bunce, G., Burward-Hoy, J. M., Butsyk, S., Campbell, S., Caringi, A., Castera, P., Chai, J.-S., Chang, B. S., Charvet, J.-L., Chen, C.-H., Chernichenko, S., Chi, C. Y., Chiba, J., Chiu, M., Choi, I. J., Choi, J. B., Choi, S., Choudhury, R. K., Christiansen, P., Chujo, T., Chung, P., Churn, A., Chvala, O., Cianciolo, V., Citron, Z., Cleven, C. R., Cobigo, Y., Cole, B. A., Comets, M. P., Conesa del Valle, Z., Connors, M., Constantin, P., Cronin, N., Crossette, N., Csanád, M., Csörgő, T., Dahms,

885 T., Dairaku, S., Danchev, I., Danley, T. W., Das, K., Datta, A., Daugherty, M. S.,  
 886 David, G., Dayananda, M. K., Deaton, M. B., DeBlasio, K., Dehmelt, K., Delagrange,  
 887 H., Denisov, A., d'Enterria, D., Deshpande, A., Desmond, E. J., Dharmawardane, K. V.,  
 888 Dietzsch, O., Ding, L., Dion, A., Diss, P. B., Do, J. H., Donadelli, M., D'Orazio, L.,  
 889 Drachenberg, J. L., Drapier, O., Drees, A., Drees, K. A., Dubey, A. K., Durham, J. M.,  
 890 Durum, A., Dutta, D., Dzhordzhadze, V., Edwards, S., Efremenko, Y. V., Egdemir, J.,  
 891 Ellinghaus, F., Emam, W. S., Engelmores, T., Enokizono, A., En'yo, H., Espagnon, B.,  
 892 Esumi, S., Eyser, K. O., Fadem, B., Feege, N., Fields, D. E., Finger, M., Finger, M.,  
 893 Fleuret, F., Fokin, S. L., Forestier, B., Fraenkel, Z., Frantz, J. E., Franz, A., Frawley,  
 894 A. D., Fujiwara, K., Fukao, Y., Fung, S.-Y., Fusayasu, T., Gadrat, S., Gainey, K., Gal,  
 895 C., Gallus, P., Garg, P., Garishvili, A., Garishvili, I., Gastineau, F., Ge, H., Germain, M.,  
 896 Giordano, F., Glenn, A., Gong, H., Gong, X., Gonin, M., Gosset, J., Goto, Y., Granier de  
 897 Cassagnac, R., Grau, N., Greene, S. V., Grim, G., Grosse Perdekamp, M., Gu, Y., Gunji,  
 898 T., Guo, L., Guragain, H., Gustafsson, H.-A., Hachiya, T., Hadj Henni, A., Haegemann,  
 899 C., Haggerty, J. S., Hagiwara, M. N., Hahn, K. I., Hamagaki, H., Hamblen, J., Hamilton,  
 900 H. F., Han, R., Han, S. Y., Hanks, J., Harada, H., Hartouni, E. P., Haruna, K., Harvey,  
 901 M., Hasegawa, S., Haseler, T. O. S., Hashimoto, K., Haslum, E., Hasuko, K., Hayano, R.,  
 902 Hayashi, S., He, X., Heffner, M., Hemmick, T. K., Hester, T., Heuser, J. M., Hiejima, H.,  
 903 Hill, J. C., Hobbs, R., Hohlmann, M., Hollis, R. S., Holmes, M., Holzmann, W., Homma,  
 904 K., Hong, B., Horaguchi, T., Hori, Y., Hornback, D., Hoshino, T., Hotvedt, N., Huang, J.,  
 905 Huang, S., Hur, M. G., Ichihara, T., Ichimiya, R., Iinuma, H., Ikeda, Y., Imai, K., Imazu,  
 906 Y., Imrek, J., Inaba, M., Inoue, Y., Iordanova, A., Isenhowe, D., Isenhowe, L., Ishihara,  
 907 M., Isinhue, A., Isobe, T., Issah, M., Isupov, A., Ivanishchev, D., Iwanaga, Y., Jacak,  
 908 B. V., Javani, M., Jeon, S. J., Jezghani, M., Jia, J., Jiang, X., Jin, J., Jinnouchi, O.,  
 909 Johnson, B. M., Jones, T., Joo, K. S., Jouan, D., Jumper, D. S., Kajihara, F., Kametani,  
 910 S., Kamihara, N., Kamin, J., Kanda, S., Kaneta, M., Kaneti, S., Kang, B. H., Kang, J. H.,  
 911 Kang, J. S., Kanou, H., Kapustinsky, J., Karatsu, K., Kasai, M., Kawagishi, T., Kawall,  
 912 D., Kawashima, M., Kazantsev, A. V., Kelly, S., Kempel, T., Key, J. A., Khachatryan, V.,  
 913 Khandai, P. K., Khanzadeev, A., Kijima, K. M., Kikuchi, J., Kim, A., Kim, B. I., Kim, C.,  
 914 Kim, D. H., Kim, D. J., Kim, E., Kim, E.-J., Kim, G. W., Kim, H. J., Kim, K.-B., Kim,

915 M., Kim, Y.-J., Kim, Y. K., Kim, Y.-S., Kimelman, B., Kinney, E., Kiss, A., Kistenev, E.,  
 916 Kitamura, R., Kiyomichi, A., Klatsky, J., Klay, J., Klein-Boesing, C., Kleinjan, D., Kline,  
 917 P., Koblesky, T., Kochenda, L., Kochetkov, V., Kofarago, M., Komatsu, Y., Komkov,  
 918 B., Konno, M., Koster, J., Kotchetkov, D., Kotov, D., Kozlov, A., Král, A., Kravitz, A.,  
 919 Krizek, F., Kroon, P. J., Kubart, J., Kunde, G. J., Kurihara, N., Kurita, K., Kurosawa,  
 920 M., Kweon, M. J., Kwon, Y., Kyle, G. S., Lacey, R., Lai, Y. S., Lajoie, J. G., Lebedev,  
 921 A., Le Bornec, Y., Leckey, S., Lee, B., Lee, D. M., Lee, G. H., Lee, J., Lee, K. B.,  
 922 Lee, K. S., Lee, M. K., Lee, S., Lee, S. H., Lee, S. R., Lee, T., Leitch, M. J., Leite, M.  
 923 A. L., Leitgab, M., Lenzi, B., Lewis, B., Li, X., Li, X. H., Lichtenwalner, P., Liebing, P.,  
 924 Lim, H., Lim, S. H., Linden Levy, L. A., Liška, T., Litvinenko, A., Liu, H., Liu, M. X.,  
 925 Love, B., Lynch, D., Maguire, C. F., Makdisi, Y. I., Makek, M., Malakhov, A., Malik,  
 926 M. D., Manion, A., Manko, V. I., Mannel, E., Mao, Y., Maruyama, T., Mašek, L., Masui,  
 927 H., Masumoto, S., Matathias, F., McCain, M. C., McCumber, M., McGaughey, P. L.,  
 928 McGlinchey, D., McKinney, C., Means, N., Meles, A., Mendoza, M., Meredith, B., Miake,  
 929 Y., Mibe, T., Midori, J., Mignerey, A. C., Mikeš, P., Miki, K., Miller, T. E., Milov, A.,  
 930 Mioduszewski, S., Mishra, D. K., Mishra, G. C., Mishra, M., Mitchell, J. T., Mitrovski,  
 931 M., Miyachi, Y., Miyasaka, S., Mizuno, S., Mohanty, A. K., Mohapatra, S., Montuenga,  
 932 P., Moon, H. J., Moon, T., Morino, Y., Morreale, A., Morrison, D. P., Moskowitz, M.,  
 933 Moss, J. M., Motschwiller, S., Moukhanova, T. V., Mukhopadhyay, D., Murakami, T.,  
 934 Murata, J., Mwai, A., Nagae, T., Nagamiya, S., Nagashima, K., Nagata, Y., Nagle, J. L.,  
 935 Naglis, M., Nagy, M. I., Nakagawa, I., Nakagomi, H., Nakamiya, Y., Nakamura, K. R.,  
 936 Nakamura, T., Nakano, K., Nam, S., Nattrass, C., Nederlof, A., Netrakanti, P. K., Newby,  
 937 J., Nguyen, M., Nihashi, M., Niida, T., Nishimura, S., Norman, B. E., Nouicer, R., Novák,  
 938 T., Novitzky, N., Nukariya, A., Nyanin, A. S., Nystrand, J., Oakley, C., Obayashi, H.,  
 939 O'Brien, E., Oda, S. X., Ogilvie, C. A., Ohnishi, H., Oide, H., Ojha, I. D., Oka, M.,  
 940 Okada, K., Omiwade, O. O., Onuki, Y., Orjuela Koop, J. D., Osborn, J. D., Oskarsson,  
 941 A., Otterlund, I., Ouchida, M., Ozawa, K., Pak, R., Pal, D., Palounek, A. P. T., Pantuev,  
 942 V., Papavassiliou, V., Park, B. H., Park, I. H., Park, J., Park, J. S., Park, S., Park, S. K.,  
 943 Park, W. J., Pate, S. F., Patel, L., Patel, M., Pei, H., Peng, J.-C., Pereira, H., Perepelitsa,  
 944 D. V., Perera, G. D. N., Peresedov, V., Peressounko, D., Perry, J., Petti, R., Pinkenburg,

945 C., Pinson, R., Pisani, R. P., Proissl, M., Purschke, M. L., Purwar, A. K., Qu, H., Rak,  
 946 J., Rakotozafindrabe, A., Ramson, B. J., Ravinovich, I., Read, K. F., Rembeczki, S.,  
 947 Reuter, M., Reygers, K., Reynolds, D., Riabov, V., Riabov, Y., Richardson, E., Rinn, T.,  
 948 Riveli, N., Roach, D., Roche, G., Rolnick, S. D., Romana, A., Rosati, M., Rosen, C. A.,  
 949 Rosendahl, S. S. E., Rosnet, P., Rowan, Z., Rubin, J. G., Rukoyatkin, P., Ružička, P.,  
 950 Rykov, V. L., Ryu, M. S., Ryu, S. S., Sahlmueller, B., Saito, N., Sakaguchi, T., Sakai, S.,  
 951 Sakashita, K., Sakata, H., Sako, H., Samsonov, V., Sano, M., Sano, S., Sarsour, M., Sato,  
 952 H. D., Sato, S., Sato, T., Sawada, S., Schaefer, B., Schmoll, B. K., Sedgwick, K., Seele,  
 953 J., Seidl, R., Sekiguchi, Y., Semenov, V., Sen, A., Seto, R., Sett, P., Sexton, A., Sharma,  
 954 D., Shaver, A., Shea, T. K., Shein, I., Shevel, A., Shibata, T.-A., Shigaki, K., Shimomura,  
 955 M., Shohjoh, T., Shoji, K., Shukla, P., Sickles, A., Silva, C. L., Silvermyr, D., Silvestre,  
 956 C., Sim, K. S., Singh, B. K., Singh, C. P., Singh, V., Skolnik, M., Skutnik, S., Slunečka,  
 957 M., Smith, W. C., Snowball, M., Solano, S., Soldatov, A., Soltz, R. A., Sondheim, W. E.,  
 958 Sorensen, S. P., Sourikova, I. V., Staley, F., Stankus, P. W., Steinberg, P., Stenlund, E.,  
 959 Stepanov, M., Ster, A., Stoll, S. P., Stone, M. R., Sugitate, T., Suire, C., Sukhanov, A.,  
 960 Sullivan, J. P., Sumita, T., Sun, J., Sziklai, J., Tabaru, T., Takagi, S., Takagui, E. M.,  
 961 Takahara, A., Taketani, A., Tanabe, R., Tanaka, K. H., Tanaka, Y., Taneja, S., Tanida, K.,  
 962 Tannenbaum, M. J., Tarafdar, S., Taranenko, A., Tarján, P., Tennant, E., Themann, H.,  
 963 Thomas, D., Thomas, T. L., Tieulent, R., Timilsina, A., Todoroki, T., Togawa, M., Toia,  
 964 A., Tojo, J., Tomášek, L., Tomášek, M., Torii, H., Towell, C. L., Towell, R., Towell, R. S.,  
 965 Tram, V.-N., Tserruya, I., Tsuchimoto, Y., Tsuji, T., Tuli, S. K., Tydesjö, H., Tyurin,  
 966 N., Vale, C., Valle, H., van Hecke, H. W., Vargyas, M., Vazquez-Zambrano, E., Veicht,  
 967 A., Velkovska, J., Vértési, R., Vinogradov, A. A., Virius, M., Voas, B., Vossen, A., Vrba,  
 968 V., Vznuzdaev, E., Wagner, M., Walker, D., Wang, X. R., Watanabe, D., Watanabe, K.,  
 969 Watanabe, Y., Watanabe, Y. S., Wei, F., Wei, R., Wessels, J., Whitaker, S., White, A. S.,  
 970 White, S. N., Willis, N., Winter, D., Wolin, S., Woody, C. L., Wright, R. M., Wysocki, M.,  
 971 Xia, B., Xie, W., Xue, L., Yalcin, S., Yamaguchi, Y. L., Yamaura, K., Yang, R., Yanovich,  
 972 A., Yasin, Z., Ying, J., Yokkaichi, S., Yoo, J. H., Yoon, I., You, Z., Young, G. R., Younus,  
 973 I., Yu, H., Yushmanov, I. E., Zajc, W. A., Zaudtke, O., Zelenski, A., Zhang, C., Zhou, S.,

Zimanyi, J., Zolin, L., and Zou, L. (2016). Transverse energy production and charged-particle multiplicity at midrapidity in various systems from  $\sqrt{s_{NN}} = 7.7$  to 200 gev. *Phys. Rev. C*, 93:024901. vii, viii, 5, 22, 23, 33, 37, 39

[4] Adare, A., Afanasiev, S., Aidala, C., Ajitanand, N. N., Akiba, Y., Al-Bataineh, H., Alexander, J., Al-Jamel, A., Aoki, K., Aphecetche, L., and et al. (2007). Scaling Properties of Azimuthal Anisotropy in Au+Au and Cu+Cu Collisions at  $s_{NN}=200\text{GeV}$ . *Physical Review Letters*, 98(16):162301. vi, 14, 15, 16

[5] Adler, S. S., Afanasiev, S., Aidala, C., Ajitanand, N. N., Akiba, Y., Al-Jamel, A., Alexander, J., Aoki, K., Aphecetche, L., Armendariz, R., Aronson, S. H., Auerbeck, R., Awes, T. C., Azmoun, B., Babintsev, V., Baldisseri, A., Barish, K. N., Barnes, P. D., Bassalleck, B., Bathe, S., Batsouli, S., Baublis, V., Bauer, F., Bazilevsky, A., Belikov, S., Bennett, R., Berdnikov, Y., Bjorndal, M. T., Boissevain, J. G., Borel, H., Boyle, K., Brooks, M. L., Brown, D. S., Bruner, N., Bucher, D., Buesching, H., Bumazhnov, V., Bunce, G., Burward-Hoy, J. M., Butsyk, S., Camard, X., Campbell, S., Chai, J.-S., Chand, P., Chang, W. C., Chernichenko, S., Chi, C. Y., Chiba, J., Chiu, M., Choi, I. J., Choudhury, R. K., Chujo, T., Cianciolo, V., Cleven, C. R., Cobigo, Y., Cole, B. A., Comets, M. P., Constantin, P., Csanád, M., Csörgő, T., Cussonneau, J. P., Dahms, T., Das, K., David, G., Deák, F., Delagrange, H., Denisov, A., d'Enterria, D., Deshpande, A., Desmond, E. J., Devismes, A., Dietzsch, O., Dion, A., Drachenberg, J. L., Drapier, O., Drees, A., Dubey, A. K., Durum, A., Dutta, D., Dzhordzhadze, V., Efremenko, Y. V., Egdemir, J., Enokizono, A., En'yo, H., Espagnon, B., Esumi, S., Fields, D. E., Finck, C., Fleuret, F., Fokin, S. L., Forestier, B., Fox, B. D., Fraenkel, Z., Frantz, J. E., Franz, A., Frawley, A. D., Fukao, Y., Fung, S.-Y., Gadrat, S., Gastineau, F., Germain, M., Glenn, A., Gonin, M., Gosset, J., Goto, Y., Granier de Cassagnac, R., Grau, N., Greene, S. V., Grosse Perdekamp, M., Gunji, T., Gustafsson, H.-A., Hachiya, T., Hadj Henni, A., Haggerty, J. S., Hagiwara, M. N., Hamagaki, H., Hansen, A. G., Harada, H., Hartouni, E. P., Haruna, K., Harvey, M., Haslum, E., Hasuko, K., Hayano, R., He, X., Heffner, M., Hemmick, T. K., Heuser, J. M., Hidas, P., Hiejima, H., Hill, J. C., Hobbs, R., Holmes, M., Holzmann, W., Homma, K., Hong, B., Hoover, A., Horaguchi, T., Hur, M. G., Ichihara, T.,

1003 Iinuma, H., Ikonnikov, V. V., Imai, K., Inaba, M., Inuzuka, M., Isenhowe, D., Isenhowe,  
 1004 L., Ishihara, M., Isobe, T., Issah, M., Isupov, A., Jacak, B. V., Jia, J., Jin, J., Jinnouchi,  
 1005 O., Johnson, B. M., Johnson, S. C., Joo, K. S., Jouan, D., Kajihara, F., Kametani,  
 1006 S., Kamihara, N., Kaneta, M., Kang, J. H., Katou, K., Kawabata, T., Kawagishi, T.,  
 1007 Kazantsev, A. V., Kelly, S., Khachaturov, B., Khanzadeev, A., Kikuchi, J., Kim, D. J.,  
 1008 Kim, E., Kim, E. J., Kim, G.-B., Kim, H. J., Kim, Y.-S., Kinney, E., Kiss, A., Kistenev, E.,  
 1009 Kiyomichi, A., Klein-Boesing, C., Kobayashi, H., Kochenda, L., Kochetkov, V., Kohara,  
 1010 R., Komkov, B., Konno, M., Kotchetkov, D., Kozlov, A., Kroon, P. J., Kuberg, C. H.,  
 1011 Kunde, G. J., Kurihara, N., Kurita, K., Kweon, M. J., Kwon, Y., Kyle, G. S., Lacey, R.,  
 1012 Lajoie, J. G., Lebedev, A., Le Bornec, Y., Leckey, S., Lee, D. M., Lee, M. K., Leitch,  
 1013 M. J., Leite, M. A. L., Li, X. H., Lim, H., Litvinenko, A., Liu, M. X., Maguire, C. F.,  
 1014 Makdisi, Y. I., Malakhov, A., Malik, M. D., Manko, V. I., Mao, Y., Martinez, G., Masui,  
 1015 H., Matathias, F., Matsumoto, T., McCain, M. C., McGaughey, P. L., Miake, Y., Miller,  
 1016 T. E., Milov, A., Mioduszewski, S., Mishra, G. C., Mitchell, J. T., Mohanty, A. K.,  
 1017 Morrison, D. P., Moss, J. M., Moukhanova, T. V., Mukhopadhyay, D., Muniruzzaman,  
 1018 M., Murata, J., Nagamiya, S., Nagata, Y., Nagle, J. L., Naglis, M., Nakamura, T., Newby,  
 1019 J., Nguyen, M., Norman, B. E., Nyanin, A. S., Nystrand, J., O'Brien, E., Ogilvie, C. A.,  
 1020 Ohnishi, H., Ojha, I. D., Okada, K., Omiwade, O. O., Oskarsson, A., Otterlund, I., Oyama,  
 1021 K., Ozawa, K., Pal, D., Palounek, A. P. T., Pantuev, V., Papavassiliou, V., Park, J., Park,  
 1022 W. J., Pate, S. F., Pei, H., Penev, V., Peng, J.-C., Pereira, H., Peresedov, V., Peressounko,  
 1023 D., Pierson, A., Pinkenburg, C., Pisani, R. P., Purschke, M. L., Purwar, A. K., Qu, H.,  
 1024 Qualls, J. M., Rak, J., Ravinovich, I., Read, K. F., Reuter, M., Reygers, K., Riabov,  
 1025 V., Riabov, Y., Roche, G., Romana, A., Rosati, M., Rosendahl, S. S. E., Rosnet, P.,  
 1026 Rukoyatkin, P., Rykov, V. L., Ryu, S. S., Sahlmueller, B., Saito, N., Sakaguchi, T., Sakai,  
 1027 S., Samsonov, V., Sanfratello, L., Santo, R., Sarsour, M., Sato, H. D., Sato, S., Sawada,  
 1028 S., Schutz, Y., Semenov, V., Seto, R., Sharma, D., Shea, T. K., Shein, I., Shibata, T.-A.,  
 1029 Shigaki, K., Shimomura, M., Shohjoh, T., Shoji, K., Sickles, A., Silva, C. L., Silvermyr, D.,  
 1030 Sim, K. S., Singh, C. P., Singh, V., Skutnik, S., Smith, W. C., Soldatov, A., Soltz, R. A.,  
 1031 Sondheim, W. E., Sorensen, S. P., Sourikova, I. V., Staley, F., Stankus, P. W., Stenlund,  
 1032 E., Stepanov, M., Ster, A., Stoll, S. P., Sugitate, T., Suire, C., Sullivan, J. P., Sziklai, J.,

Tabaru, T., Takagi, S., Takagui, E. M., Taketani, A., Tanaka, K. H., Tanaka, Y., Tanida, K., Tannenbaum, M. J., Taranenko, A., Tarján, P., Thomas, T. L., Togawa, M., Tojo, J., Torii, H., Towell, R. S., Tram, V.-N., Tserruya, I., Tsuchimoto, Y., Tuli, S. K., Tydesjö, H., Tyurin, N., Uam, T. J., Vale, C., Valle, H., van Hecke, H. W., Velkovska, J., Velkovsky, M., Vértesi, R., Veszprémi, V., Vinogradov, A. A., Volkov, M. A., Vznuzdaev, E., Wagner, M., Wang, X. R., Watanabe, Y., Wessels, J., White, S. N., Willis, N., Winter, D., Wohn, F. K., Woody, C. L., Wysocki, M., Xie, W., Yanovich, A., Yokkaichi, S., Young, G. R., Younus, I., Yushmanov, I. E., Zajc, W. A., Zaudtke, O., Zhang, C., Zhou, S., Zimányi, J., Zolin, L., and Zong, X. (2014). Transverse-energy distributions at midrapidity in  $p + p$ ,  $d + \text{Au}$ , and  $\text{Au} + \text{Au}$  collisions at  $\sqrt{s_{\text{NN}}} = 62.4 \sim 200$  gev and implications for particle-production models. *Phys. Rev. C*, 89:044905. 20

[6] Adler, S. S., Afanasiev, S., Aidala, C., Ajitanand, N. N., Akiba, Y., Alexander, J., Amirikas, R., Aphecetche, L., Aronson, S. H., Auerbeck, R., Awes, T. C., Azmoun, R., Babintsev, V., Baldissieri, A., Barish, K. N., Barnes, P. D., Bassalleck, B., Bathe, S., Batsouli, S., Baublis, V., Bazilevsky, A., Belikov, S., Berdnikov, Y., Bhagavatula, S., Boissevain, J. G., Borel, H., Borenstein, S., Brooks, M. L., Brown, D. S., Bruner, N., Bucher, D., Buesching, H., Bumazhnov, V., Bunce, G., Burward-Hoy, J. M., Butsyk, S., Camard, X., Chai, J.-S., Chand, P., Chang, W. C., Chernichenko, S., Chi, C. Y., Chiba, J., Chiu, M., Choi, I. J., Choi, J., Choudhury, R. K., Chujo, T., Cianciolo, V., Cobigo, Y., Cole, B. A., Constantin, P., d’Enterria, D. G., David, G., Delagrange, H., Denisov, A., Deshpande, A., Desmond, E. J., Dietzsch, O., Drapier, O., Drees, A., Rietz, R. d., Durum, A., Dutta, D., Efremenko, Y. V., Chenawi, K. E., Enokizono, A., En’yo, H., Esumi, S., Ewell, L., Fields, D. E., Fleuret, F., Fokin, S. L., Fox, B. D., Fraenkel, Z., Frantz, J. E., Franz, A., Frawley, A. D., Fung, S.-Y., Garpman, S., Ghosh, T. K., Glenn, A., Gogiberidze, G., Gonin, M., Gosset, J., Goto, Y., Cassagnac, R. G. d., Grau, N., Greene, S. V., Perdekamp, M. G., Guryn, W., Gustafsson, H.-A., Hachiya, T., Haggerty, J. S., Hamagaki, H., Hansen, A. G., Hartouni, E. P., Harvey, M., Hayano, R., He, X., Heffner, M., Hemmick, T. K., Heuser, J. M., Hibino, M., Hill, J. C., Holzmann, W., Homma, K., Hong, B., Hoover, A., Ichihara, T., Ikonnikov, V. V., Imai, K., Isenhower, D., Ishihara,

1062 M., Issah, M., Isupov, A., Jacak, B. V., Jang, W. Y., Jeong, Y., Jia, J., Jinnouchi, O.,  
 1063 Johnson, B. M., Johnson, S. C., Joo, K. S., Jouan, D., Kametani, S., Kamihara, N.,  
 1064 Kang, J. H., Kapoor, S. S., Katou, K., Kelly, S., Khachaturov, B., Khanzadeev, A.,  
 1065 Kikuchi, J., Kim, D. H., Kim, D. J., Kim, D. W., Kim, E., Kim, G.-B., Kim, H. J.,  
 1066 Kistenev, E., Kiyomichi, A., Kiyoyama, K., Klein-Boesing, C., Kobayashi, H., Kochenda,  
 1067 L., Kochetkov, V., Koehler, D., Kohama, T., Kopytine, M., Kotchetkov, D., Kozlov, A.,  
 1068 Kroon, P. J., Kuberg, C. H., Kurita, K., Kuroki, Y., Kweon, M. J., Kwon, Y., Kyle,  
 1069 G. S., Lacey, R., Ladygin, V., Lajoie, J. G., Lebedev, A., Leckey, S., Lee, D. M., Lee, S.,  
 1070 Leitch, M. J., Li, X. H., Lim, H., Litvinenko, A., Liu, M. X., Liu, Y., Maguire, C. F.,  
 1071 Makdisi, Y. I., Malakhov, A., Manko, V. I., Mao, Y., Martinez, G., Marx, M. D., Masui,  
 1072 H., Matathias, F., Matsumoto, T., McGaughey, P. L., Melnikov, E., Mendenhall, M.,  
 1073 Messer, F., Miake, Y., Milan, J., Miller, T. E., Milov, A., Mioduszewski, S., Mischke,  
 1074 R. E., Mishra, G. C., Mitchell, J. T., Mohanty, A. K., Morrison, D. P., Moss, J. M.,  
 1075 Mühlbacher, F., Mukhopadhyay, D., Muniruzzaman, M., Murata, J., Nagamiya, S., Nagle,  
 1076 J. L., Nakamura, T., Nandi, B. K., Nara, M., Newby, J., Nilsson, P., Nyanin, A. S.,  
 1077 Nystrand, J., O'Brien, E., Ogilvie, C. A., Ohnishi, H., Ojha, I. D., Okada, K., Ono, M.,  
 1078 Onuchin, V., Oskarsson, A., Otterlund, I., Oyama, K., Ozawa, K., Pal, D., Palounek, A.  
 1079 P. T., Pantuev, V. S., Papavassiliou, V., Park, J., Parmar, A., Pate, S. F., Peitzmann,  
 1080 T., Peng, J.-C., Peresedov, V., Pinkenburg, C., Pisani, R. P., Plasil, F., Purschke, M. L.,  
 1081 Purwar, A. K., Rak, J., Ravinovich, I., Read, K. F., Reuter, M., Reygers, K., Riabov, V.,  
 1082 Riabov, Y., Roche, G., Romana, A., Rosati, M., Rosnet, P., Ryu, S. S., Sadler, M. E.,  
 1083 Saito, N., Sakaguchi, T., Sakai, M., Sakai, S., Samsonov, V., Sanfratello, L., Santo, R.,  
 1084 Sato, H. D., Sato, S., Sawada, S., Schutz, Y., Semenov, V., Seto, R., Shaw, M. R., Shea,  
 1085 T. K., Shibata, T.-A., Shigaki, K., Shiina, T., Silva, C. L., Silvermyr, D., Sim, K. S., Singh,  
 1086 C. P., Singh, V., Sivertz, M., Soldatov, A., Soltz, R. A., Sondheim, W. E., Sorensen, S. P.,  
 1087 Sourikova, I. V., Staley, F., Stankus, P. W., Stenlund, E., Stepanov, M., Ster, A., Stoll,  
 1088 S. P., Sugitate, T., Sullivan, J. P., Takagui, E. M., Taketani, A., Tamai, M., Tanaka, K. H.,  
 1089 Tanaka, Y., Tanida, K., Tannenbaum, M. J., Tarján, P., Tepe, J. D., Thomas, T. L., Tojo,  
 1090 J., Torii, H., Towell, R. S., Tserruya, I., Tsuruoka, H., Tuli, S. K., Tydesjö, H., Tyurin,  
 1091 N., Hecke, H. W. v., Velkovska, J., Velkovsky, M., Villatte, L., Vinogradov, A. A., Volkov,



- 1092 M. A., Vznuzdaev, E., Wang, X. R., Watanabe, Y., White, S. N., Wohn, F. K., Woody,  
1093 C. L., Xie, W., Yang, Y., Yanovich, A., Yokkaichi, S., Young, G. R., Yushmanov, I. E.,  
1094 Zajc, W. A., Zhang, C., Zhou, S., Zhou, S. J., and Zolin, L. (2005). Systematic studies of  
1095 the centrality and  $\sqrt{s_{NN}}$  dependence of the  $de_T/d\eta$  and  $dn_{ch}/d\eta$  in heavy ion collisions at  
1096 midrapidity. *Phys. Rev. C*, 71:034908. 21
- 1097 [7] Aitchison, I. and Hey, A. (2003). *Gauge Theories in Particle Physics, Volume II: QCD*  
1098 *and the Electroweak Theory, Third Edition*. Graduate Student Series in Physics. CRC  
1099 Press. 3
- 1100 [8] Anderson, M. et al. (2003). The Star time projection chamber: A Unique tool for studying  
1101 high multiplicity events at RHIC. *Nucl. Instrum. Meth.*, A499:659–678. vii, 25, 26
- 1102 [9] Ayala, A. (2016). Hadronic matter at the edge: A survey of some theoretical approaches  
1103 to the physics of the qcd phase diagram. *Journal of Physics: Conference Series*,  
1104 761(1):012066. vi, 5, 6
- 1105 [10] Bali, G. S. (2001). QCD forces and heavy quark bound states. *Phys. Rept.*, 343:1–136.  
1106 4
- 1107 [11] Bethe, H. A. and Ashkin, J. (1953). Passage of radiations through matter experimental  
1108 nuclear physics vol 1 ed e segre. 24
- 1109 [12] Bjorken, J. D. (1983). Highly relativistic nucleus-nucleus collisions: The central rapidity  
1110 region. *Phys. Rev. D*, 27:140–151. 12
- 1111 [13] Chatrchyan, S., Khachatryan, V., Sirunyan, A. M., Tumasyan, A., Adam, W., Bergauer,  
1112 T., Dragicevic, M., Erö, J., Fabjan, C., Friedl, M., Frühwirth, R., Ghete, V. M., Hammer,  
1113 J., Hörmann, N., Hrubec, J., Jeitler, M., Kiesenhofer, W., Knünz, V., Krammer, M., Liko,  
1114 D., Mikulec, I., Pernicka, M., Rahbaran, B., Rohringer, C., Rohringer, H., Schöffbeck, R.,  
1115 Strauss, J., Taurok, A., Wagner, P., Waltenberger, W., Walzel, G., Widl, E., Wulz, C.-E.,  
1116 Mossolov, V., Shumeiko, N., Suarez Gonzalez, J., Bansal, S., Cornelis, T., De Wolf, E. A.,  
1117 Janssen, X., Luyckx, S., Maes, T., Mucibello, L., Ochsanu, S., Roland, B., Rougny,  
1118 R., Selvaggi, M., Staykova, Z., Van Haeevermaet, H., Van Mechelen, P., Van Remortel,

1119 N., Van Spilbeeck, A., Blekman, F., Blyweert, S., D'Hondt, J., Gonzalez Suarez, R.,  
 1120 Kalogeropoulos, A., Maes, M., Olbrechts, A., Van Doninck, W., Van Mulders, P.,  
 1121 Van Onsem, G. P., Villella, I., Clerbaux, B., De Lentdecker, G., Dero, V., Gay, A. P. R.,  
 1122 Hreus, T., Léonard, A., Marage, P. E., Reis, T., Thomas, L., Vander Velde, C., Vanlaer, P.,  
 1123 Wang, J., Adler, V., Beernaert, K., Cimmino, A., Costantini, S., Garcia, G., Grunewald,  
 1124 M., Klein, B., Lellouch, J., Marinov, A., McCartin, J., Ocampo Rios, A. A., Ryckbosch, D.,  
 1125 Strobbe, N., Thyssen, F., Tytgat, M., Verwilligen, P., Walsh, S., Yazgan, E., Zaganidis,  
 1126 N., Basegmez, S., Bruno, G., Castello, R., Ceard, L., Delaere, C., du Pree, T., Favart, D.,  
 1127 Forthomme, L., Giammanco, A., Hollar, J., Lemaitre, V., Liao, J., Militaru, O., Nuttens,  
 1128 C., Pagano, D., Pin, A., Piotrkowski, K., Schul, N., Vizán García, J. M., Beliy, N.,  
 1129 Caebergs, T., Daubie, E., Hammad, G. H., Alves, G. A., Correa Martins Junior, M.,  
 1130 De Jesus Damiao, D., Martins, T., Pol, M. E., Souza, M. H. G., Aldá Júnior, W. L.,  
 1131 Carvalho, W., Custódio, A., Da Costa, E. M., De Oliveira Martins, C., Fonseca De Souza,  
 1132 S., Matos Figueiredo, D., Mundim, L., Nogima, H., Oguri, V., Prado Da Silva, W. L.,  
 1133 Santoro, A., Soares Jorge, L., Sznajder, A., Bernardes, C. A., Dias, F. A., Fernandez  
 1134 Perez Tomei, T. R., Gregores, E. M., Lagana, C., Marinho, F., Mercadante, P. G., Novaes,  
 1135 S. F., Padula, S. S., Genchev, V., Iaydjiev, P., Piperov, S., Rodozov, M., Stoykova, S.,  
 1136 Sultanov, G., Tcholakov, V., Trayanov, R., Vutova, M., Dimitrov, A., Hadjiiska, R.,  
 1137 Kozhuharov, V., Litov, L., Pavlov, B., Petkov, P., Bian, J. G., Chen, G. M., Chen, H. S.,  
 1138 Jiang, C. H., Liang, D., Liang, S., Meng, X., Tao, J., Wang, J., Wang, X., Wang, Z.,  
 1139 Xiao, H., Xu, M., Zang, J., Zhang, Z., Asawatangtrakuldee, C., Ban, Y., Guo, S., Guo,  
 1140 Y., Li, W., Liu, S., Mao, Y., Qian, S. J., Teng, H., Wang, S., Zhu, B., Zou, W., Avila,  
 1141 C., Gomez, J. P., Gomez Moreno, B., Osorio Oliveros, A. F., Sanabria, J. C., Godinovic,  
 1142 N., Lelas, D., Plestina, R., Polic, D., Puljak, I., Antunovic, Z., Kovac, M., Brigljevic, V.,  
 1143 Duric, S., Kadija, K., Luetic, J., Morovic, S., Attikis, A., Galanti, M., Mavromanolakis,  
 1144 G., Mousa, J., Nicolaou, C., Ptochos, F., Razis, P. A., Finger, M., Finger, M., Assran,  
 1145 Y., Elgammal, S., Ellithi Kamel, A., Khalil, S., Mahmoud, M. A., Radi, A., Kadastik,  
 1146 M., Müntel, M., Raidal, M., Rebane, L., Tiko, A., Azzolini, V., Eerola, P., Fedi, G.,  
 1147 Voutilainen, M., Härkönen, J., Heikkinen, A., Karimäki, V., Kinnunen, R., Kortelainen,  
 1148 M. J., Lampén, T., Lassila-Perini, K., Lehti, S., Lindén, T., Luukka, P., Mäenpää, T.,

1149 Peltola, T., Tuominen, E., Tuominiemi, J., Tuovinen, E., Ungaro, D., Wendland, L.,  
 1150 Banzuzi, K., Karjalainen, A., Korpela, A., Tuuva, T., Besancon, M., Choudhury, S.,  
 1151 Dejardin, M., Denegri, D., Fabbro, B., Faure, J. L., Ferri, F., Ganjour, S., Givernaud,  
 1152 A., Gras, P., Hamel de Monchenault, G., Jarry, P., Locci, E., Malcles, J., Millischer, L.,  
 1153 Nayak, A., Rander, J., Rosowsky, A., Shreyber, I., Titov, M., Baffioni, S., Beaudette,  
 1154 F., Benhabib, L., Bianchini, L., Bluj, M., Broutin, C., Busson, P., Charlot, C., Daci,  
 1155 N., Dahms, T., Dobrzynski, L., Granier de Cassagnac, R., Haguenaue, M., Miné, P.,  
 1156 Mironov, C., Nguyen, M., Ochando, C., Paganini, P., Sabes, D., Salerno, R., Sirois, Y.,  
 1157 Veelken, C., Zabi, A., Agram, J.-L., Andrea, J., Bloch, D., Bodin, D., Brom, J.-M.,  
 1158 Cardaci, M., Chabert, E. C., Collard, C., Conte, E., Drouhin, F., Ferro, C., Fontaine, J.-  
 1159 C., Gelé, D., Goerlach, U., Juillot, P., Le Bihan, A.-C., Van Hove, P., Fassi, F., Mercier,  
 1160 D., Beauceron, S., Beaupere, N., Bondu, O., Boudoul, G., Chasserat, J., Chierici, R.,  
 1161 Contardo, D., Depasse, P., El Mamouni, H., Fay, J., Gascon, S., Gouzevitch, M., Ille,  
 1162 B., Kurca, T., Lethuillier, M., Mirabito, L., Perries, S., Sordini, V., Tosi, S., Tschudi,  
 1163 Y., Verdier, P., Viret, S., Tsamalaidze, Z., Anagnostou, G., Beranek, S., Edelhoff, M.,  
 1164 Feld, L., Heracleous, N., Hindrichs, O., Jussen, R., Klein, K., Merz, J., Ostapchuk, A.,  
 1165 Perieanu, A., Raupach, F., Sammet, J., Schael, S., Sprenger, D., Weber, H., Wittmer,  
 1166 B., Zhukov, V., Ata, M., Caudron, J., Dietz-Laursonn, E., Erdmann, M., Güth, A.,  
 1167 Hebbeker, T., Heidemann, C., Hoepfner, K., Klingebiel, D., Kreuzer, P., Lingemann,  
 1168 J., Magass, C., Merschmeyer, M., Meyer, A., Olschewski, M., Papacz, P., Pieta, H.,  
 1169 Reithler, H., Schmitz, S. A., Sonnenschein, L., Steggemann, J., Teyssier, D., Weber, M.,  
 1170 Bontenackels, M., Cherepanov, V., Flügge, G., Geenen, H., Geisler, M., Haj Ahmad, W.,  
 1171 Hoehle, F., Kargoll, B., Kress, T., Kuessel, Y., Nowack, A., Perchalla, L., Pooth, O.,  
 1172 Rennefeld, J., Sauerland, P., Stahl, A., Aldaya Martin, M., Behr, J., Behrenhoff, W.,  
 1173 Behrens, U., Bergholz, M., Bethani, A., Borrás, K., Burgmeier, A., Cakir, A., Calligaris,  
 1174 L., Campbell, A., Castro, E., Costanza, F., Dammann, D., Diez Pardos, C., Eckerlin, G.,  
 1175 Eckstein, D., Flucke, G., Geiser, A., Glushkov, I., Gunnellini, P., Habib, S., Hauk, J.,  
 1176 Jung, H., Kasemann, M., Katsas, P., Kleinwort, C., Kluge, H., Knutsson, A., Krämer, M.,  
 1177 Krücker, D., Kuznetsova, E., Lange, W., Lohmann, W., Lutz, B., Mankel, R., Marfin, I.,

1178 Marienfeld, M., Melzer-Pellmann, I.-A., Meyer, A. B., Mnich, J., Mussgiller, A., Naumann-  
 1179 Emme, S., Olzem, J., Perrey, H., Petrukhin, A., Pitzl, D., Raspereza, A., Ribeiro Cipriano,  
 1180 P. M., Riedl, C., Ron, E., Rosin, M., Salfeld-Nebgen, J., Schmidt, R., Schoerner-Sadenius,  
 1181 T., Sen, N., Spiridonov, A., Stein, M., Walsh, R., Wissing, C., Autermann, C., Blobel,  
 1182 V., Draeger, J., Enderle, H., Erfle, J., Gebbert, U., Görner, M., Hermanns, T., Höing,  
 1183 R. S., Kaschube, K., Kaussen, G., Kirschenmann, H., Klanner, R., Lange, J., Mura, B.,  
 1184 Nowak, F., Peiffer, T., Pietsch, N., Sander, C., Schettler, H., Schleper, P., Schlieckau, E.,  
 1185 Schmidt, A., Schröder, M., Schum, T., Sola, V., Stadie, H., Steinbrück, G., Thomsen,  
 1186 J., Vanelderen, L., Barth, C., Berger, J., Chwalek, T., De Boer, W., Dierlamm, A.,  
 1187 Feindt, M., Guthoff, M., Hackstein, C., Hartmann, F., Heinrich, M., Held, H., Hoffmann,  
 1188 K. H., Honc, S., Katkov, I., Komaragiri, J. R., Lobelle Pardo, P., Martschei, D., Mueller,  
 1189 S., Müller, T., Niegel, M., Nürnberg, A., Oberst, O., Oehler, A., Ott, J., Quast, G.,  
 1190 Rabbertz, K., Ratnikov, F., Ratnikova, N., Röcker, S., Scheurer, A., Schilling, F.-P.,  
 1191 Schott, G., Simonis, H. J., Stober, F. M., Troendle, D., Ulrich, R., Wagner-Kuhr, J.,  
 1192 Weiler, T., Zeise, M., Daskalakis, G., Gerasis, T., Kesisoglou, S., Kyriakis, A., Loukas,  
 1193 D., Manolakos, I., Markou, A., Markou, C., Mavrommatis, C., Ntomari, E., Gouskos, L.,  
 1194 Mertzimekis, T. J., Panagiotou, A., Saoulidou, N., Evangelou, I., Foudas, C., Kokkas, P.,  
 1195 Manthos, N., Papadopoulos, I., Patras, V., Bencze, G., Hajdu, C., Hidas, P., Horvath, D.,  
 1196 Sikler, F., Veszpremi, V., Vesztergombi, G., Beni, N., Czellar, S., Molnar, J., Palinkas, J.,  
 1197 Szillasi, Z., Karancsi, J., Raics, P., Trocsanyi, Z. L., Ujvari, B., Beri, S. B., Bhatnagar,  
 1198 V., Dhingra, N., Gupta, R., Jindal, M., Kaur, M., Mehta, M. Z., Nishu, N., Saini, L. K.,  
 1199 Sharma, A., Singh, J., Ahuja, S., Bhardwaj, A., Choudhary, B. C., Kumar, A., Kumar,  
 1200 A., Malhotra, S., Naimuddin, M., Ranjan, K., Sharma, V., Shivpuri, R. K., Banerjee,  
 1201 S., Bhattacharya, S., Dutta, S., Gomber, B., Jain, S., Jain, S., Khurana, R., Sarkar,  
 1202 S., Sharan, M., Abdulsalam, A., Choudhury, R. K., Dutta, D., Kailas, S., Kumar, V.,  
 1203 Mehta, P., Mohanty, A. K., Pant, L. M., Shukla, P., Aziz, T., Ganguly, S., Guchait, M.,  
 1204 Maity, M., Majumder, G., Mazumdar, K., Mohanty, G. B., Parida, B., Sudhakar, K.,  
 1205 Wickramage, N., Banerjee, S., Dugad, S., Arfaei, H., Bakhshiansohi, H., Etesami, S. M.,  
 1206 Fahim, A., Hashemi, M., Hesari, H., Jafari, A., Khakzad, M., Mohammadi Najafabadi,  
 1207 M., Paktinat Mehdiabadi, S., Safarzadeh, B., Zeinali, M., Abbrescia, M., Barbone, L.,

1208 Calabria, C., Chhibra, S. S., Colaleo, A., Creanza, D., De Filippis, N., De Palma, M.,  
 1209 Fiore, L., Iaselli, G., Lusito, L., Maggi, G., Maggi, M., Marangelli, B., My, S., Nuzzo,  
 1210 S., Pacifico, N., Pompili, A., Pugliese, G., Selvaggi, G., Silvestris, L., Singh, G., Zito,  
 1211 G., Abbiendi, G., Benvenuti, A. C., Bonacorsi, D., Braibant-Giacomelli, S., Brigliadori,  
 1212 L., Capiluppi, P., Castro, A., Cavallo, F. R., Cuffiani, M., Dallavalle, G. M., Fabbri, F.,  
 1213 Fanfani, A., Fasanella, D., Giacomelli, P., Grandi, C., Guiducci, L., Marcellini, S., Masetti,  
 1214 G., Meneghelli, M., Montanari, A., Navarria, F. L., Odorici, F., Perrotta, A., Primavera,  
 1215 F., Rossi, A. M., Rovelli, T., Siroli, G., Travaglini, R., Albergo, S., Cappello, G., Chiorboli,  
 1216 M., Costa, S., Potenza, R., Tricomi, A., Tuve, C., Barbagli, G., Ciulli, V., Civinini, C.,  
 1217 D'Alessandro, R., Focardi, E., Frosali, S., Gallo, E., Gonzi, S., Meschini, M., Paoletti,  
 1218 S., Sguazzoni, G., Tropiano, A., Benussi, L., Bianco, S., Colafranceschi, S., Fabbri, F.,  
 1219 Piccolo, D., Fabbricatore, P., Musenich, R., Benaglia, A., De Guio, F., Di Matteo, L.,  
 1220 Fiorendi, S., Gennai, S., Ghezzi, A., Malvezzi, S., Manzoni, R. A., Martelli, A., Massironi,  
 1221 A., Menasce, D., Moroni, L., Paganoni, M., Pedrini, D., Ragazzi, S., Redaelli, N., Sala,  
 1222 S., Tabarelli de Fatis, T., Buontempo, S., Carrillo Montoya, C. A., Cavallo, N., De Cosa,  
 1223 A., Dogangun, O., Fabozzi, F., Iorio, A. O. M., Lista, L., Meola, S., Merola, M., Paolucci,  
 1224 P., Azzi, P., Bacchetta, N., Bellan, P., Bisello, D., Branca, A., Carlin, R., Checchia, P.,  
 1225 Dorigo, T., Dosselli, U., Gasparini, F., Gasparini, U., Gozzelino, A., Kanishchev, K.,  
 1226 Lacaprara, S., Lazzizzera, I., Margoni, M., Meneguzzo, A. T., Nespolo, M., Ronchese,  
 1227 P., Simonetto, F., Torassa, E., Vanini, S., Zotto, P., Zumerle, G., Gabusi, M., Ratti,  
 1228 S. P., Riccardi, C., Torre, P., Vitulo, P., Biasini, M., Bilei, G. M., Fanò, L., Lariccia, P.,  
 1229 Lucaroni, A., Mantovani, G., Menichelli, M., Nappi, A., Romeo, F., Saha, A., Santocchia,  
 1230 A., Taroni, S., Azzurri, P., Bagliesi, G., Boccali, T., Broccolo, G., Castaldi, R., D'Agnolo,  
 1231 R. T., Dell'Orso, R., Fiori, F., Foà, L., Giassi, A., Kraan, A., Ligabue, F., Lomtadze, T.,  
 1232 Martini, L., Messineo, A., Palla, F., Rizzi, A., Serban, A. T., Spagnolo, P., Squillacioti, P.,  
 1233 Tenchini, R., Tonelli, G., Venturi, A., Verdini, P. G., Barone, L., Cavallari, F., Del Re, D.,  
 1234 Diemoz, M., Grassi, M., Longo, E., Meridiani, P., Micheli, F., Nourbakhsh, S., Organtini,  
 1235 G., Paramatti, R., Rahatlou, S., Sigamani, M., Soffi, L., Amapane, N., Arcidiacono, R.,  
 1236 Argiro, S., Arneodo, M., Biino, C., Cartiglia, N., Costa, M., Demaria, N., Graziano,  
 1237 A., Mariotti, C., Maselli, S., Migliore, E., Monaco, V., Musich, M., Obertino, M. M.,

1238 Pastrone, N., Pelliccioni, M., Potenza, A., Romero, A., Ruspa, M., Sacchi, R., Solano, A.,  
 1239 Staiano, A., Vilela Pereira, A., Belforte, S., Candelise, V., Cossutti, F., Della Ricca, G.,  
 1240 Gobbo, B., Marone, M., Montanino, D., Penzo, A., Schizzi, A., Heo, S. G., Kim, T. Y.,  
 1241 Nam, S. K., Chang, S., Kim, D. H., Kim, G. N., Kong, D. J., Park, H., Ro, S. R., Son,  
 1242 D. C., Son, T., Kim, J. Y., Kim, Z. J., Song, S., Choi, S., Gyun, D., Hong, B., Jo, M.,  
 1243 Kim, H., Kim, T. J., Lee, K. S., Moon, D. H., Park, S. K., Choi, M., Kim, J. H., Park,  
 1244 C., Park, I. C., Park, S., Ryu, G., Cho, Y., Choi, Y., Choi, Y. K., Goh, J., Kim, M. S.,  
 1245 Kwon, E., Lee, B., Lee, J., Lee, S., Seo, H., Yu, I., Bilinskas, M. J., Grigelionis, I., Janulis,  
 1246 M., Juodagalvis, A., Castilla-Valdez, H., De La Cruz-Burelo, E., Heredia-de La Cruz, I.,  
 1247 Lopez-Fernandez, R., Magaña Villalba, R., Martínez-Ortega, J., Sánchez-Hernández, A.,  
 1248 Villasenor-Cendejas, L. M., Carrillo Moreno, S., Vazquez Valencia, F., Salazar Ibarguen,  
 1249 H. A., Casimiro Linares, E., Morelos Pineda, A., Reyes-Santos, M. A., Krofcheck, D.,  
 1250 Bell, A. J., Butler, P. H., Doesburg, R., Reucroft, S., Silverwood, H., Ahmad, M.,  
 1251 Asghar, M. I., Hoorani, H. R., Khalid, S., Khan, W. A., Khurshid, T., Qazi, S., Shah,  
 1252 M. A., Shoaib, M., Bialkowska, H., Boimska, B., Frueboes, T., Gokieli, R., Górski,  
 1253 M., Kazana, M., Nawrocki, K., Romanowska-Rybinska, K., Szleper, M., Wrochna, G.,  
 1254 Zalewski, P., Brona, G., Bunkowski, K., Cwiok, M., Dominik, W., Doroba, K., Kalinowski,  
 1255 A., Konecki, M., Krolkowski, J., Almeida, N., Bargassa, P., David, A., Faccioli, P.,  
 1256 Ferreira Parracho, P. G., Gallinaro, M., Seixas, J., Varela, J., Vischia, P., Belotelov,  
 1257 I., Bunin, P., Gavrilenko, M., Golutvin, I., Gorbunov, I., Kamenev, A., Karjavin, V.,  
 1258 Kozlov, G., Lanev, A., Malakhov, A., Moisenz, P., Palichik, V., Pereygin, V., Shmatov,  
 1259 S., Smirnov, V., Volodko, A., Zarubin, A., Evstyukhin, S., Golovtsov, V., Ivanov, Y.,  
 1260 Kim, V., Levchenko, P., Murzin, V., Oreshkin, V., Smirnov, I., Sulimov, V., Uvarov,  
 1261 L., Vavilov, S., Vorobyev, A., Vorobyev, A., Andreev, Y., Dermenev, A., Gninenko,  
 1262 S., Golubev, N., Kirsanov, M., Krasnikov, N., Matveev, V., Pashenkov, A., Tliso, D.,  
 1263 Toropin, A., Epshteyn, V., Erofeeva, M., Gavrilov, V., Kossov, M., Lychkovskaya, N.,  
 1264 Popov, V., Safronov, G., Semenov, S., Stolin, V., Vlasov, E., Zhokin, A., Belyaev, A.,  
 1265 Boos, E., Ershov, A., Gribushin, A., Klyukhin, V., Kodolova, O., Korotkikh, V., Lokhtin,  
 1266 I., Markina, A., Obraztsov, S., Perfilov, M., Petrushanko, S., Popov, A., Sarycheva, L.,  
 1267 Savrin, V., Snigirev, A., Vardanyan, I., Andreev, V., Azarkin, M., Dremin, I., Kirakosyan,

1268 M., Leonidov, A., Mesyats, G., Rusakov, S. V., Vinogradov, A., Azhgirey, I., Bayshev, I.,  
 1269 Bitioukov, S., Grishin, V., Kachanov, V., Konstantinov, D., Korablev, A., Krychkine,  
 1270 V., Petrov, V., Ryutin, R., Sobol, A., Tourtchanovitch, L., Troshin, S., Tyurin, N.,  
 1271 Uzunian, A., Volkov, A., Adzic, P., Djordjevic, M., Ekmedzic, M., Krpic, D., Milosevic, J.,  
 1272 Aguilar-Benitez, M., Alcaraz Maestre, J., Arce, P., Battilana, C., Calvo, E., Cerrada, M.,  
 1273 Chamizo Llatas, M., Colino, N., De La Cruz, B., Delgado Peris, A., Domínguez Vázquez,  
 1274 D., Fernandez Bedoya, C., Fernández Ramos, J. P., Ferrando, A., Flix, J., Fouz, M. C.,  
 1275 Garcia-Abia, P., Gonzalez Lopez, O., Goy Lopez, S., Hernandez, J. M., Josa, M. I., Merino,  
 1276 G., Puerta Pelayo, J., Quintario Olmeda, A., Redondo, I., Romero, L., Santaolalla, J.,  
 1277 Soares, M. S., Willmott, C., Albajar, C., Codispoti, G., de Trocóniz, J. F., Brun, H.,  
 1278 Cuevas, J., Fernandez Menendez, J., Folgueras, S., Gonzalez Caballero, I., Lloret Iglesias,  
 1279 L., Piedra Gomez, J., Brochero Cifuentes, J. A., Cabrillo, I. J., Calderon, A., Chuang,  
 1280 S. H., Duarte Campderros, J., Felcini, M., Fernandez, M., Gomez, G., Gonzalez Sanchez,  
 1281 J., Jorda, C., Lopez Virto, A., Marco, J., Marco, R., Martinez Rivero, C., Matorras,  
 1282 F., Munoz Sanchez, F. J., Rodrigo, T., Rodríguez-Marrero, A. Y., Ruiz-Jimeno, A.,  
 1283 Scodellaro, L., Sobron Sanudo, M., Vila, I., Vilar Cortabitarte, R., Abbaneo, D., Auffray,  
 1284 E., Auzinger, G., Baillon, P., Ball, A. H., Barney, D., Benitez, J. F., Bernet, C., Bianchi,  
 1285 G., Bloch, P., Bocci, A., Bonato, A., Botta, C., Breuker, H., Camporesi, T., Cerminara,  
 1286 G., Christiansen, T., Coarasa Perez, J. A., D'Enterria, D., Dabrowski, A., De Roeck,  
 1287 A., Di Guida, S., Dobson, M., Dupont-Sagorin, N., Elliott-Peisert, A., Frisch, B., Funk,  
 1288 W., Georgiou, G., Giffels, M., Gigi, D., Gill, K., Giordano, D., Giunta, M., Glege, F.,  
 1289 Gomez-Reino Garrido, R., Govoni, P., Gowdy, S., Guida, R., Hansen, M., Harris, P.,  
 1290 Hartl, C., Harvey, J., Hegner, B., Hinzmann, A., Innocente, V., Janot, P., Kaadze, K.,  
 1291 Karavakis, E., Kousouris, K., Lecoq, P., Lee, Y.-J., Lenzi, P., Lourenço, C., Mäki, T.,  
 1292 Malberti, M., Malgeri, L., Mannelli, M., Masetti, L., Meijers, F., Mersi, S., Meschi, E.,  
 1293 Moser, R., Mozer, M. U., Mulders, M., Musella, P., Nesvold, E., Orimoto, T., Orsini, L.,  
 1294 Palencia Cortezon, E., Perez, E., Perrozzi, L., Petrilli, A., Pfeiffer, A., Pierini, M., Pimiä,  
 1295 M., Piparo, D., Polese, G., Quertenmont, L., Racz, A., Reece, W., Rodrigues Antunes, J.,  
 1296 Rolandi, G., Rommerskirchen, T., Rovelli, C., Rovere, M., Sakulin, H., Santanastasio, F.,  
 1297 Schäfer, C., Schwick, C., Segoni, I., Sekmen, S., Sharma, A., Siegrist, P., Silva, P., Simon,

1298 M., Sphicas, P., Spiga, D., Spiropulu, M., Tsirou, A., Veres, G. I., Vlimant, J. R., Wöhri,  
 1299 H. K., Worm, S. D., Zeuner, W. D., Bertl, W., Deiters, K., Erdmann, W., Gabathuler,  
 1300 K., Horisberger, R., Ingram, Q., Kaestli, H. C., König, S., Kotlinski, D., Langenegger, U.,  
 1301 Meier, F., Renker, D., Rohe, T., Sibille, J., Bäni, L., Bortignon, P., Buchmann, M. A.,  
 1302 Casal, B., Chanon, N., Deisher, A., Dissertori, G., Dittmar, M., Dünser, M., Eugster, J.,  
 1303 Freudenreich, K., Grab, C., Hits, D., Lecomte, P., Lustermann, W., Martinez Ruiz del  
 1304 Arbol, P., Mohr, N., Moortgat, F., Nägeli, C., Nef, P., Nessi-Tedaldi, F., Pandolfi, F.,  
 1305 Pape, L., Pauss, F., Peruzzi, M., Ronga, F. J., Rossini, M., Sala, L., Sanchez, A. K.,  
 1306 Starodumov, A., Stieger, B., Takahashi, M., Tauscher, L., Thea, A., Theofilatos, K.,  
 1307 Treille, D., Urscheler, C., Wallny, R., Weber, H. A., Wehrli, L., Aguilo, E., Amsler, C.,  
 1308 Chiochia, V., De Visscher, S., Favaro, C., Ivova Rikova, M., Millan Mejias, B., Otiougova,  
 1309 P., Robmann, P., Snoek, H., Tupputi, S., Verzetti, M., Chang, Y. H., Chen, K. H., Kuo,  
 1310 C. M., Li, S. W., Lin, W., Liu, Z. K., Lu, Y. J., Mekterovic, D., Singh, A. P., Volpe, R., Yu,  
 1311 S. S., Bartalini, P., Chang, P., Chang, Y. H., Chang, Y. W., Chao, Y., Chen, K. F., Dietz,  
 1312 C., Grundler, U., Hou, W.-S., Hsiung, Y., Kao, K. Y., Lei, Y. J., Lu, R.-S., Majumder, D.,  
 1313 Petrakou, E., Shi, X., Shiu, J. G., Tzeng, Y. M., Wan, X., Wang, M., Adiguzel, A., Bakirci,  
 1314 M. N., Cerci, S., Dozen, C., Dumanoglu, I., Eskut, E., Girgis, S., Gokbulut, G., Gurpinar,  
 1315 E., Hos, I., Kangal, E. E., Karapinar, G., Kayis Topaksu, A., Onengut, G., Ozdemir, K.,  
 1316 Ozturk, S., Polatoz, A., Sogut, K., Sunar Cerci, D., Tali, B., Topakli, H., Vergili, L. N.,  
 1317 Vergili, M., Akin, I. V., Aliev, T., Bilin, B., Bilmis, S., Deniz, M., Gamsizkan, H., Guler,  
 1318 A. M., Ocalan, K., Ozpineci, A., Serin, M., Sever, R., Surat, U. E., Yalvac, M., Yildirim,  
 1319 E., Zeyrek, M., Gülmez, E., Isildak, B., Kaya, M., Kaya, O., Ozkorucuklu, S., Sonmez, N.,  
 1320 Cankocak, K., Levchuk, L., Bostock, F., Brooke, J. J., Clement, E., Cussans, D., Flacher,  
 1321 H., Frazier, R., Goldstein, J., Grimes, M., Heath, G. P., Heath, H. F., Kreczko, L.,  
 1322 Metson, S., Newbold, D. M., Nirunpong, K., Poll, A., Senkin, S., Smith, V. J., Williams,  
 1323 T., Basso, L., Bell, K. W., Belyaev, A., Brew, C., Brown, R. M., Cockerill, D. J. A.,  
 1324 Coughlan, J. A., Harder, K., Harper, S., Jackson, J., Kennedy, B. W., Olaiya, E., Petyt,  
 1325 D., Radburn-Smith, B. C., Shepherd-Themistocleous, C. H., Tomalin, I. R., Womersley,  
 1326 W. J., Bainbridge, R., Ball, G., Beuselinck, R., Buchmuller, O., Colling, D., Cripps, N.,  
 1327 Cutajar, M., Dauncey, P., Davies, G., Della Negra, M., Ferguson, W., Fulcher, J., Futyan,



D., Gilbert, A., Guneratne Bryer, A., Hall, G., Hatherell, Z., Hays, J., Iles, G., Jarvis, M., Karapostoli, G., Lyons, L., Magnan, A.-M., Marrouche, J., Mathias, B., Nandi, R., Nash, J., Nikitenko, A., Papageorgiou, A., Pela, J., Pesaresi, M., Petridis, K., Pioppi, M., Raymond, D. M., Rogerson, S., Rose, A., Ryan, M. J., Seez, C., Sharp, P., Sparrow, A., Stoye, M., Tapper, A., Vazquez Acosta, M., Virdee, T., Wakefield, S., Wardle, N., Whyntie, T., Chadwick, M., Cole, J. E., Hobson, P. R., Khan, A., Kyberd, P., Leslie, D., Martin, W., Reid, I. D., Symonds, P., Teodorescu, L., Turner, M., Hatakeyama, K., Liu, H., Scarborough, T., Charaf, O., Henderson, C., Rumerio, P., Avetisyan, A., Bose, T., Fantasia, C., Heiste (2012). Measurement of the pseudorapidity and centrality dependence of the transverse energy density in pb-pb collisions at  $\sqrt{s_{\text{NN}}} = 2.76$  TeV. *Phys. Rev. Lett.*, 109:152303. 6, 20

[14] Collaboration, T. A., Aamodt, K., Quintana, A. A., Achenbach, R., Acounis, S., Adamov, D., Adler, C., Aggarwal, M., Agnese, F., Rinella, G. A., Ahammed, Z., Ahmad, A., Ahmad, N., Ahmad, S., Akindinov, A., Akishin, P., Aleksandrov, D., Alessandro, B., Alfaro, R., Alfarone, G., Alici, A., Alme, J., Alt, T., Altinpinar, S., Amend, W., Andrei, C., Andres, Y., Andronic, A., Anelli, G., Anfreville, M., Angelov, V., Anzo, A., Anson, C., Antici, T., Antonenko, V., Antonczyk, D., Antinori, F., Antinori, S., Antonioli, P., Aphecetche, L., Appelshuser, H., Aprodu, V., Arba, M., Arcelli, S., Argentieri, A., Armesto, N., Arnaldi, R., Arefiev, A., Arsene, I., Asryan, A., Augustinus, A., Awes, T. C., ysto, J., Azmi, M. D., Bablock, S., Badal, A., Badyal, S. K., Baechler, J., Bagnasco, S., Bailhache, R., Bala, R., Baldisseri, A., Baldit, A., Bn, J., Barbera, R., Barberis, P.-L., Barbet, J. M., Barnfoldi, G., Barret, V., Bartke, J., Bartos, D., Basile, M., Basmanov, V., Bastid, N., Batigne, G., Batyunya, B., Baudot, J., Baumann, C., Bearden, I., Becker, B., Belikov, J., Bellwied, R., Belmont-Moreno, E., Belogianni, A., Belyaev, S., Benato, A., Beney, J. L., Benhabib, L., Benotto, F., Beol, S., Berceanu, I., Bercuci, A., Berdermann, E., Berdnikov, Y., Bernard, C., Berny, R., Berst, J. D., Bertelsen, H., Betev, L., Bhasin, A., Baskar, P., Bhati, A., Bianchi, N., Bielik, J., Bielikov, J., Bimbot, L., Blanchard, G., Blanco, F., Blanco, F., Blau, D., Blume, C., Blyth, S., Boccioni, M., Bogdanov, A., Bggild, H., Bogolyubsky, M., Boldizsr, L., Bombara, M., Bombonati, C., Bondila, M., Bonnet,

1357 D., Bonvicini, V., Borel, H., Borotto, F., Borshchov, V., Bortoli, Y., Borysov, O., Bose,  
 1358 S., Bosisio, L., Botje, M., Bttger, S., Bourdaud, G., Bourrion, O., Bouvier, S., Braem,  
 1359 A., Braun, M., Braun-Munzinger, P., Bravina, L., Bregant, M., Bruckner, G., Brun, R.,  
 1360 Bruna, E., Brunasso, O., Bruno, G. E., Bucher, D., Budilov, V., Budnikov, D., Buesching,  
 1361 H., Buncic, P., Burns, M., Burachas, S., Busch, O., Bushop, J., Cai, X., Caines, H.,  
 1362 Calaon, F., Caldogno, M., Cali, I., Camerini, P., Campagnolo, R., Campbell, M., Cao,  
 1363 X., Capitani, G. P., Romeo, G. C., Cardenas-Montes, M., Carduner, H., Carena, F.,  
 1364 Carena, W., Cariola, P., Carminati, F., Casado, J., Diaz, A. C., Caselle, M., Castellanos,  
 1365 J. C., Castor, J., Catanescu, V., Cattaruzza, E., Cavazza, D., Cerello, P., Ceresa, S.,  
 1366 ern, V., Chambert, V., Chapeland, S., Charpy, A., Charrier, D., Chartoire, M., Charvet,  
 1367 J. L., Chattopadhyay, S., Chattopadhyay, S., Chepurnov, V., Chernenko, S., Cherney,  
 1368 M., Cheshkov, C., Cheynis, B., Chochula, P., Chiavassa, E., Barroso, V. C., Choi, J.,  
 1369 Christakoglou, P., Christiansen, P., Christensen, C., Chykalov, O. A., Cicalo, C., Cifarelli-  
 1370 Strolin, L., Ciobanu, M., Cindolo, F., Cirstoiu, C., Clausse, O., Cleymans, J., Cobanoglu,  
 1371 O., Coffin, J.-P., Coli, S., Colla, A., Colledani, C., Combaret, C., Combet, M., Comets,  
 1372 M., Balbastre, G. C., del Valle, Z. C., Contin, G., Contreras, J., Cormier, T., Corsi, F.,  
 1373 Cortese, P., Costa, F., Crescio, E., Crochet, P., Cuautle, E., Cussonneau, J., Dahlinger,  
 1374 M., Dainese, A., Dalsgaard, H. H., Daniel, L., Das, I., Das, T., Dash, A., Silva, R. D.,  
 1375 Davenport, M., Daues, H., Caro, A. D., de Cataldo, G., Cuveland, J. D., Falco, A. D.,  
 1376 de Gaspari, M., de Girolamo, P., de Groot, J., Gruttola, D. D., Haas, A. D., Marco, N. D.,  
 1377 Pasquale, S. D., Remigis, P. D., de Vaux, D., Decock, G., Delagrange, H., Franco, M. D.,  
 1378 Dellacasa, G., Dell'Olio, C., Dell'Olio, D., Deloff, A., Demanov, V., Dnes, E., D'Erasmo,  
 1379 G., Derkach, D., Devaux, A., Bari, D. D., Bartolomeo, A. D., Giglio, C. D., Liberto,  
 1380 S. D., Mauro, A. D., Nezza, P. D., Dialinas, M., Diaz, L., Valdes, R. D., Dietel, T., Dima,  
 1381 R., Ding, H., Dinca, C., Divi, R., Dobretsov, V., Dobrin, A., Doenigus, B., Dobrowolski,  
 1382 T., Domnguez, I., Dorn, M., Drouet, S., Dubey, A. E., Ducroux, L., Dumitrache, F.,  
 1383 Dumonteil, E., Dupieux, P., Duta, V., Majumdar, A. D., Majumdar, M. D., Dyhre,  
 1384 T., Efimov, L., Efremov, A., Elia, D., Emschermann, D., Engster, C., Enokizono, A.,  
 1385 Espagnon, B., Estienne, M., Evangelista, A., Evans, D., Evrard, S., Fabjan, C. W.,  
 1386 Fabris, D., Faivre, J., Falchieri, D., Fantoni, A., Farano, R., Fearick, R., Fedorov, O.,

1387 Fekete, V., Felea, D., Feofilov, G., Tllez, A. F., Ferretti, A., Fichera, F., Filchagin, S.,  
 1388 Filoni, E., Finck, C., Fini, R., Fiore, E. M., Flierl, D., Floris, M., Fodor, Z., Foka, Y.,  
 1389 Fokin, S., Force, P., Formenti, F., Fragiaco, E., Fragiadakis, M., Fraissard, D., Franco,  
 1390 A., Franco, M., Frankenfeld, U., Fratino, U., Fresneau, S., Frolov, A., Fuchs, U., Fujita, J.,  
 1391 Furget, C., Furini, M., Girard, M. F., Gaardhje, J.-J., Gabrielli, A., Gadrat, S., Gagliardi,  
 1392 M., Gago, A., Gaido, L., Torreira, A. G., Gallio, M., Gandolfi, E., Ganoti, P., Ganti, M.,  
 1393 Garabatos, J., Lopez, A. G., Garizzo, L., Gaudichet, L., Gemme, R., Germain, M., Gheata,  
 1394 A., Gheata, M., Ghidini, B., Ghosh, P., Giolu, G., Giraudo, G., Giubellino, P., Glasow,  
 1395 R., Glssel, P., Ferreira, E. G., Gutierrez, C. G., Gonzales-Trueba, L. H., Gorbunov, S.,  
 1396 Gorbunov, Y., Gos, H., Gosset, J., Gotovac, S., Gottschlag, H., Gottschalk, D., Grabski,  
 1397 V., Grassi, T., Gray, H., Grebenyuk, O., Grebieszko, K., Gregory, C., Grigoras, C.,  
 1398 Grion, N., Grigoriev, V., Grigoryan, A., Grigoryan, C., Grigoryan, S., Grishuk, Y., Gros,  
 1399 P., Grosse-Oetringhaus, J., Grossiord, J.-Y., Grosso, R., Grynyov, B., Guarnaccia, C.,  
 1400 Guber, F., Guerin, F., Guernane, R., Guerzoni, M., Guichard, A., Guida, M., Guilloux,  
 1401 G., Gulkanyan, H., Gulbrandsen, K., Gunji, T., Gupta, A., Gupta, V., Gustafsson, H.-  
 1402 A., Gutbrod, H., Hadjidakis, C., Haiduc, M., Hamar, G., Hamagaki, H., Hamblen, J.,  
 1403 Hansen, J. C., Hardy, P., Hatzifotiadou, D., Harris, J. W., Hartig, M., Harutyunyan, A.,  
 1404 Hayrapetyan, A., Hasch, D., Hasegan, D., Hehner, J., Heine, N., Heinz, M., Helstrup, H.,  
 1405 Herghelegiu, A., Herlant, S., Corral, G. H., Herrmann, N., Hetland, K., Hille, P., Hinke,  
 1406 H., Hippolyte, B., Hoch, M., Hoebbel, H., Hoedlmoser, H., Horaguchi, T., Horner, M.,  
 1407 Hristov, P., Hrivnov, I., Hu, S., Guo, C. H., Humanic, T., Hurtado, A., Hwang, D. S.,  
 1408 Ianigro, J. C., Idzik, M., Igoikin, S., Ilkaev, R., Ilkiv, I., Imhoff, M., Innocenti, P. G.,  
 1409 Ionescu, E., Ippolitov, M., Irfan, M., Insa, C., Inuzuka, M., Ivan, C., Ivanov, A., Ivanov,  
 1410 M., Ivanov, V., Jacobs, P., Jacholkowski, A., Janurov, L., Janik, R., Jasper, M., Jena, C.,  
 1411 Jirde, L., Johnson, D. P., Jones, G. T., Jorgensen, C., Jouve, F., Jovanovi, P., Junique,  
 1412 A., Jusko, A., Jung, H., Jung, W., Kadija, K., Kamal, A., Kamermans, R., Kapusta, S.,  
 1413 Kaidalov, A., Kakoyan, V., Kalcher, S., Kang, E., Kapitan, J., Kaplan, V., Karadzhev, K.,  
 1414 Karavichev, O., Karavicheva, T., Karpechev, E., Karpio, K., Kazantsev, A., Kebschull,  
 1415 U., Keidel, R., Khan, M. M., Khanzadeev, A., Kharlov, Y., Kikola, D., Kileng, B., Kim,  
 1416 D., Kim, D. S., Kim, D. W., Kim, H. N., Kim, J. S., Kim, S., Kinson, J. B., Kiprich, S. K.,

1417 Kisel, I., Kiselev, S., Kisiel, A., Kiss, T., Kiworra, V., Klay, J., Bsing, C. K., Kliemant, M.,  
 1418 Klimov, A., Klovning, A., Kluge, A., Kluit, R., Kniese, S., Kolevaton, R., Kollegger, T.,  
 1419 Kolojvari, A., Kondratiev, V., Kornas, E., Koshurnikov, E., Kotov, I., Kour, R., Kowalski,  
 1420 M., Kox, S., Kozlov, K., Krlik, I., Kramer, F., Kraus, I., Kravkov, A., Krawutschke, T.,  
 1421 Krivda, M., Kryshen, E., Kucheriaev, Y., Kugler, A., Kuhn, C., Kuijer, P., Kumar, L.,  
 1422 Kumar, N., Kumpumaeki, P., Kurepin, A., Kurepin, A. N., Kushpil, S., Kushpil, V.,  
 1423 Kutovsky, M., Kvaerno, H., Kweon, M., Labb, J.-C., Lackner, F., de Guevara, P. L.,  
 1424 Lafage, V., Rocca, P. L., Lamont, M., Lara, C., Larsen, D. T., Laurenti, G., Lazzeroni,  
 1425 C., Bornec, Y. L., Bris, N. L., Gailliard, C. L., Lebedev, V., Lecoq, J., Lee, K. S., Lee, S. C.,  
 1426 Lefvre, F., Legrand, I., Lehmann, T., Leistam, L., Lenoir, P., Lenti, V., Leon, H., Monzon,  
 1427 I. L., Lvai, P., Li, Q., Li, X., Librizzi, F., Lietava, R., Lindegaard, N., Lindenstruth, V.,  
 1428 Lippmann, C., Lisa, M., Listratenko, O. M., Littel, F., Liu, Y., Lo, J., Lobanov, V.,  
 1429 Loginov, V., Noriega, M. L., Lpez-Ramrez, R., Torres, E. L., Lorenzo, P. M., Lvhidden,  
 1430 G., Lu, S., Ludolphs, W., Lunardon, M., Luquin, L., Lusso, S., Lutz, J.-R., Luvisetto,  
 1431 M., Lyapin, V., Maevskaya, A., Magureanu, C., Mahajan, A., Majahan, S., Mahmoud,  
 1432 T., Mairani, A., Mahapatra, D., Makarov, A., Makhlyueva, I., Malek, M., Malkiewicz,  
 1433 T., Mal'Kevich, D., Malzacher, P., Mamonov, A., Manea, C., Mangotra, L. K., Maniero,  
 1434 D., Manko, V., Manso, F., Manzari, V., Mao, Y., Marcel, A., Marchini, S., Mare, J.,  
 1435 Margagliotti, G. V., Margotti, A., Marin, A., Marin, J.-C., Marras, D., Martinengo, P.,  
 1436 Martnez, M. I., Martinez-Davalos, A., Garcia, G. M., Martini, S., Chiesa, A. M., Marzocca,  
 1437 C., Masciocchi, S., Masera, M., Masetti, M., Maslov, N. I., Masoni, A., Massera, F., Mast,  
 1438 M., Mastroserio, A., Matthews, Z. L., Mayer, B., Mazza, G., Mazzaro, M. D., Mazzoni,  
 1439 A., Meddi, F., Meleshko, E., Menchaca-Rocha, A., Meneghini, S., Meoni, M., Perez, J. M.,  
 1440 Mereu, P., Meunier, O., Miake, Y., Michalon, A., Michinelli, R., Miftakhov, N., Mignone,  
 1441 M., Mikhailov, K., Milosevic, J., Minaev, Y., Minafra, F., Mischke, A., Mikowiec, D.,  
 1442 Mitsyn, V., Mitu, C., Mohanty, B., Moisa, D., Molnar, L., Mondal, M., Mondal, N.,  
 1443 Zetina, L. M., Monteno, M., Morando, M., Morel, M., Moretto, S., Morhardt, T., Morsch,  
 1444 A., Moukhanova, T., Mucchi, M., Muccifora, V., Mudnic, E., Mller, H., Mller, W., Munoz,  
 1445 J., Mura, D., Musa, L., Muraz, J. F., Musso, A., Nania, R., Nandi, B., Nappi, E., Navach,  
 1446 F., Navin, S., Nayak, T., Nazarenko, S., Nazarov, G., Nellen, L., Nendaz, F., Nianine,

1447 A., Nicassio, M., Nielsen, B. S., Nikolaev, S., Nikolic, V., Nikulin, S., Nikulin, V., Nilsen,  
 1448 B., Nitti, M., Noferini, F., Nomokonov, P., Nooren, G., Noto, F., Nouais, D., Nyiri,  
 1449 A., Nystrand, J., Odyniec, G., Oeschler, H., Oinonen, M., Oldenburg, M., Oleks, I.,  
 1450 Olsen, E. K., Onuchin, V., Oppedisano, C., Orsini, F., Ortiz-Velzquez, A., Oskamp, C.,  
 1451 Oskarsson, A., Osmic, F., sterman, L., Otterlund, I., Ovrebeek, G., Oyama, K., Pachr,  
 1452 M., Pagano, P., Pai, G., Pajares, C., Pal, S., Pal, S., Plla, G., Palmeri, A., Pancaldi,  
 1453 G., Panse, R., Pantaleo, A., Pappalardo, G. S., Pastirk, B., Pastore, C., Patarakin, O.,  
 1454 Paticchio, V., Patimo, G., Pavlinov, A., Pawlak, T., Peitzmann, T., Pnichot, Y., Pepato,  
 1455 A., Pereira, H., Peresunko, D., Perez, C., Griffio, J. P., Perini, D., Perrino, D., Peryt, W.,  
 1456 Pesci, A., Peskov, V., Pestov, Y., Peters, A. J., Petrek, V., Petridis, A., Petris, M., Petrov,  
 1457 V., Petrov, V., Petrovici, M., Peyr, J., Piano, S., Piccotti, A., Pichot, P., Piemonte, C.,  
 1458 Pikna, M., Pilastrini, R., Pillot, P., Pinazza, O., Pini, B., Pinsky, L., Morais, V. P.,  
 1459 Pismennaya, V., Piuz, F., Platt, R., Ploskon, M., Plumeri, S., Pluta, J., Pocheptsov,  
 1460 T., Podesta, P., Poggio, F., Poghossyan, M., Poghossyan, T., Polk, K., Polichtchouk, B.,  
 1461 Polozov, P., Polyakov, V., Pommeresch, B., Pompei, F., Pop, A., Popescu, S., Posa, F.,  
 1462 Pospil, V., Potukuchi, B., Pouthas, J., Prasad, S., Preghenella, R., Prino, F., Prodan, L.,  
 1463 Prono, G., Protsenko, M. A., Pruneau, C. A., Przybyla, A., Pshenichnov, I., Puddu, G.,  
 1464 Pujahari, P., Pulvirenti, A., Punin, A., Punin, V., Putschke, J., Quartieri, J., Quercigh,  
 1465 E., Rachevskaya, I., Rachevski, A., Rademakers, A., Radomski, S., Radu, A., Rak, J.,  
 1466 Ramello, L., Raniwala, R., Raniwala, S., Rasmussen, O. B., Rasson, J., Razin, V., Read,  
 1467 K., Real, J., Redlich, K., Reichling, C., Renard, C., Renault, G., Renfordt, R., Reolon,  
 1468 A. R., Reshetin, A., Revol, J.-P., Reygers, K., Ricaud, H., Riccati, L., Ricci, R. A., Richter,  
 1469 M., Riedler, P., Rigalleau, L. M., Riggi, F., Riegler, W., Rindel, E., Riso, J., Rivetti, A.,  
 1470 Rizzi, M., Rizzi, V., Cahuantzi, M. R., Red, K., Rhrich, D., Romn-Lpez, S., Romanato, M.,  
 1471 Romita, R., Ronchetti, F., Rosinsky, P., Rosnet, P., Rossegger, S., Rossi, A., Rostchin,  
 1472 V., Rotondo, F., Roukoutakis, F., Rousseau, S., Roy, C., Roy, D., Roy, P., Royer, L.,  
 1473 Rubin, G., Rubio, A., Rui, R., Rusanov, I., Russo, G., Ruuskanen, V., Ryabinkin, E.,  
 1474 Rybicki, A., Sadovsky, S., afak, K., Sahoo, R., Saini, J., Saiz, P., Salur, S., Sambyal,  
 1475 S., Samsonov, V., ndor, L., Sandoval, A., Sann, H., Santiard, J.-C., Santo, R., Santoro,  
 1476 R., Sargsyan, G., Saturnini, P., Scapparone, E., Scarlassara, F., Schackert, B., Schiaua,

1477 C., Schicker, R., Schioler, T., Schippers, J. D., Schmidt, C., Schmidt, H., Schneider, R.,  
 1478 Schossmaier, K., Schukraft, J., Schutz, Y., Schwarz, K., Schweda, K., Schyns, E., Scioli,  
 1479 G., Scomparin, E., Snow, H., Sedykh, S., Segato, G., Sellitto, S., Semeria, F., Senyukov,  
 1480 S., Seppnen, H., Serici, S., Serkin, L., Serra, S., Sesselmann, T., Sevcenco, A., Sgura, I.,  
 1481 Shabratova, G., Shahoyan, R., Sharkov, E., Sharma, S., Shigaki, K., Shileev, K., Shukla,  
 1482 P., Shurygin, A., Shurygina, M., Sibiriak, Y., Siddi, E., Siemiarczuk, T., Sigward, M. H.,  
 1483 Silenzi, A., Silvermyr, D., Silvestri, R., Simili, E., Simion, V., Simon, R., Simonetti, L.,  
 1484 Singaraju, R., Singhal, V., Sinha, B., Sinha, T., Siska, M., Sitr, B., Sitta, M., Skaali,  
 1485 B., Skowronski, P., Slodkowski, M., Smirnov, N., Smykov, L., Snellings, R., Snoeys, W.,  
 1486 Soegaard, C., Soerensen, J., Sokolov, O., Soldatov, A., Soloviev, A., Soltveit, H., Soltz,  
 1487 R., Sommer, W., Soos, C., Soramel, F., Sorensen, S., Soyk, D., Spyropoulou-Stassinaki,  
 1488 M., Stachel, J., Staley, F., Stan, I., Stavinskiy, A., Steckert, J., Stefanini, G., Stefanek,  
 1489 G., Steinbeck, T., Stelzer, H., Stenlund, E., Stocco, D., Stockmeier, M., Stoicea, G.,  
 1490 Stolpovsky, P., Strme, P., Stutzmann, J. S., Su, G., Sugitate, T., umbera, M., Suire, C.,  
 1491 Susa, T., Kumar, K. S., Swoboda, D., Symons, J., Szarka, I., Szostak, A., Szuba, M.,  
 1492 Szymanski, P., Tadel, M., Tagridis, C., Tan, L., Takaki, D. T., Taureg, H., Tauro, A.,  
 1493 Tavlet, M., Munoz, G. T., Thder, J., Tieulent, R., Timmer, P., Tolyhy, T., Topilskaya,  
 1494 N., de Matos, C. T., Torii, H., Toscano, L., Tosello, F., Tournaire, A., Traczyk, T., Trger,  
 1495 G., Tromeur, W., Truesdale, D., Trzaska, W., Tsiledakis, G., Tsilis, E., Tsvetkov, A.,  
 1496 Turcato, M., Turrise, R., Tuveri, M., Tveter, T., Tydesjo, H., Tykarski, L., Tywoniuk, K.,  
 1497 Ugolini, E., Ullaland, K., Urbn, J., Urciuoli, G. M., Usai, G. L., Usseglio, M., Vacchi, A.,  
 1498 Vala, M., Valiev, F., Vyvre, P. V., Brink, A. V. D., Eijndhoven, N. V., Kolk, N. V. D.,  
 1499 van Leeuwen, M., Vannucci, L., Vanzetto, S., Vanuxem, J.-P., Vargas, M. A., Varma,  
 1500 R., Vascotto, A., Vasiliev, A., Vassiliou, M., Vasta, P., Vechernin, V., Venaruzzo, M.,  
 1501 Vercellin, E., Vergara, S., Verhoeven, W., Veronese, F., Vetlitskiy, I., Vernet, R., Victorov,  
 1502 V., Vidak, L., Viesti, G., Vikhlyantsev, O., Vilakazi, Z., Baillie, O. V., Vinogradov, A.,  
 1503 Vinogradov, L., Vinogradov, Y., Virgili, T., Viyogi, Y., Vodopianov, A., Volpe, G., Vranic,  
 1504 D., Vrlkov, J., Vulpesu, B., Wabnitz, C., Wagner, V., Wallet, L., Wan, R., Wang, Y.,  
 1505 Wang, Y., Wheadon, R., Weis, R., Wen, Q., Wessels, J., Westergaard, J., Wiechula, J.,  
 1506 Wiesenaecker, A., Wikne, J., Wilk, A., Wilk, G., Williams, C., Willis, N., Windelband, B.,

1507 Witt, R., Woehri, H., Wyllie, K., Xu, C., Yang, C., Yang, H., Yermia, F., Yin, Z., Yin, Z.,  
 1508 Ky, B. Y., Yushmanov, I., Yuting, B., Zabrodin, E., Zagato, S., Zagreev, B., Zaharia, P.,  
 1509 Zalite, A., Zampa, G., Zampolli, C., Zanevskiy, Y., Zarochentsev, A., Zaudtke, O., Zvada,  
 1510 P., Zbroszczyk, H., Zepeda, A., Zeter, V., Zgura, I., Zhalov, M., Zhou, D., Zhou, S., Zhu,  
 1511 G., Zichichi, A., Zinchenko, A., Zinovjev, G., Zoccarato, Y., Zubarev, A., Zucchini, A.,  
 1512 and Zuffa, M. (2008). The alice experiment at the cern lhc. *Journal of Instrumentation*,  
 1513 3(08):S08002. 24

1514 [15] Connors, M., Nattrass, C., Reed, R., and Salur, S. (2017). Review of Jet Measurements  
 1515 in Heavy Ion Collisions. vi, 10, 11, 13

1516 [16] Elia, D. and the ALICE Collaboration (2013). Strangeness production in alice. *Journal*  
 1517 *of Physics: Conference Series*, 455(1):012005. 16

1518 [17] Evans, L. and Bryant, P. (2008). Lhc machine. *Journal of Instrumentation*,  
 1519 3(08):S08001. 9

1520 [18] Floris, M. (2014). Hadron yields and the phase diagram of strongly interacting matter.  
 1521 *Nuclear Physics A*, 931:103 – 112. QUARK MATTER 2014. 6

1522 [19] Foka, P. and Janik, M. A. (2016). An overview of experimental results from ultra-  
 1523 relativistic heavy-ion collisions at the cern lhc: Bulk properties and dynamical evolution.  
 1524 *Reviews in Physics*, 1:154 – 171. 10

1525 [20] Gyulassy, M. (2004). The QGP discovered at RHIC. In *Structure and dynamics*  
 1526 *of elementary matter. Proceedings, NATO Advanced Study Institute, Camyuva-Kemer,*  
 1527 *Turkey, September 22-October 2, 2003*, pages 159–182. 7

1528 [21] Heuser, J. M. (2013). The compressed baryonic matter experiment at fair. *Nuclear*  
 1529 *Physics A*, 904-905:941c – 944c. The Quark Matter 2012. 5

1530 [22] Hilke, H. J. (2010). Time projection chambers. *Reports on Progress in Physics*,  
 1531 73(11):116201. 25

- [23] Huovinen, P., Kolb, P. F., Heinz, U., Ruuskanen, P. V., and Voloshin, S. A. (2001).  
Radial and elliptic flow at RHIC: further predictions. *Physics Letters B*, 503:58–64. 14
- [24] Jacobs, P. and Wang, X.-N. (2005). Matter in extremis: ultrarelativistic nuclear  
collisions at RHIC. *Progress in Particle and Nuclear Physics*, 54:443–534. 14
- [25] Kapusta, J. I. (1979). Quantum chromodynamics at high temperature. *Nuclear Physics*  
*B*, 148(3):461 – 498. 3
- [26] Luo, X. (2016). Exploring the qcd phase structure with beam energy scan in heavy-  
ion collisions. *Nuclear Physics A*, 956:75 – 82. The XXV International Conference on  
Ultrarelativistic Nucleus-Nucleus Collisions: Quark Matter 2015. 18
- [27] Miller, M. L., Reygers, K., Sanders, S. J., and Steinberg, P. (2007). Glauber modeling  
in high energy nuclear collisions. *Ann. Rev. Nucl. Part. Sci.*, 57:205–243. 10
- [28] Nattrass, C. (2009). System, energy, and flavor dependence of jets through di-hadron  
correlations in heavy ion collisions. v, 10, 25
- [29] Odyniec, G. (2013). The rhic beam energy scan program in star and what’s next ...  
*Journal of Physics: Conference Series*, 455(1):012037. 18
- [30] Ozaki, S. and Roser, T. (2015). Relativistic heavy ion collider, its construction and  
upgrade. *Progress of Theoretical and Experimental Physics*, 2015(3):03A102. vi, 8
- [31] Paquet, J.-F., Shen, C., Denicol, G., Luzum, M., Schenke, B., Jeon, S., and Gale, C.  
(2016). Thermal and prompt photons at rhic and the lhc. *Nuclear Physics A*, 956:409 –  
412. The XXV International Conference on Ultrarelativistic Nucleus-Nucleus Collisions:  
Quark Matter 2015. 14, 15
- [32] Preghenella, R. (2011). Transverse momentum spectra of identified charged hadrons  
with the ALICE detector in Pb-Pb collisions at  $\sqrt{s_{NN}} = 2.76$  TeV. *PoS, EPS-*  
*HEP2011:118*. 23
- [33] Qin, G.-Y. and Wang, X.-N. (2015). Jet quenching in high-energy heavy-ion collisions.  
*International Journal of Modern Physics E*, 24:1530014–438. 17



- [34] Satz, H. (2006). Colour deconfinement and quarkonium binding. *Journal of Physics G: Nuclear and Particle Physics*, 32(3):R25. 4, 5
- [35] Schenke, B. (2017). Origins of collectivity in small systems. *Nuclear Physics A*, 967:105 – 112. The 26th International Conference on Ultra-relativistic Nucleus-Nucleus Collisions: Quark Matter 2017. 14
- [36] Shao, M., Barannikova, O. Yu., Dong, X., Fisyak, Y., Ruan, L., Sorensen, P., and Xu, Z. (2006). Extensive particle identification with TPC and TOF at the STAR experiment. *Nucl. Instrum. Meth.*, A558:419–429. 25
- [37] Shuryak, E. V. (1988). The qcd vacuum and quark-gluon plasma. *Zeitschrift für Physik C Particles and Fields*, 38(1):141–145. 3
- [38] Snellings, R. (2011). Elliptic flow: a brief review. *New Journal of Physics*, 13(5):055008. 14
- [39] Stock, R. (2004). Ultra-relativistic nucleus-nucleus collisions. Proceedings, 17th International Conference, Quark Matter 2004, Oakland, USA, January 11-17, 2004. *J. Phys.*, G30:S633–S648. 7
- [40] Strickland, M. (2014). Anisotropic hydrodynamics: Motivation and methodology. *Nuclear Physics A*, 926:92–101. 14
- [41] Stcker, H. (2005). Collective flow signals the quarkgluon plasma. *Nuclear Physics A*, 750(1):121 – 147. Quark-Gluon Plasma. New Discoveries at RHIC: Case for the Strongly Interacting Quark-Gluon Plasma. Contributions from the RBRC Workshop held May 14-15, 2004. vii, 18
- [42] Vovchenko, V., Anchishkin, D., and Csernai, L. P. (2014). Time dependence of partition into spectators and participants in relativistic heavy-ion collisions. *Phys. Rev. C*, 90:044907. vi, 12
- [43] Wilde, M. (2013). Measurement of Direct Photons in pp and Pb-Pb Collisions with ALICE. *Nucl. Phys.*, A904-905:573c–576c. 15

- 1584 [44] Wong, C.-Y. (1994). *Introduction to high-energy heavy-ion collisions*. World scientific.
- 1585 vi, 15, 16, 17, 76

# Appendices

## A Kinematic Variables

The description of the collision physics and the interpretation of its results are aided by the construction of variables that undergo simple transformations under a change of reference frame. Two such variables, rapidity and pseudorapidity, are described in this section.

The rapidity,  $y$ , of a particle is defined as:

$$y \equiv \frac{1}{2} \ln \frac{p_0 + p_z}{p_0 - p_z} \quad (1)$$

$$= \frac{1}{2} \ln \frac{E + p_z}{E - p_z}, \quad (2)$$

where  $p_0$  and  $p_z$  are the components of its contravariant four-momentum  $p = (p_0, p_x, p_y, p_z)$  with  $p_0 = \frac{E}{c}$ ,  $E$  being the relativistic energy of the particle and  $c$ , the speed of light, being equal to 1 in natural units.

The rapidity of a particle is used as a relativistic description of its velocity. Unlike the canonical velocity of a particle, its rapidity transforms simply additively under a Lorentz boost of the frame of reference. For example, suppose a particle has a rapidity  $y$  in the laboratory frame. Let  $y'$  denote its rapidity as measured in a frame that is Lorentz boosted with a velocity  $\beta$  in the  $z$ -direction with respect to the laboratory frame. Then the relationship between the rapidities in the two different frames is simply

$$y' = y - y_\beta \quad (3)$$

Here,

$$y_\beta = \frac{1}{2} \ln \frac{1 + \beta}{1 - \beta} \quad (4)$$

is the rapidity the particle would have in the laboratory frame if it were moving with a velocity  $\beta$  in the  $z$ -direction with respect to the laboratory frame, as can be verified from equation 1 with  $p_0 = \gamma m$  and  $p_z = \gamma \beta m$ ,  $\gamma$  being the Lorentz factor  $\frac{1}{\sqrt{1-\beta^2}}$  [44].

The convenience provided by this construct comes with a cost. As evident from equation 1, the calculation of the rapidity of a particle requires the measurement of two different

1607 observables associated with it, such as the energy and the  $z$ -direction momentum. However,  
 1608 experimental constraints may sometimes only facilitate the measurement of the direction of  
 1609 the detected particle with respect to the beam axis. What's more convenient in such a case  
 1610 is the use of another variable construct called pseudorapidity,  $\eta$ , defined as:

$$\eta \equiv -\ln \tan \frac{\theta}{2}, \quad (5)$$

1611 where  $\theta$  is the angle the particle's momentum vector,  $\mathbf{p}$ , makes with the  $z$ -direction. The  
 1612 above equation can also be written in terms of the momentum as:

$$\eta = \frac{1}{2} \ln \frac{|\mathbf{p}| + p_z}{|\mathbf{p}| - p_z} \quad (6)$$

1613 From equations 1 and 6, it is evident that  $\eta \approx y$  when  $|\mathbf{p}| \approx p_0$ , i.e., when the momentum  
 1614 is large. The transformation of the particle distribution from the  $y$ -space to the  $\eta$ -space is  
 1615 discussed in section 4.3.2.